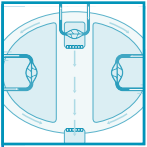


CEREBROSPINAL FLUID SECRETION BY THE CHOROID PLEXUS

Helle H. Damkier, Peter D. Brown, and Jeppe Praetorius

Department of Biomedicine, Health, Aarhus University, Aarhus, Denmark; and Faculty of Life Sciences, Michael Smith Building, Manchester University, Manchester, United Kingdom



Damkier HH, Brown PD, Praetorius J. Cerebrospinal Fluid Secretion by the Choroid Plexus. *Physiol Rev* 93: 1847–1892, 2013; doi:10.1152/physrev.00004.2013.—

The choroid plexus epithelium is a cuboidal cell monolayer, which produces the majority of the cerebrospinal fluid. The concerted action of a variety of integral membrane proteins mediates the transepithelial movement of solutes and water across the epithelium. Secretion by the choroid plexus is characterized by an extremely high rate and by the unusual cellular polarization of well-known epithelial transport proteins. This review focuses on the specific ion and water transport by the choroid plexus cells, and then attempts to integrate the action of specific transport proteins to formulate a model of cerebrospinal fluid secretion. Significant emphasis is placed on the concept of isotonic fluid transport across epithelia, as there is still surprisingly little consensus on the basic biophysics of this phenomenon. The role of the choroid plexus in the regulation of fluid and electrolyte balance in the central nervous system is discussed, and choroid plexus dysfunctions are described in a very diverse set of clinical conditions such as aging, Alzheimer's disease, brain edema, neoplasms, and hydrocephalus. Although the choroid plexus may only have an indirect influence on the pathogenesis of these conditions, the ability to modify epithelial function may be an important component of future therapies.

I.	INTRODUCTION	1847
II.	STRUCTURE OF THE CHOROID PLEXUSES...	1848
III.	THE UNIQUE POLARITY OF THE CHOROID...	1852
IV.	MODELS FOR WATER AND SOLUTE...	1854
V.	EARLY INVESTIGATIONS OF THE...	1862
VI.	MOVEMENT OF SMALL MONOVALENT...	1866
VII.	MOVEMENT OF SMALL MONOVALENT...	1871
VIII.	TRANSCELLULAR WATER TRANSPORT	1873
IX.	CURRENT MODEL FOR CSF SECRETION...	1873
X.	REGULATION OF CSF WATER AND...	1876
XI.	MECHANISMS AND REGULATION OF...	1878
XII.	PATHOPHYSIOLOGY RELATING TO...	1880
XIII.	PERSPECTIVES AND FUTURE...	1883

I. INTRODUCTION

For decades, the choroid plexuses have attracted much attention because of their contribution to cerebrospinal fluid (CSF) formation and because they are strikingly dissimilar to most other transporting epithelia. The choroid plexus epithelium (CPE) is a secretory epithelium par excellence with unique cellular transport mechanisms that have been revealed by contributions from many laboratories and through the application of a wide variety of methods. The cells of the CPE are among the most efficient tissues in terms of secretory rate. The CSF is formed at a rate of $\sim 0.4 \text{ ml} \cdot \text{min}^{-1} \cdot \text{g tissue}^{-1}$, a transport rate only paralleled in mammals by the cells of the renal proximal tubule and pancreatic ducts (32, 72). The total volume of CSF in the

entire human CNS amounts to 150 ml, and ~ 500 – 600 ml are produced in 24 h; thus the CSF is replaced three to four times per day (49, 351). The CPE has appealed to scientists working in the fields of epithelial transport, cell biology, cell polarization, and neuroscience, because of these unusual transport characteristics of the epithelium.

More than four decades have now passed since the canonical and still most comprehensive review to date of the choroid plexus function was written by Helen F. Cserr in 1971 (49). In the sections below, we seek to provide a thorough and updated overview of the transport physiology of the CPE. Recent advances in understanding the regulation of CSF secretion are also discussed, and we highlight the limitations of our current understanding of CSF formation and choroid plexus physiology. It should be noted that important topics such as the CPE-mediated transport of organic solutes, nutrient and drug transport, and the release of mediators and hormones that do not relate to ion and water secretion fall outside the scope of this article. These topics have been reviewed recently elsewhere (84, 139, 158, 302). The potential direct or indirect roles of the choroid plexuses in pathophysiological states, such as choroid plexus adenomas, hydrocephalus, increased intracranial pressure, and the control of ventilation, however, are discussed. Our overriding aim is to attract the interest of physiologists and neuroscientists in general and of transport physiologists in particular, to the complexities of the choroid plexuses.

In a "Historical Note," Hadju (112) credited the first descriptions of CSF to Hippocrates (460 to 370 BC) as being "water surrounding the brain" (119), and later to Galen (129 to 200 AD) as forming an "excremental liquid" in the ventricles (100). In 1744, Swedenborg referred to the CSF as "lymph" that was being dispensed from the roof of the fourth ventricle to the medulla oblongata and the spinal cord. A few years later, von Haller presented evidence that the "water" in the brain was actually secreted into the ventricles. From this point onward, other prominent scientists who made crucial contributions to CSF research include the following: Willis, Magendie, Mestrezat, and Cushing. The choroid plexuses were first suggested as sites of CSF secretion by Faivre in 1854 (90) and by Cushing in 1914 (53). The first direct experimental evidence for this was presented in 1960 by Rougemont and colleagues (64), who also showed that CSF was not a simple ultrafiltrate of plasma. Despite the compelling evidence by Rougemont and many others, the significance of the CPE in CSF formation is still often debated. Nevertheless, it is now generally accepted that the four choroid plexuses secrete the majority of the intraventricular CSF. Most recent estimates indicate that ~80% of the CSF is secreted by the choroid plexuses, with the remaining 20% coming from the interstitial fluid of the brain which is generated by the blood-brain barrier (BBB) (262). In humans, the reported surface area of the BBB is 20 m² (19), while the surface area estimate of the choroid plexus is only 0.021 m², or ~0.1% of the BBB (77). In rats, however, the best estimate of luminal surface area is 75 cm² (157), with a brain capillaries surface area of ~155 cm², or only twice the area of the choroid plexus. One reason for the discrepancy between the estimates is the possible underestimation of the surface area in the human CPE. The calculations did not take into account the surface extension of the luminal microvilli in CPE. However, even with a maximal 50-fold surface extension by microvilli, there is still ample space for other explanations of the discrepancy. Another reason for the discrepancy could be that a much larger relative BBB surface area is required in the much more complex human brain. In any case, the secretory capacity of the choroid plexus per surface area is far greater than for the BBB, and this may well be a main reason the large contribution to CSF secretion by the CPE.

Demonstrating that the choroid plexuses actually secrete fluid, however, exercised the ingenuity of many scientists for much of the 20th century. Their work is reviewed in depth by Davson et al. (62) and is only briefly summarized here: 1) removal of the choroid plexus from one ventricle, caused changes in ventricle volume consistent with a secretory role for the choroid plexuses; 2) measurements of the difference in hematocrit between arterial blood entering and venous blood leaving the choroid plexus, demonstrated fluid loss from the blood as it transits the choroid plexus; 3) determination of the composition of fluid collected under oil from the surface of the exposed choroid plexus, showed

that this fluid was almost identical to CSF collected from the cisterna magna and therefore was not simply an exudate formed by ultra-filtration of blood plasma; and 4) the demonstration of the active secretion of Na⁺, Cl⁻, and HCO₃⁻ from "blood" to "ventricle" in choroid plexus tissue isolated from the bullfrog and mounted in an Ussing chamber. Each of the different experimental approaches employed has some limitations, as discussed by Davson et al. (62); however, together these data provided strong evidence for the role of the choroid plexus in CSF secretion.

In the last few years, even more persuasive evidence for the role of the CPE in CSF secretion has been generated using transgenic mice. These studies have shown that the rate of CSF secretion is reduced in animals in which the genes for specific transport proteins are silenced, as judged noninvasively by MRI imaging of ventricular volume or by measuring intracranial pressure. Proteins studied in this way include NCBE (137) and AQP1 (234), both of which are strongly expressed in choroid plexus but importantly show limited expression elsewhere in the brain ventricular system. In a further refinement to these methods, it has also been shown that the ionic composition of the CSF is altered in mice lacking the NBCe2 transporter (151) and the KCNE2 channel protein (269). These data on transgenic mice are perhaps the most convincing evidence to date supporting the role of the choroid plexuses as the major sites of CSF secretion.

II. STRUCTURE OF THE CHOROID PLEXUSES AND THE VENTRICULAR SYSTEM

A. Choroid Plexus Structure

Four choroid plexuses reside inside the ventricular system of the brain: one in each of the two lateral ventricles, one in the third, and one in the fourth ventricle. The choroid plexuses arise as extensions of the ependymal lining of the ventricles during development. In the mature brain, most of these branched or sheetlike surface extensions floats in the ventricular cavities surrounded by the CSF. Together, the four choroid plexuses comprise a major part of the blood-CSF barrier (BCSFB). The arachnoid membrane and the circumventricular organs constitute the remainder of the BCSFB. The BCSFB should not to be confused with the BBB formed between the tight endothelial cell layer of the cerebral blood vessels and the interstitial fluid of the brain (FIGURES 1 AND 3). The tight endothelial layer of the BBB forms a barrier, which limits the access to the brain parenchyma for most substances, whereas the capillary endothelium in the BCSFB is quite leaky.

The choroid plexuses have a relatively simple structure. They consist of a single layer of cuboidal to low cylindrical epithelial cells that reside on a basement membrane (FIGURE 2, A and B). Electron microscopic analysis of the epithelial cells reveals a relatively large number of mitochondria

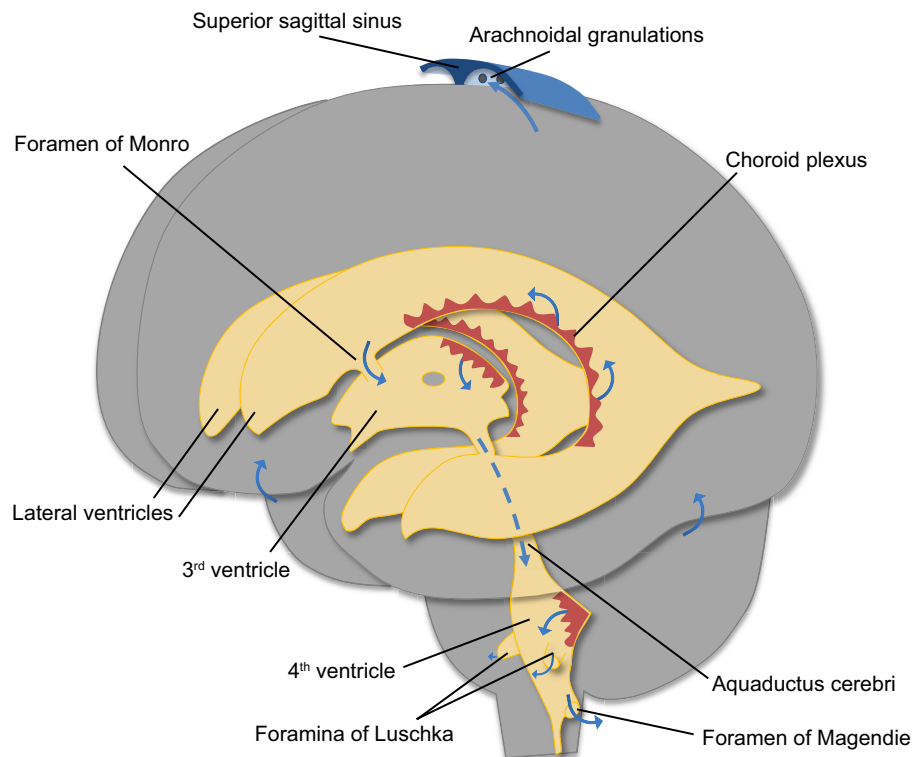


FIGURE 1. Organization of the ventricular system of the brain. The brain parenchyma is shown in gray, the ventricles and aquaducts are in yellow, and the choroid plexuses are marked in red. Cerebrospinal fluid is formed by the choroid plexus of the two lateral ventricles, the 3rd and 4th ventricles. Lateral ventricle fluid converges in the 3rd ventricle through the foramen of Monro and reaches the 4th ventricle via the aquaductus cerebri (Sylvius). The cerebrospinal fluid exits from the 4th ventricle through the foramina of Magendie and Luschka to the outer surface of the central nervous system. The majority of the fluid is reabsorbed in the arachnoidal granulations draining to the superior sagittal sinus.

spread throughout the cytoplasm, a central nucleus, and abundant Golgi apparatus located laterally and toward the ventricular lumen. The cytoplasm also contains vesicles, which increase in size towards the luminal surface (203). As mentioned above, the surface area of the luminal membrane of the CPE is greatly enhanced by the presence of dense microvilli (**FIGURE 2C**). The basal and lateral surfaces are rather flat, but they develop a strongly folded labyrinth with the neighboring cell at the transition from lateral to basal surface (203). This pronounced folding in the membrane expands the basal surface area and is perhaps to some extent restricting the diffusion of solutes from the interstitium to the intercellular compartment, i.e., the lateral intercellular space.

Along with microvilli, both primary cilia and motile cilia are found on the luminal surface (224). The most recent understanding is that CPE cells either have one primary cilium or small tufts of smaller motile cilia (16). Structural defects in cilia cause hydrocephalus due to an increase in CSF production by the choroid plexus (309). Experimental removal of cilia by chloral hydrate causes an increase in soluble adenylyl cyclase and cAMP leading to increased transcytosis in a primary CPE cell line (224), suggesting a sensory function of this structure. Mice with defective cilia due to *Tg737orpk* mutations exhibit

dramatically altered choroid plexus function, including changes in intracellular cAMP, pH, CSF composition, and resulting hydrocephalus (15, 16). The molecular mechanisms behind the ciliary function and dysfunction are not completely understood, but it has been suggested that the beating cilia prevent the creation of unstirred layers, whereas the primary cilia may serve as osmosensors and/or chemosensors.

The CPE cells are connected by junctional complexes at the luminal membrane (**FIGURE 2A**), consisting of tight junctions, adherens junctions, and desmosomes. The tight junctions express several members of the claudin protein family (167). Cellular claudin composition is a major determinant for the selective tightness of an epithelium. The strong expression of claudin-2 and -11 in the choroid plexus tight junctions means that they closely resemble those of the proximal tubules, which are very water permeable (345). In fact, the choroid plexus is often compared with the proximal tubule with reference to the large amount of fluid movement, albeit in opposite directions.

Beneath the epithelial basement membrane is a network of fenestrated capillaries that are surrounded by connective tissue composed of fibroblasts and immune cells (**FIGURE 2, B AND D**). The fenestrations of the capillaries are sealed

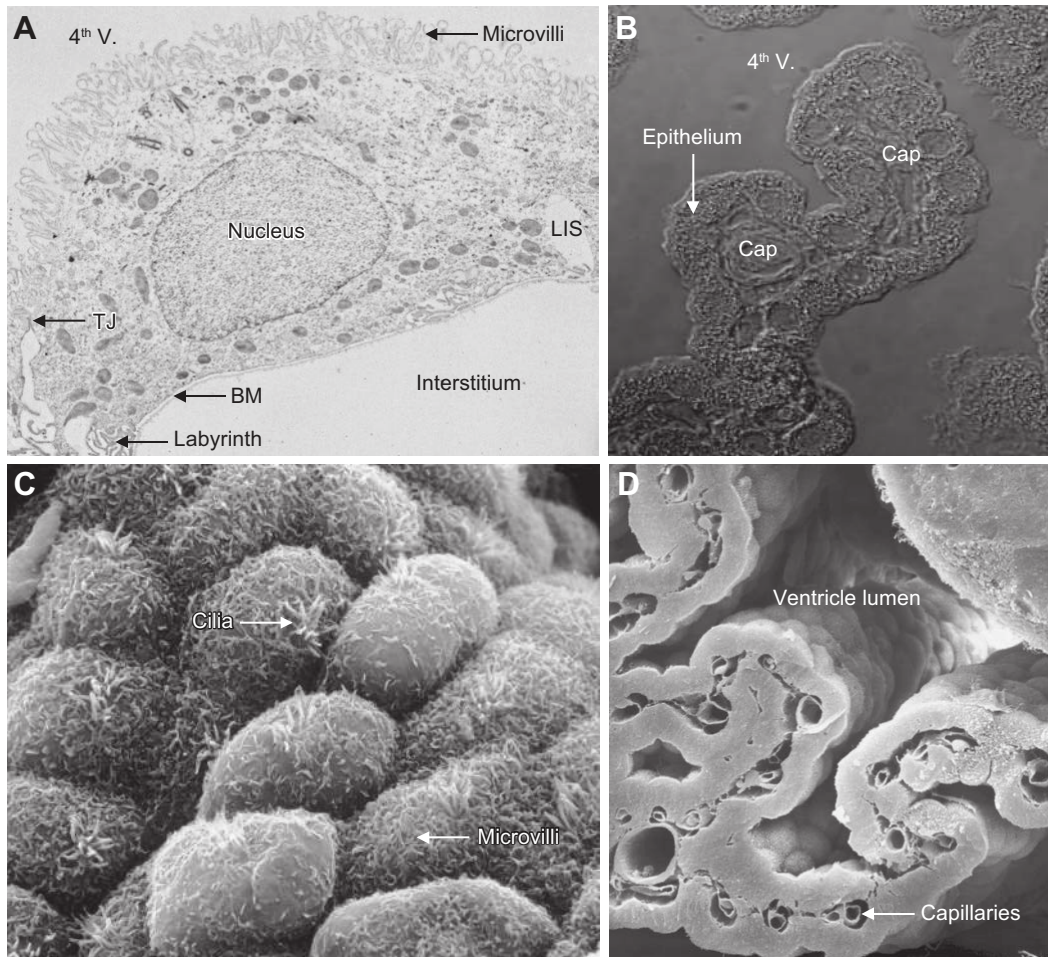


FIGURE 2. Choroid plexus ultrastructure. *A*: transmission electron micrograph of a rat choroid plexus epithelial cell. The luminal surface contains numerous microvilli and is separated from the lateral intercellular space (LIS) by tight junctions (TJ). A labyrinth of plasma membrane infoldings is seen at the border between the relatively smooth lateral and basal membranes. The basement membrane (BM) separates the epithelium from the interstitium, which in this image lacks its connective tissue because of the preparation technique. *B*: differential interference contrast micrograph of the tip of a 4th ventricle (4th V). Choroid plexus villus with its capillaries (Cap) in the sparse interstitial connective tissue and the single layer of cuboidal epithelium. *C*: scanning electron micrograph of the ventricular surface of human choroid plexus. Examples of microvilli and motile cilia are indicated. *D*: cryo-fractured preparation of mouse choroid plexus. The capillaries of the sheetlike choroid plexus and the lateral ventricle lumen are indicated. (*C* and *D* are purchased from Corbis images.)

with thin diaphragms, which permit ions, water, and small molecules (e.g., nutrients, vitamins, etc.) to pass relatively easily into the interstitial fluid of each plexus. It is, therefore, mainly the epithelial cells that constitute the BCSFB.

B. Blood Supply and Innervation of the Choroid Plexus

The choroid plexuses receive blood from both the internal carotid arteries and the vertebral artery. In the two lateral ventricles, the choroid plexuses are supplied by the anterior choroidal artery, which branches from the internal carotid (via the medial cerebral artery), and by the posterior choroidal artery branching from the vertebral artery (via the

posterior cerebral artery). The latter also supplies the choroid plexus in the third ventricle. The choroid plexus in the fourth ventricle is supplied from the anterior and posterior inferior cerebellar arteries arising from the basilar and vertebral arteries, respectively. The choroid plexuses are perfused with blood at a rate of 4 ml/min per gram of choroid plexus tissue, which is approximately 10 times higher than the rate of the blood supply to the brain parenchyma (157). This high rate of perfusion means that blood flow is not normally rate-limiting for the process of CSF secretion.

Blood flow to the choroid plexuses is controlled by the sympathetic nervous system via fibers arising from the superior cervical ganglion. Both the capillaries and epithelial cells are innervated by these adrenergic fibers. The capillaries possess both α and β_2 adrenergic receptors, and stimulation of these

causes vasoconstriction or vasodilatation, respectively. On the other hand, the epithelial cells contain β_1 receptors, which upon stimulation cause a decrease in the rate of cerebrospinal fluid secretion. This is believed to be mediated via a decrease in carbonic anhydrase activity (323). The capillaries and epithelial cells also receive parasympathetic cholinergic nerve fibers most likely arising from the glossopharyngeal and vagal nerves (179). Parasympathetic stimulation reduces CSF production, probably by a nitric oxide mediated decrease in $\text{Na}^+\text{-K}^+$ -ATPase activity (85).

C. Ventricular Circulation and Outflow of CSF

Each of the choroid plexuses secretes CSF into the respective brain ventricle (**FIGURES 1 AND 3**). Once in the ventricle, the CSF is in contact with the ependymal epithelium, which lines the ventricles and constitutes a leaky barrier between the ventricle and the brain interior. Throughout the brain, the CSF and the interstitial fluid of the brain parenchyma are separated only by the leaky ependymal and the perivascular space that surrounds the large blood vessels (310). As more CSF is produced, there is a constant directional flow from the lateral ventricles towards the fourth ventricle and beyond. Thus the CSF secreted in the lateral ventricles flows through the foram-

ina of Monro into the third ventricle. From here the fluid flows through the aqueduct of Sylvius to the fourth ventricle. CSF then leaves the ventricular system via the foramina of Luschka and Magendie into the subarachnoid space. In the subarachnoid space, the CSF is no longer in contact with the ependyma but is now separated from the outer surface of the brain by the pia mater.

Although there is no agreement on the topic, most researchers believe that the CSF returns to venous blood in the brain sinuses, mainly via the arachnoid granulations and arachnoid villi. The arachnoid granulations consist of a central core that resembles the subarachnoid space. A capsule consisting of endothelial cells from the venous layer, and connective tissue and fibroblasts from the dura mater covers the core. The most apical portion of the granulation is covered only by an arachnoid layer and is in direct contact with the venous lumen (161). The reabsorption rate is dependent on the pressure gradient between the subarachnoid space and the venous sinus pressure. A small fraction of CSF may return to the blood system via the perineural sheets of cranial nerves to the cervical lymph nodes (50), and in certain pathological conditions with increased intracranial pressure, CSF can be forced into the extracellular space in the periventricular white matter through the ependymal barrier (298).

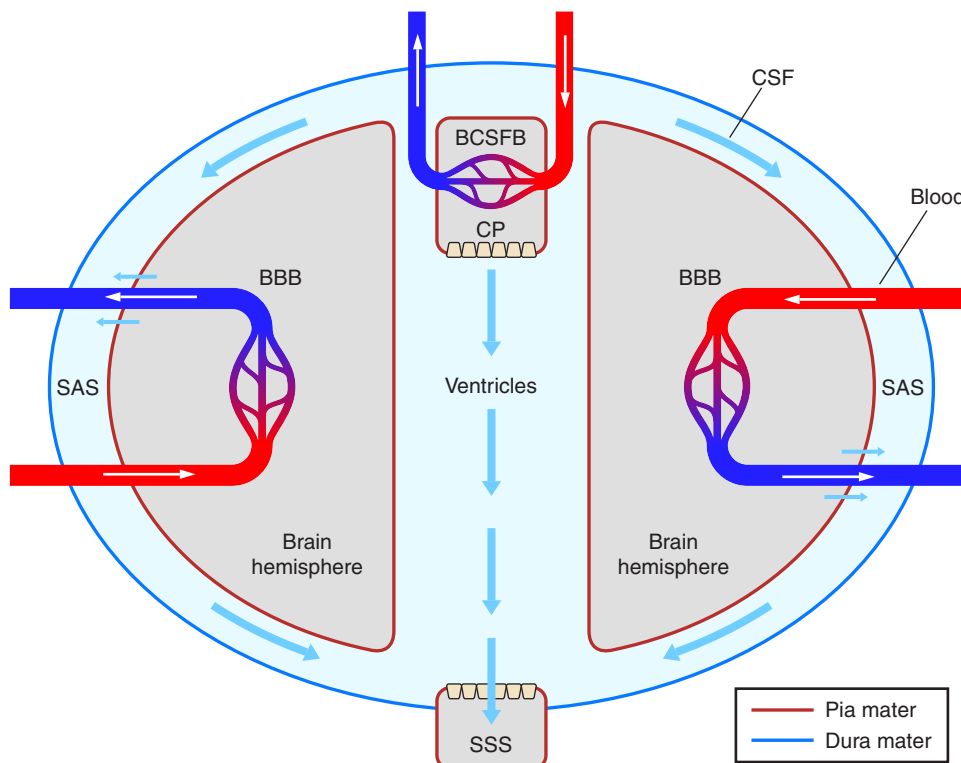


FIGURE 3. The fluid compartments in the brain. Cerebrospinal fluid (CSF, blue arrows) is primarily produced by the choroid plexus (CP) or blood CSF barrier (BCSFB) and flows through the ventricle system into the subarachnoid space (SAS) between the dura and the pia mater. CSF returns to the venous blood through the arachnoid granulations into the superior sagittal sinus (SSS). The blood supply to the majority of the brain is restricted by the blood-brain barrier (BBB). The brain interstitial fluid makes up the final portion of CSF and drains to the CSF through the perivascular spaces.

D. Development of the Choroid Plexuses

The choroid plexuses are derived from the dorsal part of the neural tube, which in humans develops early in the fourth week of gestation (230). The ends of the neural tube close as the anterior part of the tube develops into the brain and the posterior into the spinal cord. As the neural tube closes, the initial CSF is amniotic fluid trapped by the closing tube. The ventricles subsequently expand faster than the brain tissue grows. A transient occlusion of the spinal cord elicits an increase in intraventricular hydrostatic pressure that enables the expansion of the ventricles (68). The expansion is mediated by the osmotic gradient generated in the embryonic CSF, which is secreted by the neuroepithelium (188). The CP in the roof of the fourth ventricle is the first to appear in the 9th week of gestation, shortly after neural tube closure. The lateral ventricle choroid plexuses develop from the neuroepithelium and mesenchyme from the roof of the third ventricle and medial wall of the cerebral hemisphere. The fully developed lateral ventricle choroid plexus extends from the foramen of Monro and posterior to the choroidal fissure. The choroid plexus of the third ventricle is the last to develop and forms from the roof of the ventricle. The third ventricle choroid plexus is a continuation of the lateral ventricle choroid plexus through the foramen of Monro (276). The functional capacities of the choroid plexuses are fully developed shortly after the structures are formed (213, 144).

The development of the epithelium has four stages (82): 1) the tissue appears as pseudostratified cells without apparent glycogen content; 2) development of low columnar cells containing glycogen with apical nuclei; 3) cuboidal cells without glycogen and a central to apical nucleus; and finally 4) the mature choroid plexus with cuboidal epithelial cells with basal or central nuclei and no glycogen (82). The role of glycogen is not completely understood, but it may play a role in the development of glycosaminoglycans in the basement membrane. Notably, carbonic anhydrase appears in the developing human choroid plexus as soon as the tissue starts to form, and it persists throughout development into the mature CPE. Immature choroid plexus cells contain common plasma proteins like albumin, α -fetoprotein, transthyretin, and transferrin. With the exception of transthyretin, these proteins are not found in mature choroid plexus. Tight junctions are formed even in early choroid plexuses, and they appear essential for further epithelial differentiation (167).

III. THE UNIQUE POLARITY OF THE CHOROID PLEXUS EPITHELIUM

Epithelia cover the internal and external surfaces of multicellular organisms. They act in the first instance as barriers against aggressive chemicals, thermal changes, and microorganisms. However, they serve many other vital functions, such as sensing the external environment and mediating selective transport (absorption and secretion) to maintain a

constant and appropriate internal milieu. CPE cells appear to perform all these functions, and as in other epithelia (13, 37, 209), this requires the asymmetrical distribution of membrane proteins, i.e., cellular polarization (**FIGURE 4**). The polarized distribution of plasma membrane proteins requires the correct sorting of the membrane proteins, and this is an absolute requirement for sustaining life in higher organisms. Each type of epithelium expresses a specific array of different types of transport proteins depending on the required function. Membrane proteins are each targeted to either the outward-facing luminal membrane or the inward-facing basolateral membrane. In most epithelia, any given membrane protein seems always to target either the basolateral or the luminal membrane, e.g., the $\text{Na}^+\text{-K}^+\text{-ATPase}$ is normally expressed exclusively in the basolateral membrane.

One striking feature of the choroid plexus that has attracted the attention of both physiologists and cell biologists is the apparent inverse polarization of the epithelial cells. It should be restated that the CPE cells are polarized in a similar way as every known epithelium, i.e., they have a basolateral membrane residing on a basement membrane facing the interstitium/blood side, and separation of the basolateral and luminal membranes by tight junctions (**FIGURES 2A AND 4**). The epithelial cells also possess adherens junctions beneath the tight junctions, and contain a supranuclear microtubule-organizing center. Finally, the luminal membrane bears both microvilli and kinocilia as described above. All these are typical features of polarized epithelial cells. Nevertheless, the $\text{Na}^+\text{-K}^+\text{-ATPase}$ and similarly “basolateral transporters” such as NKCC1, KCC4, and NHE1 (see below) are all expressed in the luminal membrane of the choroid plexus. In contrast, other typical “basolateral transporters,” such as AE2, KCC3, and NBCn1, occupy the same membrane domain as in other epithelia. This highly unusual and almost unique distribution of membrane proteins remains a focus of those interested in protein trafficking (251).

In general, the cellular distribution of plasma membrane proteins is determined by three mechanisms: 1) primary protein structure, 2) sorting in vesicles destined for specific membrane domains, and 3) membrane stabilization by cytoskeletal anchoring (3, 37, 209). Thus, for many membrane proteins, specific consensus amino acid motifs are included during protein synthesis in the endoplasmic reticulum. These amino acids or special glycosylated motifs added en route are recognized by chaperone molecules in the rough endoplasmic reticulum (RER)-Golgi axis. These motifs determine the sorting of proteins into transport vesicles that are targeted either to the luminal or basolateral membrane from the *trans*-Golgi network (TGN). The plasma membrane abundance of a protein also reflects the balance between insertion of new protein, the stabilization

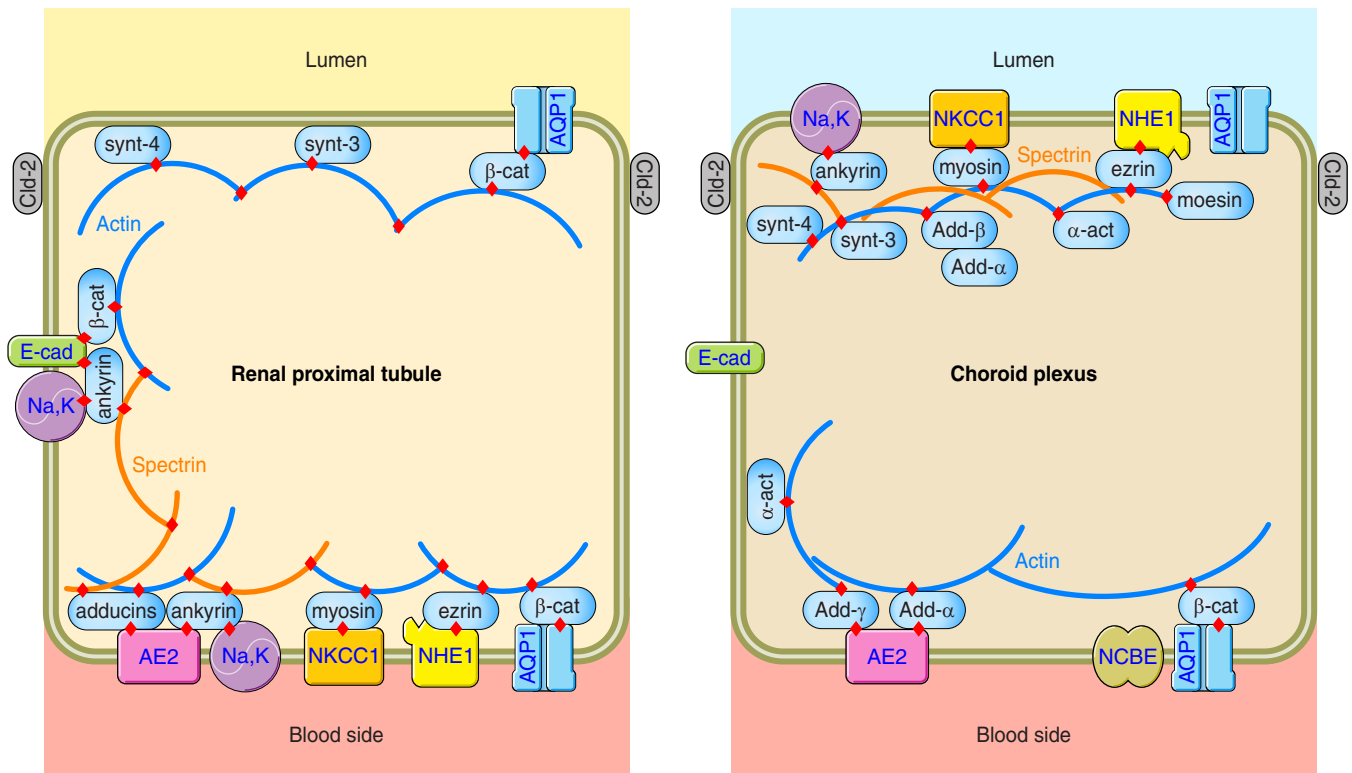


FIGURE 4. Polarity of choroid plexus epithelial cells. The cartoon shows the typical distribution of the actin and spectrin cytoskeleton in an epithelial cell such as the renal proximal tubule cell compared with the atypical distribution in the choroid plexus cell. Integral plasma membrane proteins involved in cellular solute and water transport are anchored to the cytoskeleton through adaptor or anchoring proteins, such as ankyrins, adducins, catenins, ezrin-radixin-moesin proteins, and syntaxins. The distribution of $\text{Na}^+\text{-K}^+\text{-ATPase}$ (Na,K), aquaporin-1 (AQP1), anion exchanger 2 (AE2), $\text{Na}^+\text{-K}^+\text{-2Cl}^-$ cotransporter 1 (NKCC1), the Na^+/H^+ exchanger 1 (NHE1), and E-cadherin (E-cad) is shown for both cell types as well as the tight junction protein claudin-2. The mechanism behind the atypical polarity of the choroid plexus epithelial cell is at present unknown.

in the membrane by cytoskeletal anchoring, and protein retrieval for breakdown.

Explanations for the unusual expression of proteins in the CPE have been sought at each level of protein synthesis and sorting. There is no evidence for the CPE-specific membrane targeting being the result of changes in primary structure for the luminal $\text{Na}^+\text{-K}^+\text{-ATPase}$, NHE1, or NKCC1 proteins (Damkier and Praetorius, unpublished observations). Thus the mechanisms for the atypical protein targeting in CPE may be sought for among differences in either TGN sorting of membrane-bound vesicles or in plasma membrane retention. To date, TGN sorting has not been systematically investigated in the choroid plexus, but some progress has been made regarding the atypical selective membrane retention (see below). The basic paradigm is that membrane proteins can either exist as free-floating proteins in the lipid bilayer or as fixed proteins, anchored to the actin or spectrin cytoskeleton through adaptor proteins such as ankyrins, adducins, myosins, ezrin/moesin, or catenins (FIGURE 4). To understand the cell biological principles involved in choroid plexus polarization, it is necessary first to consider more general principles of cell polarization in the following paragraph.

There are two central questions in cell polarization: 1) How is polarity induced? 2) How do the first proteins reach a given domain? If one first envisions a nonpolarized cell meeting a neighboring cell, these cells can form early adherens junctions and tight junctions. These junctions then seal off the luminal and basolateral domains in a beltlike fashion (209). Once this process is complete, diffusion of membrane proteins across the junctional complexes is restricted, so any newly synthesized membrane protein must arrive by vesicular carriers. These vesicles can target the intended membrane domain via the system of SNAP-SNARE proteins and Rab proteins targeting the vesicle to the intended membrane domain. However, this specificity requires that the given membrane domain already contain membrane proteins specific to that domain. The membrane domain specificity is either determined by proteins sorted during the formation of cell junctions by guided lateral diffusion in the membrane, or by some other mechanism inserting vesicles to a specific domain without needing the target SNARE and Rab protein of that domain.

Evidence from neurons, which also display cellular polarity, provides support for such a dual mechanism (227). If we assume the transition of a uniform rounded cell to a mature

neuron is similar to the induction of epithelial polarity, then we can equate the axon of the neuron to the epithelial luminal membrane, whereas the dendrites and cell body of the neuron equate to the basolateral membrane. In neurons, the earliest event in the neurons leading to asymmetry is the cytosolic accumulation of actin fibers beneath the plasma membrane at a site that does not display any previous specialization. While vesicles from the TGN destined for the cell membrane could reach all areas of the surface before the actin accumulation, it appears that certain vesicles are unable to penetrate the actin mesh and, thus, are excluded from the membrane above it. The actin accumulation occurs exactly at the site where the axon grows out and specific vesicles are only delivered to the dendritic and cell body surfaces. From this point, the membrane domains will differ in membrane protein contents including docking proteins for further vesicular cargo and specialization. In epithelial cells, a similar actin network forms during the generation of cell junctions beneath the luminal membrane: the terminal web. One may envisage that insertion of vesicles into the luminal membrane would be somehow restricted or selective to aid the initial cell polarization as observed in developing axons (227).

The earliest mechanistic insight into the atypical distribution of membrane proteins in the choroid plexus came from two studies published in the early 1990s. In the first, Marrs et al. (200) found that the $\text{Na}^+\text{-K}^+\text{-ATPase}$ was complexed by erythroid ankyrin and fodrin to the luminal surface in a triton-resistant membrane protein fraction. The now accepted nomenclature defines the erythroid ankyrin A as ankyrin 1, whereas the former brain (and cardiac) ankyrin B is ankyrin 2 and cardiac/neuronal ankyrin G is now ankyrin 3. Fodrin is a nonerythroid spectrin heterodimer composed of αII and βII subunits (erythroid type is αI and βI). There are two α spectrins (αI and αII) and five β spectrins (βI to βV) forming the spectrin dimers. Marrs et al. (200) also found that B-cadherin was expressed in the choroid plexus, and found in a triton-soluble fraction, also complexed with ankyrin and fodrin. Overexpression studies in fibroblasts were performed to test whether the presence of B-cadherin was involved in the lack of basolateral $\text{Na}^+\text{-K}^+\text{-ATPase}$. It was concluded that only E-cadherin expression was accompanied by basolateral $\text{Na}^+\text{-K}^+\text{-ATPase}$ localization, whereas B-cadherin expression led to diffuse distribution of the membrane protein. Whether this was based on selective targeting of $\text{Na}^+\text{-K}^+\text{-ATPase}$ vesicles to the apical membrane in the absence of E-cadherin, or to a lack of E-cadherin-dependent retention of the protein in the basolateral membrane remains unknown.

In the second paper, Alper et al. (5) applied a variety of antibodies to demonstrate that the vast majority of ankyrin, fodrin (spectrin), actin, myosin, and α -actinin colocalize with the $\text{Na}^+\text{-K}^+\text{-ATPase}$ in the luminal plasma membrane domain in the choroid plexus. This is the opposite to most

other epithelia, where ankyrin/spectrin cytoskeleton is predominantly found at the basolateral membrane domains. In agreement with the study by Marrs et al. (200), spectrin was also found at the basolateral domain but in a much lower abundance. However, the immunohistochemical localization of ankyrin with the luminal membrane in the Alper study (5) was in stark contrast to the biochemical detection of ankyrin in both domains of the cell by Marrs et al. (200). Apart from the methodological difference, this discrepancy may have been caused by differences in the ankyrin subtype or antibody performance between the two studies. In Alper's study (5), the antibodies were directed against human erythroid ankyrin (ANK1), while they were anti-chicken ANK1 in the Marrs study (200). No other ankyrins nor spectrin forms have been studied thus far in relation to the choroid plexus. Recently, Lobas et al. (184) localized E-cadherin as well as β -catenin to the basolateral membrane domain and ezrin to the luminal membrane domain. We have recently verified the expression of E-cadherin in murine choroid plexus (Christensen, Damkier, and Praetorius, unpublished data), thereby challenging the interpretation by Marrs et al. that the pan-cadherin antibody recognized B-cadherin in the choroid plexus.

It was recently shown that the subluminal ezrin distribution in the CPE was completely disrupted in mice with genetic ablation of the NaHCO_3 transporter Ncbe (59). This is accompanied with redistribution of the NHE1 from the atypical position in the luminal membrane to the usual localization at the basolateral membrane. Ncbe gene knockout was also accompanied by a collapse of the ventricular volume, indicating a greatly reduced CSF secretion by the CPE. In the same study, however, we found that the abundances of other key transporters such as the $\text{Na}^+\text{-K}^+\text{-ATPase}$ and AQP1 in the luminal membrane were markedly reduced in the knockouts (59). Thus it is not established whether the loss of Ncbe expression is the primary cause for the decreased CSF volume. A similar decrease in ventricular volume was observed by Lobas et al. (184), when protocadherin gamma was deleted in ciliated cells including CPE cells. In this study, there were no obvious changes in the CPE specific polarity with regards to tight junction proteins, E-cadherin, or ezrin. Clearly, a systematic and coherent comparison of the spectrin cytoskeleton and anchor protein distribution is warranted to more precisely define the determinants for the atypical polarization of CPE.

IV. MODELS FOR WATER AND SOLUTE TRANSPORT ACROSS EPITHELIA

Many cellular substances are not evenly distributed across plasma membranes. The distribution of a given solute across the membrane depends on the electrochemical forces acting on the solute and the permeability of the membrane to that solute. In most animal cells, the active and electrogenic extrusion of Na^+ in exchange for K^+ by the $\text{Na}^+\text{-K}^+$

ATPase is the major generator of ionic and charge asymmetry. This mechanism therefore drives most secondary active transport of other solutes into and out of cells. These general mechanisms are present in all mammalian cells. In transporting epithelia, the asymmetric distribution of plasma membrane transport proteins enables net transcellular transport of ions, other solutes, and water in a given direction, i.e., vectorial transport. In addition to transcellular movement of solutes and water, some epithelia facilitate the paracellular transport of certain molecules via tight junctions (26). One prominent example is the paracellular reabsorption of Mg^{2+} in the renal thick ascending limb of Henle's loop, where the lumen-positive potential difference across the epithelium drives Mg^{2+} through claudin-16 (previous paracellin-1) to the interstitium (293). In electrically leaky epithelia, cations or anions are able to pass the tight junction to some extent, while electrically tight epithelia virtually exclude such transport. In subsequent sections, we will discuss the vectorial transport of Na^+ , Cl^- , and HCO_3^- by the CPE from the blood side to the brain ventricles. In this section, however, we first consider the potential mechanisms of transepithelial H_2O transport.

In some epithelia where large transepithelial gradients exist, e.g., the renal collecting duct, the routes of vectorial water transport are quite well established (25). In contrast, the explanations of how transport occurs when the osmotic gradients are small or even undetectable remain controversial. Several models have been proposed to explain how water transport is coupled to solute movement across epithelia to yield almost isotonic net transport. These models were developed predominantly for absorptive epithelia; however, the choroid plexus has also been investigated as a key example of a secretory epithelium. Despite the involvement of some of the most prominent physiologists in epithelial transport, there is still no general agreement on this fundamental matter. Here, we provide a brief overview of the proposed models and their limitations to form a basis for the current model of the secretory processes in the choroid plexus.

A. Three-Compartment Model

The phenomenon of apparent isosmolar transport of water and solute across epithelia was first described by Reid (265). Since then, isosmotic transport has been described in small intestine, gall bladder, renal proximal tubules, and the choroid plexus epithelium (10, 52, 69, 70, 338, 339, 346). In 1962, Curran and MacIntosh (51) proposed the three-compartment model to explain isosmotic solute and water transport across epithelia. The three-compartment model involved a semipermeable membrane or barrier facing the lumen, a middle compartment, and a nonselective membrane or barrier facing the interstitial side (FIGURE 5A). The semipermeable barrier was highly water permeable but had a low solute permeability (high solute reflection), whereas the

nonselective barrier was almost freely permeable to solutes and water (low solute reflection). The active transport of solutes into the middle compartment from the adjacent cells increased the osmolarity here, and water followed across the semipermeable membrane to regain isosmolarity. The solute and water transport also increased the hydrostatic pressure in the middle compartment. This pressure thus drove water and solutes from the middle compartment across the nonselective membrane into the interstitial side of the epithelium. The nature of the different compartments and barriers, however, were not defined in this model (51).

B. Standing Gradient Model

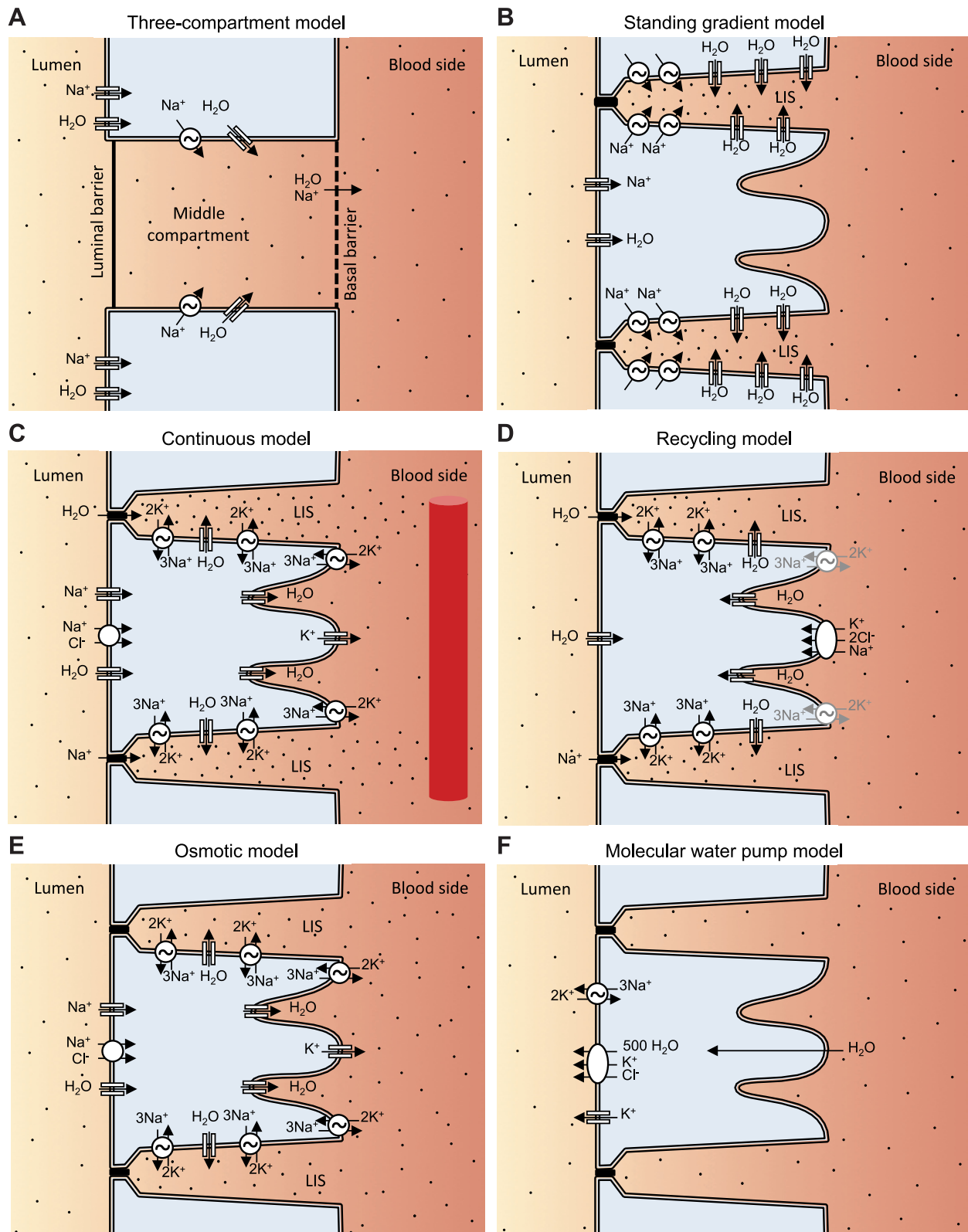
In the very influential standing gradient model, the three-compartment model was extended and the morphological nature of the compartments was identified (71, 343). The model depended strictly on transcellular transport, in which the solute, such as Na^+ , was taken into cells across the luminal membrane (i.e., the reflective or semipermeable membrane in the three-compartment membrane, FIGURE 5B). A slight intracellular hyperosmolarity then favored water movement across the same membrane to restore isosmolarity. Solute was actively transported into the lateral intercellular space (LIS, middle compartment) by the $\text{Na}^+\text{-K}^+$ -ATPase in the area closest to the tight junction at the blind end of the LIS. This produced a slightly higher osmolarity in LIS than inside the cell so water followed the solute across the lateral membrane. The resulting volume expansion in the LIS generated a hydrostatic pressure gradient towards the interstitial space below the basement membrane. The pressure gradient caused the bulk extrusion of isotonic fluid from the LIS to the underlying connective tissue on the blood side. The hypertonic fluid at the blind end of the LIS gradually became isotonic towards the open end, as the major water movement from the cell to LIS occurred near the open end. Over the years, several of the requirements for the model were questioned (275, 305, 337). First, the $\text{Na}^+\text{-K}^+$ -ATPases were uniformly distributed along the entire basolateral membrane, and not restricted to the area adjacent to the tight junctions as predicted in the model. Second, the tight junctions were not impermeable in leaky epithelia. Third, it was demonstrated that the walls of the LIS did not form a restriction for diffusion of small molecules. Furthermore, with respect to the CPE, the model was not easily applicable to secretory epithelia in which there are no compartments equivalent to the LIS.

C. Modifications to the Standing Gradient Model

The standing gradient model was modified many times based on results obtained from absorptive epithelia. Boulpaep and co-workers (275) noted the inadequacies of the standing gradient hypothesis, so they offered two alterna-

tive, but not mutually exclusive, models. The continuous model dealt with the problem of “isotonic transport” by including significant paracellular component of the transport, a peritubular fluid of similar composition as the LIS,

and slight hyperosmolarity as the fluid emerged from the LIS (but not from the basal membrane). The model depended on Na^+/K^+ -ATPase in the lateral membranes and suggested that the reduction in tonicity towards isosmolar-



ity occurred across the capillary wall instead of inside the LIS or after passing the basement membrane (FIGURE 5C). Due to the high cell membrane water permeability, the model predicted that even a small difference in osmolarity of 2–3 mosM was sufficient to explain the observed isosmotic reabsorption in proximal tubules. This model was subsequently expanded into the five-compartment version, where electrical driving forces and individual ionic fluxes were taken into account. An intrinsic problem was that experimental preparations of the isolated leaky epithelia with no underlying connective tissue or capillary bed were still capable of apparent isosmotic transport. The local osmotic differences in the connective tissue depending on the position relative to the LIS were not demonstrated directly and would be difficult to sustain over time. Once again, these models were only applicable to reabsorptive epithelia.

The basolateral recycling model was proposed by Ussing, Larsen, and co-workers to explain the problem in the standing gradient model of decreasing fluid osmolarity along the LIS. The hyperosmolar absorbate was still first normalized at the mouth of the LIS where most of the water entered the LIS from the cell (173). Furthermore, the decrease in fluid osmolarity before extrusion from LIS was aided by recycling Na^+ and water across the basolateral membrane. The Na^+/K^+ -ATPase was distributed in agreement with evidence from most epithelia, i.e., uniformly on the basal and lateral surfaces. However, the model postulated that the Na^+/K^+ -ATPase must remain quiescent in the basal facing membrane where Na^+ was actually imported (in cotransport with Cl^- and probably K^+) for a new round of extrusion into LIS (FIGURE 5D). In leaky epithelia, the requirement for Na^+ recycling was greatly decreased for the fluid from the LIS to reach isosmolarity.

In the recycling model, equal amounts of water entered the cells from the luminal and basal membranes. Both these components were extruded from the cell into the LIS. To explain net water absorption, a significant amount of the water transport occurred through the tight junctions. It was not clear from the model why the Na^+/K^+ -ATPase in the basal membrane would remain quiescent compared with the identical molecules facing the LIS. The model was often applied to the renal proximal tubule; however, there was no molecular or experimental evidence for basolateral NaCl import in these cells. The model also required a lumen-positive transepithelial potential difference to drive Na^+ into LIS via the tight junctions, and this potential difference was not present in the first half of the proximal tubules. Furthermore, none of the three presented modifications to the standing gradient model was easily transposed to secretory epithelia.

D. Osmotically Driven Water Transport Model

Spring (304), like Boulpaep, proposed that even a small osmotic difference across the epithelium created by active transcellular transport of Na^+ would be sufficient to explain the observed water movement. Spring based the osmotic model on experimental evidence from proximal tubules and gall bladder with a reported hyperosmolarity of ~2–15 mosM (22, 242). These values were close to those reported from renal proximal tubules, small intestine, and indeed the CPE (107, 113, 282, 358). A notable argument in Spring's model was that the area of the luminal membrane must be $\sim 10^4$ times greater than the surface area of tight junctions (303). This was even before correcting for surface area extension by microvilli present in virtually all

FIGURE 5. Models for isotonic transport across epithelia. *A:* the three-compartment model was the founding model of isotonic transport. The luminal barrier has a high solute reflection, so all solute and water enter other structures with a selective solute permeability (here exemplified by H_2O and Na^+). From here, solute is actively pumped into the middle compartment and water follows to maintain isosmolarity. This leads to the generation of hydrostatic pressure in the middle compartment because of the isotonicity and the low solute reflection of the basal barrier. Thus the solute and fluid are transported to the basal compartment (blood side). *B:* in the standing gradient model, the middle compartment was identified as the lateral intercellular spaces (LIS). Furthermore, the concept of a solute gradient along the LIS from the blind end of the basement membrane was introduced. Na^+ is mainly injected near the blind end of LIS, whereas water transport occurs mainly into the open end of the LIS. It is still an increase in hydrostatic pressure that drives fluid out of the LIS into the blood side. *C:* the continuous model operates with an even distribution of Na^+ and water transport along the LIS. Here, the generation of a slightly hyperosmolar solution to drive water transport from the cell to the LIS. The interstitial tissue beneath the LIS has the same higher osmolarity in contrast to the osmolarity of the interstitium beneath the basal plasma membrane. Also, a paracellular contribution to solute and water was introduced. Again, hydrostatic pressure forces fluid from LIS to the blood side. *D:* the recycling model is similar to the continuous model in many aspects, but depends on recycling of a substantial amount of the water and sodium injected to the LIS across the basal plasma membrane. The majority of the net transport occurs through the tight junctions, and basal Na^+/K^+ -ATPase must remain quiescent. *E:* the osmotic model differs from the continuous model by the lack of significant paracellular water transport, and the paracellular solute transport is mainly a necessity to maintain the transepithelial voltage difference low. The model is not dependent on the variation in interstitial osmolarity or uneven distribution of transporters on the entire basolateral surface and may apply to both absorptive and secretory epithelia. The transcellular solute transport creates a slight hyperosmolarity in the LIS as well as on the basal side of the epithelium and creates an even driving force for water along the entire basolateral surface. *F:* the molecular water pump model, as opposed to the above models of absorptive epithelia, was based on studies of the secretory choroid plexus. Here, the transport of water is coupled to solute transport directly by the same transport protein, in this case the K^+/Cl^- cotransporter. The transport is driven by the outward K^+ gradient created by the Na^+/K^+ -ATPase. In addition to explaining isosmotic transport, this model suggests a mechanism even for “uphill” water transport, as 500 water molecules are transported with one of each ion. The model does not deal with the basolateral transport processes.

leaky epithelia. Thus the tight junctions were required to have at least 10^4 the water permeability of the transcellular route to account for 50% of the net water transport across the epithelium. This was several orders of magnitude larger than the observed water permeabilities.

In contrast to the previous models, the $\text{Na}^+\text{-K}^+\text{-ATPase}$ was uniformly distributed along the basolateral membrane in the osmotic model and solute was transported into both the LIS and towards the basement membrane from the entire basal cell membrane (FIGURE 5E). Thus the transported fluid had identical composition whether it arose from LIS or from the basal infoldings. In the model, selective cation or anion permeabilities ascribed to tight junctions allowed either the selective absorption of ions by the paracellular route, or back-leak of ions to the bath and thereby preserved the relatively low transepithelial potential difference that could otherwise hinder cellular uptake of solute. Spring's osmotic model, in contrast to the previous models, was independent of the architecture of the cell surfaces such as the LIS and basolateral infoldings and was therefore applicable to both absorptive and secretory epithelia.

E. Water and Ion Cotransport

Zeuthen and co-workers (193, 362) recognized that a poor relationship between AQP expression and water transport existed in some epithelia (FIGURE 5F). Furthermore, in many epithelia they saw little evidence for osmotic water transport driven by a stepwise change in osmolarity from lumen to cell and from cell to the interstitium. Based on initial studies of the choroid plexus, Zeuthen and colleagues proposed an entirely different model for isotonic and even uphill water movement, i.e., water transport, which takes places against an osmotic gradient. They proposed that ion cotransporters moved significant amounts of water into or out of cells, a so-called molecular water pump or secondary active water transport (360, 361). They suggested that the coupled ion and water cotransport was the only theoretically plausible mechanism for the uphill movement of water, which had previously been reported in studies of gall bladder, small intestine, proximal tubules, and choroid plexus. The central dogma of uphill water transport was denoted by Spring as "strength of transport," and in all cases it is only observed when there was an intact interstitial layer beneath the epithelium. Indeed, many transport physiologists believe that uphill transport is a methodological artifact caused by the preservation of connective tissue beneath the epithelium (303).

Early observations in favor of water pumps came from studies of cell volume changes in *Necturus* CPE in response to luminal hyperosmolarity (and assessed by microelectrode measurements of intracellular ion concentrations). Volume changes were shown to depend on whether mannitol, NaCl, or KCl was used to increase the osmotic load. Increasing

luminal osmolarity by 50 mosM using mannitol or NaCl caused rapid shrinkage of CP cells as expected, as water was moved from cells to the bath (360, 361). However, a robust cell swelling was induced when KCl was used to increase osmolarity. This swelling was blocked by the cotransporter inhibitor bumetanide, suggesting that swelling resulted from water influx mediated by inward KCl and H_2O cotransport (360, 361). Theoretically the mechanism requires that there is a relatively high intracellular hyperosmolarity, to prevent water leaving the cells via aquaporins driven by osmotic differences. Estimates of the intracellular osmolarity in rat choroid plexus, based on the measured Na^+ and K^+ concentrations (TABLE 2), however, do not support the existence of this high intracellular osmolarity.

The central dogma of uphill water transport was described as "strength of transport" by Spring, and in all cases observed in preparations with intact interstitial layer beneath the epithelium. The interstitial connecting tissue would be predicted to build up a hyperosmolarity similar to the bath over time because of predominant solute transport into and across the epithelium and perhaps an initial loss of water to the bath. Uphill water transport has to our knowledge never been demonstrated in denuded epithelia. However, further evidence in support for the molecular coupling of solute and water cotransport has come from the recently resolved crystal structures and subsequent transport simulations of human $\text{Na}^+\text{-glucose}$ transporter SGLT-1 and *Vibrio* SGLT (43, 281). The solute-binding pocket of the SGLT is predicted to contain 70–100 H_2O molecules trapped with the solutes in the occluded state. However, as the concentration of water in a solution is ~ 56 M, the cotransporters would be required to move more than 187 water molecules per solute, to explain hypotonic or "uphill" water transport. It will be interesting to learn how many water molecules are contained in the ion binding pocket of the KCC cotransporters studied by Zeuthen and co-workers. Thus the subject of water cotransport for now remains controversial.

F. Tight Junction-Based Models

A significant contribution from a paracellular pathway for water formed a key component of several of the aforementioned models, i.e., the continuous model, the five-compartment model, and the basolateral recycling model. Thus as much as 50% of the total transepithelial water transport was ascribed to paracellular pathways in mathematical models of proximal tubule transport (336, 344). Three mechanistic models have been proposed to explain how transport may occur via the paracellular route.

In the mechanodiffusion model (FIGURE 6A), Hill and Shachar-Hill (118) argued for a central role for tight junctions in net solute and water transport in epithelia that did

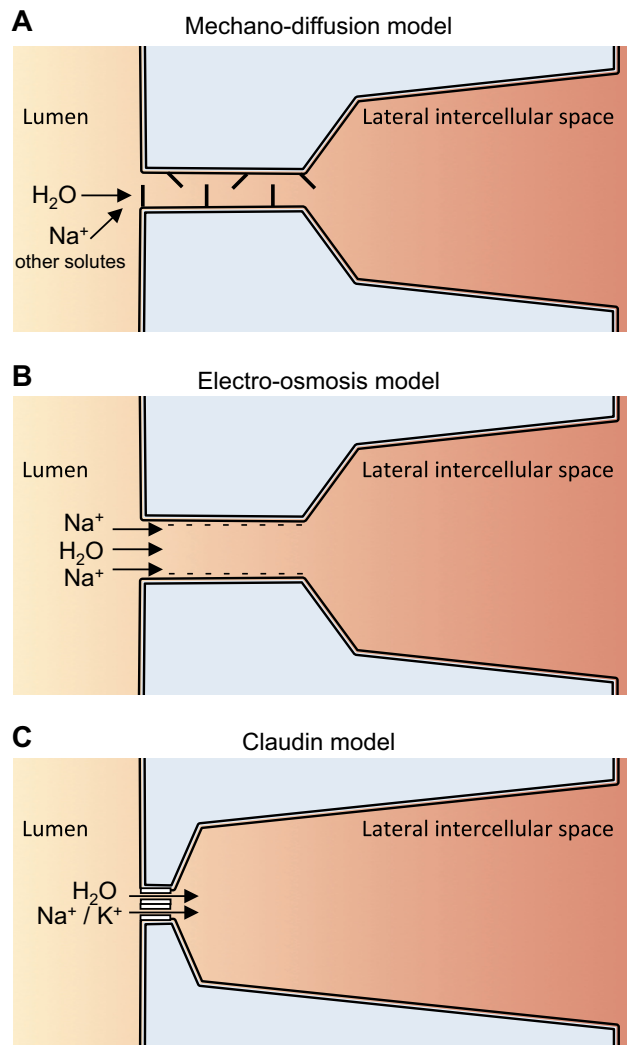


FIGURE 6. Paracellular pathways for water and solutes. **A:** the mechano-diffusion model explains paracellular transport of solutes and water by sequential opening and closures of tight junctional strands. When a tight junction strand opens, the fluid outside and inside the given tight junction pocket equilibrates. After closure and opening to the next intrajunctional pocket, the full contents of the first pocket equilibrate across the newly opened strand, etc. This way, chemical and to some extent electrical gradients will be diminished over time. It is worth noting that the mechano-diffusion model cannot explain isotonic transport or size/charge exclusion. **B:** in the electro-osmosis model, water is dragged along with positive ions that are attracted by the negative surface charge along the tight junction. Na^+ is attracted into the tight junction because of the net negatively charged surface. This movement of a major solute will drag bulk fluid in the same direction into the gap between neighboring cells is sufficiently wide to allow bulk fluid movement. **C:** certain claudins are permeable to anions or cations and mediate significant contribution to ion transport in many epithelia. Claudin-2 is expressed in the choroid plexus permeates and may permit paracellular transport of both cations and water. The transport of solutes and water molecules is not coupled, although the movement appears to occur in single file. The net transport will follow the electrochemical gradients.

not involve osmotic flow through the junctions. As in most of the above models, the movement of solute results in the development of an osmotic gradient; however, in the

mechano-diffusion model, it was claimed that paracellular transport could be hypotonic leaving the final absorbate isotonic. The mechanism of fluid transport through tight junctions involved active opening and closure of a series of compartments formed between cell walls and the strands of tight junction proteins. The bulk water was followed by modest amounts of ions that because of size exclusion lacked macromolecules. It was not explained how the selective permeability of various tight junctions could occur by this scheme. The mechanodiffusion model predicted a hypotonic LIS, which contradicted the evidence of hyperosmotic interspace and preceded the emerging field of claudin research which gave rise to a molecular basis for paracellular transport (see below).

In the electrodiffusion model (**FIGURE 6B**), Fischbarg (96) basically agreed with Hill's model with a few prominent differences. The exact mechanism by which fluid was transported through tight junctions by electrodiffusion was required to fully compensate for the relatively low surface area of the junctions compared with the apical membrane. In the electro-diffusion model, net negative charge in tight junction "channel" structure and a lumen-negative transepithelial potential difference drove paracellular Na^+ movement into the negatively charged intercellular slit of the tight junction towards the other side of epithelium. This movement dragged bulk water along into the intercellular slit as described for electro-diffusive water pumps and would have had the potential of compensating for the small surface area of the tight junctions. However, the idea was not easily reconciled with results from the proximal tubule or the choroid plexus. In the choroid plexus, the lumen-positive transepithelial potential difference would have repelled Na^+ , which would therefore have dragged water from CSF to the interstitium. In proximal tubules, the lumen-negative potential in the first half segment would have resulted in Na^+ and water movement into the renal tubule lumen.

In 1999, Lifton and co-workers (293) discovered that a specific tight junction protein, claudin-16 (then paracellin-1), could mediate Mg^{2+} transport between cells. Subsequent work has found that additional claudins, such as claudin-1, -3, and -5, are present in electrically very tight junctions, whereas others such as claudin-2, -10b, and -15 form cation-selective pores and claudin-10a and -17 are anion selective (169). Claudin-2 was first discovered by Furuse et al. (99) and is expressed in leaky epithelia, such as proximal tubules and the choroid plexus. The functional significance of claudin-2 was further elucidated in *Cldn2* knockout mice, in which proximal tubular paracellular resistance is greatly increased, and the transepithelial transport of Na^+ , Cl^- , and water is decreased (222). The role of claudin-2 in water transport was further elaborated by the demonstration that overexpression of claudin-2 induced a fivefold increase in the water permeability of the principal

cell MDCK-c7 culture model of tight epithelia (270). Imposing either osmotic gradients or Na^+ gradients enhanced water transport, and the results indicated a single-file transport of molecules through the junctions (270). A model of claudin-mediated ion and water transport as it would appear in the choroid plexus is shown in **FIGURE 6C**.

Although these data by Rosenthal and co-workers strongly suggested that claudin-2 induced water permeability to the epithelium, a fivefold increase in junctional permeability in a very water tight epithelium may not have been sufficient to contribute significantly in a leaky epithelium such as the proximal tubules and choroid plexus. The increase in permeability by claudin-2 expression was relatively small compared with the required 10^4 -fold higher tight junction permeability to compensate for the small surface area compared with the luminal membrane. Spring and co-workers found evidence against significant water flux across the tight junction into the LIS in a model of leaky MDCK cells (MDCK-II) and favored the idea that the vast majority of water transport was transcellular. In the choroid plexus it cannot be excluded that the K^+ secretion and a component of the water movement might be mediated by paracellular transport through claudin-2, as these molecules share the outward transport direction here.

There are a few other unresolved questions regarding transport in leaky epithelia that weaken any of the current models of water and solute transport. The problem related to the current discussion is how to explain the observed transepithelial movement of medium-sized molecules, such as glucose and mannitol. With the modern insight into tight junction geometry and molecular composition, there is little room for significant transport of the medium-sized molecules or the phenomenon “solvent drag” across the tight junctions. One proposed morphological possibility for such transport is the cellular junctions where three epithelial cells meet and where the tight junction proteins turn away from the surface to follow the lateral cell corners to form a funnel-like tube. This pore may be large enough to allow the permeation of some molecules, but is probably sealed by the trijunctional protein tricellulin (198). Another explanation to the reported transport of larger molecules is the edge effects occurring when mounting tissue in Ussing chambers or other artificial damages to the epithelial monolayers. Hopefully, future studies will address all of these questions.

G. Comparison of the Choroid Plexus to Other Secretory Epithelia

While the above models adequately explain isosmotic absorption of fluid and electrolytes, most of these cannot easily be applied to secretory epithelia. In most secretory epithelia, just as in absorptive epithelia (**FIGURE 7A**), the Na^+ - K^+ -ATPase is the primary molecular machine driving

epithelial transport, and in most secretory epithelia the Na^+ - K^+ -ATPase is located in the basolateral membrane. Thus, in the majority of secretory epithelia, secretion cannot occur by a reversal or “mirror image” of absorption. **FIGURE 7B** is a simplified representation of the model for secretion by a typical glandular epithelium. In this model, it is the transcellular transport of Cl^- , and not Na^+ , which is central in the secretory process. Thus Cl^- enters the epithelium via the NKCC1 in the basolateral membrane. Influx of Cl^- takes place against the electrochemical gradient by secondary active transport driven by the Na^+ gradient. Cl^- then exits the cell through Cl^- channels in the apical membrane. In contrast, the cell extrudes Na^+ by the basolateral Na^+ - K^+ -ATPase in such tissues, and Na^+ probably translocates to the lumen via the tight junctions driven by the lumen-negative voltage created by the transepithelial Cl^- transport. This model forms the basis for discussion of transport in most secretory epithelia, although it has been subject to modification in studies of specific epithelia.

The sweat glands, salivary glands, and exocrine pancreas are among the best-studied secretory epithelia. A two-stage process of secretion is observed in both sweat and salivary glands; the coil cells or acinar cells, respectively, secrete an almost isotonic fluid driven by Cl^- movement as described above. These primary secretions are then modified by the ductal cells under hormonal and nervous control to form a more or less hypotonic product with lower Na^+ and Cl^- contents, but higher K^+ and HCO_3^- concentrations (190, 191, 316). In contrast, in the exocrine pancreas, the acinar cells secrete only a little Na^+ , Cl^- , and water along with the digestive enzymes, and it is the ductal cells which secrete the majority of fluid together with Na^+ and HCO_3^- as the predominant ions (34). In the cat pancreas, there is a strikingly close correlation of almost unity between the blood-side perfusate and the pancreatic juice osmolarities over a wide range of osmolarities, but the ionic contents are always slightly higher in the fluid of the main duct (38).

AQP1 and AQP5 are expressed in the pancreatic duct cells, with AQP1 in both apical and basolateral expression and AQP5 exclusively in the apical membrane (33). These aquaporins are thought to participate in the potent water secretion by the ducts, but the hypothesis remains to be tested in experiments on AQP1 and AQP5 knockout mice and/or by inhibition of aquaporins using mercuric compounds. In the salivary glands, AQP5 is most prominently expressed in the apical membrane of the acinar cells, where it greatly increases the water permeability (109, 110), and in AQP5 knockouts salivary secretion is greatly impaired (192). AQP3 is expressed in the basolateral plasma membrane of human salivary gland acinar cells (110), but there is no evidence of aquaporin expression in the basolateral membranes of salivary gland acinar cells from other species. Little is known about aquaporin expression in sweat gland coil cells, although AQP5 knockout mice show little or no

defect in sweat secretion (226, 297). These data indicate that in some exocrine gland cells, the permeability of the cell membranes may be sufficiently high to accommodate

isotonic secretion, or that perhaps the paracellular pathway can mediate the water transport along with the well-established paracellular Na^+ secretion. With the exception of claudin-2 in pancreatic ducts and claudin-16 in salivary glands, however, no ion or water permeating claudins have been detected in exocrine glands (168, 187, 197, 241, 259). Overall, it seems that the pathways for the main ions in potent secretory epithelia are well described, except for the paracellular Na^+ pathway in the acini. Little is known, in contrast, about the relative contribution of transcellular and paracellular water transport in these tissues despite progress in the molecular mapping of potential water transporting molecules for both transcellular and paracellular transport.

By comparison to these typical secretory epithelia, ion transport in the choroid plexus is very different. The highly atypical localization of the Na^+/K^+ -ATPase in the apical membrane means that ion secretion in the choroid plexus may take place by a process akin to the reversal of the absorption in other epithelia. **FIGURE 7C** is an early model of ion transport by the choroid plexus. It shows that because of the apical localization of Na^+/K^+ -ATPase, transcellular transport of Na^+ is central to the overall transport process, i.e., it resembles the inversely directed transport in renal proximal tubules (**FIGURE 7A**). Thus the choroid plexus can

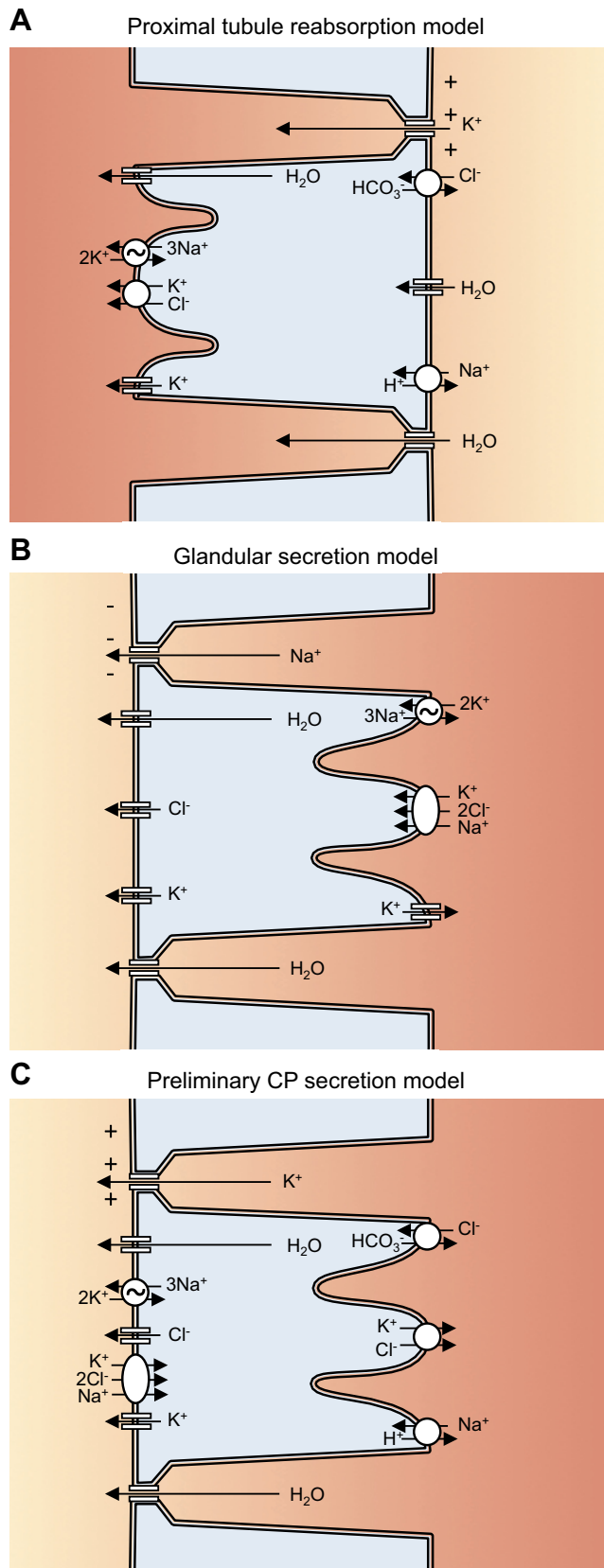


FIGURE 7. Comparison of models for typical absorptive, secretory epithelia, and the choroid plexus. **A:** reabsorption by the renal proximal tubule involves basolateral extrusion of Na^+ by the Na^+/K^+ -ATPase. This creates an inward electrochemical gradient for Na^+ , which is exploited by apical cotransporters such as Na^+/H^+ exchange to import Na^+ . Cl^- exchanges with HCO_3^- across the apical membrane and exits the cell via basolateral cotransport with K^+ . Thus K^+ recycles across the basolateral membrane. Water molecules are transported across the cells mainly through transcellular pathways, as the membranes have high intrinsic water permeabilities. **B:** the classical model for secretion from sweat or salivary glands. The Na^+/K^+ -ATPase develops an inward gradient for Na^+ and sustains inside negative charge. The NKCC imports Na^+ , K^+ , and Cl^- into the cell. Thus Na^+ is recycled across the basolateral membrane along with most K^+ exiting via basolateral K^+ channels. Cl^- is extruded across the apical membrane through Cl^- channels generating a slight lumen-negative potential difference compared with the basolateral side of the epithelium. This drives paracellular Na^+ secretion and transcellular K^+ secretion. Water takes transcellular or paracellular routes driven by a discrete luminal hyperosmolarity. **C:** a preliminary model for secretion by the choroid plexus. Before the molecular identity of the major transporters was known, the model for CSF secretion by choroid plexus was mainly based on transport inhibitor studies (for details, see **FIGURE 10**). The Na^+/K^+ -ATPase directly extruded Na^+ into the CSF and created lumen positive charge. Cl^- and to a lesser extent HCO_3^- followed through conductive pathways down the electrochemical gradient. The source for Na^+ and Cl^- for secretion was the parallel action of Na^+/H^+ exchange and $\text{Cl}^-/\text{HCO}_3^-$ exchange across the basolateral plasma membrane. Water was moved across the epithelium driven by slight luminal hyperosmolarity. HCO_3^- was generated from hydration of CO_2 catalyzed by intracellular carbonic anhydrase.

be said to have more in common with the absorptive epithelia than most if not all secretory epithelia.

The tight junctions of the choroid plexus have traditionally been described as leaky similar to those in the renal proximal tubules. However, it may be more accurate to claim that they are intermediate with respect to the electrical resistance (see below). The transepithelial potential difference across the choroid plexus is small as is the case in leaky epithelia. This, however, is not necessarily a good indicator of leakiness, and it may just reflect the careful balance between anion and cation transport in this epithelium.

The expression of tight junction proteins determines the degree to which paracellular transport of simple solutes can contribute to CSF secretion or absorption, i.e., some claudin proteins form selective pores within the tight junctions. Many claudins are expressed in the choroid plexus at the mRNA and/or protein levels, including claudin 1, 2, 3, 5, 9, 11, 12, 19, and 22 (99, 167, 313, 347). Of these, however, only claudin-2 is a pore-forming claudin characterized as both monovalent cation- and water-selective channel (169). No other pore-forming claudins, i.e., claudin 10, 15, and 17, are found in the choroid plexus. Claudin-2 expression per se does not always render an epithelium highly leaky, but it is necessary for paracellular permeability. The absence of other pore-forming claudins and factors such as the very elaborate basolateral interdigitations—the basal labyrinth may cause the intermediate resistance of the choroid plexus epithelium. However, the recorded resistance is far from the values of up to 2,000 Ω reported in truly tight epithelia.

The water permeability of the CPE tight junctions is a separate matter. The expression of specific claudins is currently believed to govern the particular permeability of epithelia, and the CPE just as the renal proximal tubules (PT) expresses the water selective claudin-2. The contribution of claudin-2 to water transport in the CPE has not been determined, but in the PT claudin-2 deficiency leads to the exact same phenotype with regards to water transport capability as in AQP1 knockout. Furthermore, there is no information available on the structure and development of the ventricular system in the claudin-2-deficient mice. Thus the relative contribution of paracellular and transcellular routes for water in CSF secretion is unknown. Given the available data, however, we suggest that the paracellular pathway makes only a minor contribution to ion and water transport in the direction from blood to CSF. A modest paracellular cation flux in the opposite direction may also serve to maintain a low transepithelial potential difference, and thereby indirectly support the transcellular electrogenic transport.

In conclusion, the transepithelial transport of ions and water appears to be essential for the overall process of CSF secretion. The following sections in this review describe how a model of

ion transport in CSF secretion by the choroid plexus has been developed and elaborated over the last 50 years.

V. EARLY INVESTIGATIONS OF THE MECHANISM OF CHOROID PLEXUS SECRETION

In the second half of the 20th century, from about 1960 to about 1985, ground-breaking experimental work aimed at determining the mechanisms of ion transport in choroid plexus function was performed using a wide variety of experimental methods. Here, we briefly describe the most prominent methods, and then provide a brief overview of the resulting data.

The method of sampling the newly formed fluid (nascent CSF) from oil-covered ventricle choroid plexus was introduced by Ames and colleagues (64) (**FIGURE 8A**). This method was of key importance, because it meant that the composition of the newly formed ventricular CSF could be compared with that of the mixed fluid from the cisterna magna and, perhaps more importantly, with blood plasma. Pappenheimer et al. (237) developed the method of ventriculo-cisternal perfusion (**FIGURE 8B**), whereby changes in CSF composition and volume were determined by infusing fluid of a known composition into the ventricles at a controlled rate, and then sampling the fluid further downstream. **FIGURE 8C** shows the approach taken by Welch (339), who sampled the blood from the arterial and venous side of the choroid plexus to determine what was extracted by the passage. These values could be compared with the bath solution surrounding CPE. This method was extended significantly by Johanson et al. (142), who employed radioactive tracers to precisely determine total water space, red blood cell volume, interstitial space, and cell water space.

Today, most work on the choroid plexus involves the use of rats and more particularly mice, where transgenic approaches have been taken. However, for technical reasons, many of the experiments performed using the *in vivo* methods have employed larger mammals such as goat, cat, dog, and rabbit, i.e., these methods are too elaborate for application to smaller species. Important contributions to our understanding of choroid plexus function were also made in nonmammalian species. In shark and some amphibian species, for example, the choroid plexus has a sheetlike morphology with epithelium on only one side. Thus the tissue can be mounted in Ussing chambers allowing transepithelial fluxes to be measured, something which is not possible with mammalian tissues. These methods were exploited particularly successfully by Wright and colleagues, who published a series of key papers on the bullfrog choroid plexus in the 1970s and early 1980s (277, 278, 350, 351, 364, 365). Wright and Zeuthen also refined the use of microelectrode impalement of amphibian CPE cells with microelectrodes for electrophysiological recordings, ion concentration, and volume measurements (277, 363–365) (**FIGURE 8D**).

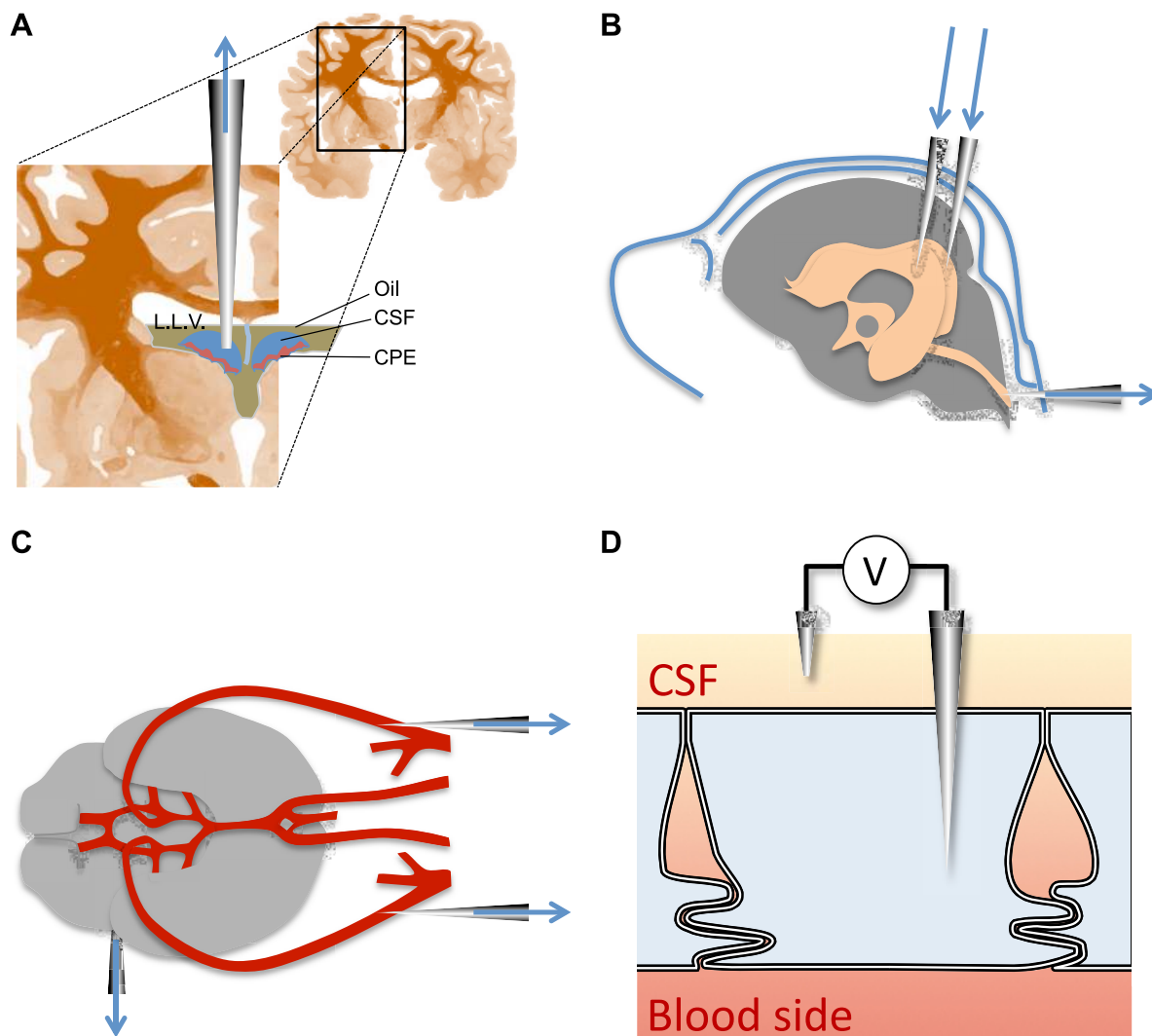


FIGURE 8. Classical methods in the study of choroid plexus function. *A:* nascent CSF sampling was accomplished in vivo by installing an oil layer in the ventricle lumen surrounding the choroid plexus. The newly formed cerebrospinal fluid was directly collected with a pipette for analysis of ionic composition. *B:* in ventriculocisternal perfusion, artificial cerebrospinal fluid is introduced in the lateral ventricles at low flow rate. The perfusate is collected from the cisterna magna in vivo, and the changes in ionic composition of the fluid after perfusion of the ventricular system can be determined. The alterations in the collected fluid can form the basis for the estimates of the CSF formed during the experiment. *C:* in vivo method with simultaneous sampling of arterial supply, the venous drainage, and cerebrospinal fluid. The ventricle system in addition to the larger blood vessels supplying the choroid plexus are cannulated and fluid samples extracted. These fluids are then analyzed for any change of ionic composition. Collection and analysis can be extended to include radioactive tracer ions. *D:* microelectrode analysis can be applied to record both the transepithelial potential difference and the membrane potential. Ion-sensitive microelectrodes are impaled into the epithelial cells with a reference electrode placed in the bath. Ion-sensitive microelectrodes have been used to study H_2O transport by monitoring changes in intracellular ion concentrations ex vivo.

One of the main outcomes of these early studies of choroid plexus function was the precise determination of the composition of newly synthesized CSF as it appears in the ventricles. The distribution of main ions between plasma and CSF determined in rabbit and dog are presented in **TABLE 1**. **TABLE 1** shows that although the values in plasma and CSF are similar, they are certainly not the same. Specifically, in both species, the concentrations of K^+ , HCO_3^- , and Ca^{2+} are lower in the CSF, whereas the Cl^- concentration

is greater in the CSF (61). A similar profile of ion concentrations is also found in the rat CSF (**TABLE 2**).

Another set of basic observations was that the CSF concentrations of K^+ , HCO_3^- (126, 127), and Ca^{2+} (145, 217) all remain virtually constant when plasma concentrations were experimentally varied. Together, these data were vital in establishing that CSF is secreted by the choroid plexuses and is not simply an ultrafiltrate of plasma (61, 62) as described in the

Table 1. The concentration of ions and osmolality in plasma and CSF from rabbit and dog

	Rabbit		Dog	
	Plasma	CSF	Plasma	CSF
Na ⁺ , mM	148	149	155	151
K ⁺ , mM	4.3	2.9	4.6	3.0
Mg ²⁺ , mM	2.0	1.7	1.4	2.0
Ca ²⁺ , mM	5.6	2.5	5.7	2.9
Cl ⁻ , mM	106	130	121	133
HCO ₃ ⁻ , mM	25	22	26	26
pH	7.46	7.27	7.42	7.42
Osmolality, mosmol/kgH ₂ O	298.5	305.2	299.6	305.2

Data from Davson and Segal (61).

introduction. The early studies also provided the first indication that the main ions transported from blood to ventricle by the choroid plexuses are Na⁺, Cl⁻, and HCO₃⁻. Furthermore, the movement of these ions created a small osmotic difference (ventricle positive, **TABLE 1**), which may be sufficient to drive the secretion of water. These data are summarized in the model of the CPE in **FIGURE 9**.

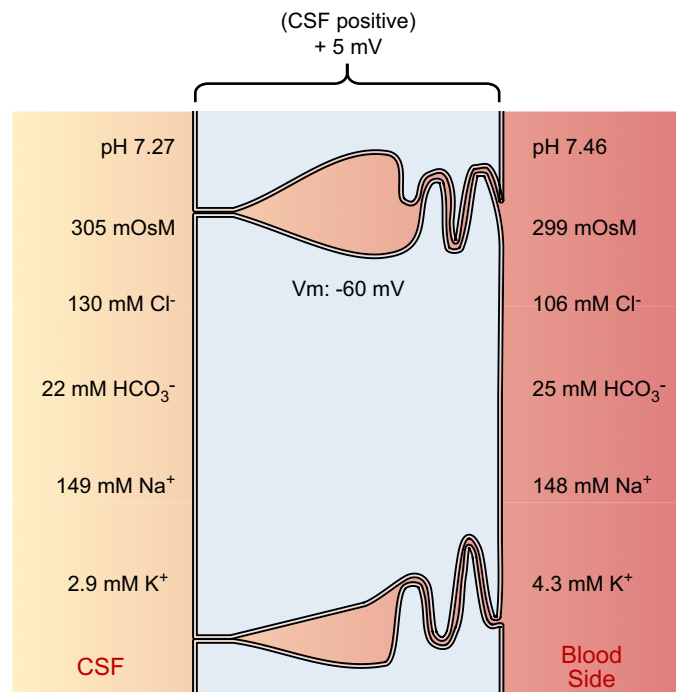
At the same time as much of this work was being performed, Wright and colleagues (278, 350) were taking advantage of the ability to mount bullfrog choroid plexus in Ussing chambers. With this method they demonstrated that Na⁺, Cl⁻, and HCO₃⁻ are actively secreted by a transcellular route across the CPE (278, 350). These observations were therefore in good agreement with the contemporary mammalian studies (see above). Zeuthen and Wright (364) also demonstrated that the epithelium mediates the net transcellular absorption of K⁺. This observation may be significant in explaining how CSF [K⁺] is maintained (see below).

The Wright group also explored the electrophysiological properties of the bullfrog choroid plexus. They measured a transepithelial resistance of ~170 Ω·cm² (261). The transepithelial resistance is important, because it gives a measure

Table 2. The concentration of ions in rat plasma, CSF, and lateral ventricle choroid plexus

	Plasma	CSF	CPE
Na ⁺ , mM	148	152	49
K ⁺ , mM	4.6	3.0	97
Cl ⁻ , mM	114	129	64
HCO ₃ ⁻ , mM	21	24	11
pH	7.44	7.34	7.05

Data from Johanson and Murphy (140).

**FIGURE 9.** Electrochemical gradients across the choroid plexus epithelium. The ionic composition of cerebrospinal fluid (CSF) and the blood side of the choroid plexus epithelium. The values are from rabbit (61). The cell has a membrane potential of approximately -60 mV and a transepithelial potential difference of 5 mV (CSF side positive).

of the leakiness of an epithelium, i.e., whether or not there is significant paracellular permeability. The resistance of a typical leaky epithelium such as the renal proximal tubule is on the order of 5–7 Ω·cm² in rabbit and dog (25, 178) and 40 Ω·cm² in amphibian *Necturus* (289). In contrast, tight epithelia in which there is no or very limited paracellular transport have resistances of up to 2,000 Ω·cm². The resistance of the bullfrog choroid plexus can therefore be said to be in the intermediate range. Thus the paracellular route may be of limited significance in the choroid plexus. Unfortunately, the electrical resistance of the intact mammalian CPE cannot be measured directly because of the morphology of the tissue. However, the recent development of methods to maintain monolayers of mammalian choroid plexus cells in primary culture has facilitated measurements of transepithelial resistance. Values obtained are in the range of 50–200 Ω·cm² (11, 150, 270, 344, 345), and therefore in good agreement with the bullfrog data.

The values for membrane potential obtained from the bullfrog, and later *Necturus*, were also in accordance with the limited amount mammalian data. In amphibians, the membrane potential ranged from -25 to -60 mV (intracellular negative and depending on experimental conditions) with an average around about -45 mV (277, 364). Similar values were obtained in studies of mammalian choroid plexus,

e.g., rabbit -64 mV (340), mouse -40 mV (269), and rat -36 mV (Brown, unpublished data). These data are important because the intracellular negative potential is important in driving anion (Cl^- and HCO_3^-) secretion by the choroid plexus. A value of -45 mV is given in the diagram in **FIGURE 9**. The transepithelial potential difference is one electrical parameter that differs between amphibian and mammalian choroid plexus, and can be an important determinant of ion movement by any paracellular route. In mammals, there is a significant body of data to suggest that the transepithelial potential difference is ~ 5 mV lumen positive, as shown in **FIGURE 9** (116, 126, 340). In the bullfrog, a value of -1 mV was recorded (278); the functional significance of this observation, however, has never been elucidated.

FIGURE 10 summarizes the results of experiments aimed at determining the identity of the transport pathways responsible for Na^+ , Cl^- , and HCO_3^- secretion by the mammalian choroid plexus. **FIGURE 10** catalogues the array of transport inhibitors applied in vivo to the choroid plexus. Many of the inhibitors, which were known to reduce ion transport in other epithelia, also negatively affected CSF secretion by the choroid plexus. First of all, the Na^+ - K^+ -ATPase inhibitor ouabain and the carbonic anhydrase inhibitor acetazolamide inhibited CSF formation by 40–100% (7, 60, 285, 350), whereas the NHE and ENaC transport blocker amiloride induced 50% reduction, but only when infused directly into the carotid arteries (60). The Na^+ - K^+ - 2Cl^- cotransport inhibitor bumetanide had no effect on CSF for-

mation from the blood side (324), and the KCC inhibitor furosemide inhibited CSF secretion when used only in doses that may be sufficient to inhibit carbonic anhydrase activity (206, 208, 263).

Ion radioactive tracer studies, Na^+ and Cl^- uptake into CPE was inhibited by bilateral application of acetazolamide, furosemide, bumetanide, amiloride, and the HCO_3^- and Cl^- transport inhibitor DIDS (143). The Cl^- uptake was most affected by a combination of DIDS and bumetanide, which almost completely blocked Cl^- entry. The inhibition of CSF secretion by DIDS occurred when the drug was applied to the basolateral side both in vivo and in vitro and CSF secretion as such was sensitive to basolateral pH and $[\text{HCO}_3^-]$ (66, 205, 278). These data suggest that CSF secretion depends on acid/base transporters in the basolateral membrane of the CPE.

The work described in this section has shown that by the mid-1980s the basic process of ion transport by the choroid plexuses had been defined. However, the lack of specificity of many of the inhibitors used in these studies meant that the precise identities of the ion transport proteins involved in CSF secretion remained unknown. From the mid-1980s onwards, all this was to change with development of molecular genetics and introduction of patch-clamp electrophysiology. These “new” disciplines contributed on two levels to our understanding of ion transport processes by the choroid plexus. First, they classified very accurately the wide diversity of ion

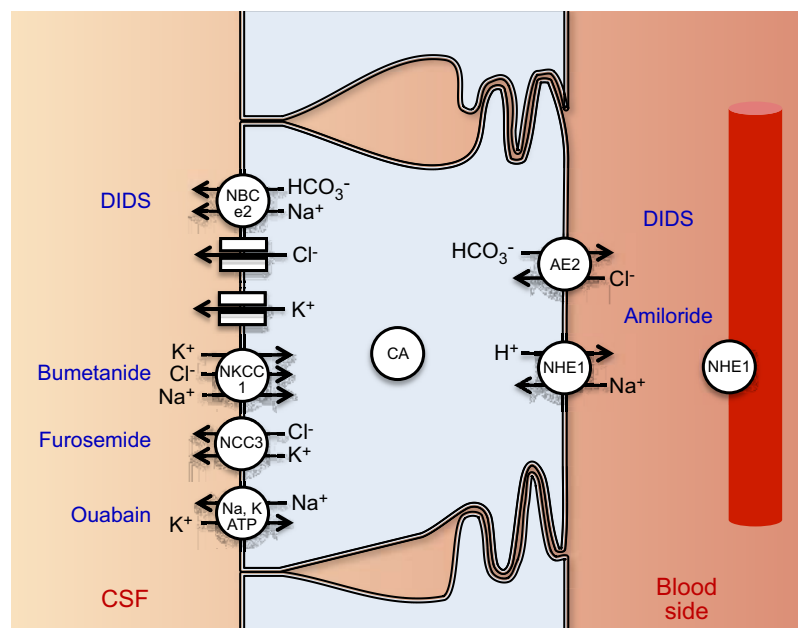


FIGURE 10. Potential sites of action for known inhibitors of cerebrospinal fluid secretion. Among the transport inhibitors applied to the luminal side of the epithelium, DIDS targets the $\text{Na}^+:\text{HCO}_3^-$ cotransport by NBCe2 and possibly Cl^- and HCO_3^- conductances. Bumetanide mainly inhibits the $\text{Na}^+:\text{K}^+:\text{2Cl}^-$ cotransporter NKCC1, whereas furosemide blocks $\text{K}^+:\text{Cl}^-$ cotransport by KCC3. Ouabain is a potent inhibitor of $\text{Na}^+:\text{K}^+:\text{ATPase}$. Applied from the basolateral side, DIDS inhibits the $\text{Cl}^-/\text{HCO}_3^-$ exchanger AE2 and amiloride blocks either the Na^+/H^+ exchanger NHE1 or Na^+ channels, such as ENaC. Amiloride may also exert an action mainly on secretion via the blood vessels of the choroid plexus. The carbonic anhydrase inhibitor acetazolamide is cell permeant and inhibits secretion regardless of the route of administration.

transport proteins, which even in the 1980s had not been fully anticipated. Second, the use of patch clamp and molecular localization methods have very clearly defined transport protein and ion channel expression in the choroid plexus (FIGURE 11). In the following sections, we provide a comprehensive survey of ion transport and ion transport protein expression in first the luminal and then the basolateral membrane of the mammalian choroid plexus.

VI. MOVEMENT OF SMALL MONOVALENT IONS ACROSS THE LUMINAL MEMBRANE

A. The $\text{Na}^+\text{-K}^+\text{-ATPase}$

$\text{Na}^+\text{-K}^+\text{-ATPases}$ hydrolyze a single ATP molecule to drive the “uphill” extrusion of three Na^+ in exchange for two K^+ . This action is necessary for creating and maintaining

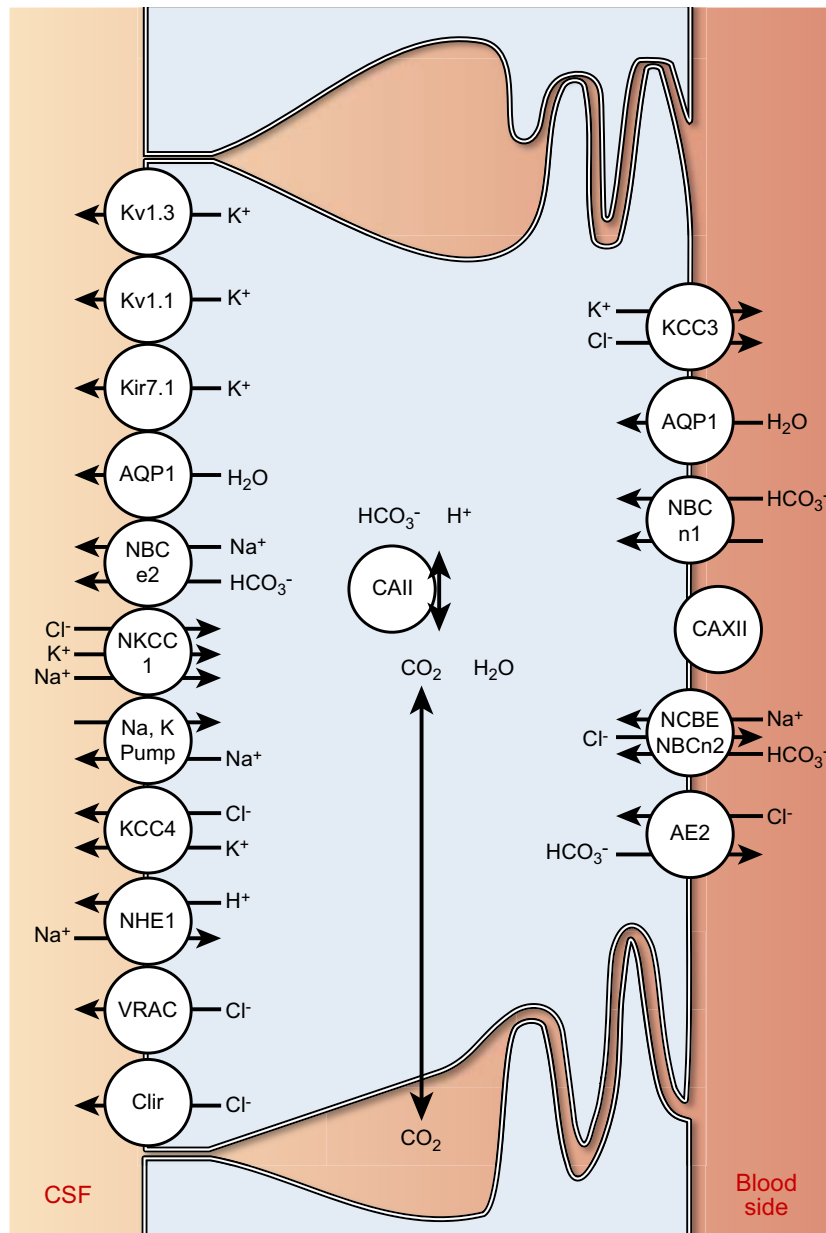


FIGURE 11. Transcellular pathways for small monovalent ions and water in the choroid plexus epithelium. The schematic representation of the choroid plexus epithelial cell shows the integral plasma membrane proteins believed to be involved in the secretion of cerebrospinal fluid. At the luminal membrane (CSF side): the potassium channels Kv1.3, Kv1.1, and Kir7.1; the water channel AQP1; the $\text{Na}^+\text{-HCO}_3^-$ cotransporter NBCe2; the $\text{Na}^+, \text{K}^+, 2\text{Cl}^-$ cotransporter NKCC1; the $\text{Na}^+\text{-K}^+\text{-ATPase}$; the $\text{K}^+\text{-Cl}^-$ cotransporter KCC4; the Na^+/H^+ exchanger NHE1; and the Cl^- conductances VRAC and Clir. At the basolateral membrane: the $\text{K}^+\text{-Cl}^-$ cotransporter KCC3, the water channel AQP1, the $\text{Na}^+\text{-HCO}_3^-$ cotransporters Nbc and NBCn1, and the $\text{Cl}^-/\text{HCO}_3^-$ exchanger AE2. Interconversion between $\text{CO}_2 + \text{H}_2\text{O}$ and $\text{H}^+ + \text{HCO}_3^-$ is catalyzed by extracellular and intracellular carbonic anhydrases (CAXII and CAII, respectively).

asymmetrical distributions of many solutes across the cell membrane. The inward directed Na^+ gradient created by the Na^+ - K^+ -ATPase drives secondary active transport of other ions and solutes necessary for specific cellular functions such as secretion. In most secretory epithelia, the Na^+ - K^+ -ATPase is essential for the secondary active transport of Cl^- which is a fundamental step in the secretory process. In these epithelia and elsewhere, the Na^+ - K^+ -ATPase is nearly always localized to the basolateral membrane protein in epithelia. In contrast, in the choroid plexus, the Na^+ - K^+ -ATPase is now known to be located in the luminal membrane (FIGURE 12A). Thus ventricular application of the Na^+ - K^+ -ATPase inhibitor ouabain abolishes the net transepithelial Na^+ flux and the CSF secretion (7). Ouabain binding and Na^+ - K^+ -ATPase immunoreactivity are demonstrated in the luminal membrane (88, 202, 253, 290, 258). The luminal localization of the Na^+ - K^+ -ATPase means that Na^+ is injected into the CSF by primary active transport, and therefore, the Na^+ - K^+ -ATPase is of fundamental importance to the process of CSF secretion. In addition to this direct role in the Na^+ extrusion, the Na^+ - K^+ -ATPase also establishes and maintains the Na^+ and K^+ gradients, which ultimately drives all the other transport proteins, which contribute to CSF secretion. Thus inhibitors of the pump, such as ouabain, are very effective at reducing CSF secretion (60, 249, 351).

Functional Na^+ - K^+ -ATPases are composed of two or three subunits. The protein complex in the CPE consists of the $\alpha 1$ -, and either $\beta 1$ - or $\beta 2$ -subunits (163, 333, 366) as well as the cAMP-sensitive accessory protein or γ -subunit, phospholemman (FXYP1) (94). The combination $\alpha 1$, $\beta 1$, FXYP1 is a very typical distribution of subunits for an epithelial cell and, hence, does not offer an explanation for the luminal localization of the Na^+ - K^+ -ATPase in the choroid plexus. The significance of the $\beta 2$ -subunits for membrane targeting in CPE remains to be established. Interestingly, phospholemman reduces the Na^+ affinity of the Na^+ - K^+ -ATPase, thereby facilitating the task of maintaining a supposedly high intracellular $[\text{Na}^+]$ (46) (TABLE 2). Sweadner and co-workers (94) suggested that phospholemman may represent a target for the PKA-activated CSF secretion by the choroid plexus. Na^+ - K^+ -ATPase expression in the choroid plexus is also regulated by α -klotho, a protein associated with longevity, which is abundantly expressed in the choroid plexus (171).

The luminal Na^+ - K^+ -ATPase transports significant amounts of K^+ from the CSF into the CPE (29, 364), and constitutes the most effective means of transporting K^+ out of the CSF. The Na^+ - K^+ -ATPases have high affinities for K^+ (K_m for K^+ : $\alpha 1\beta 1 = 0.9$ mM and $\alpha 1\beta 2 = 1.2$ mM; 47), and are therefore probably operating at maximum rate at normal $[\text{K}^+]_{\text{CSF}}$ concentrations. However, the expression of all three of $\alpha 1$, $\beta 1$, and $\beta 2$ subunits is increased in tissue isolated from rats with experi-

mentally induced hyperkalemia (163). This presumably reflects the increased need to remove CSF K^+ in these animals.

As described above, the plasma membrane anchoring protein ankyrin is predominantly expressed in the luminal domain of the CPE (5) and form high-molecular-weight complexes with the Na^+ - K^+ -ATPase (200). It remains to be established how the luminal targeting of the Na^+ - K^+ -ATPase is controlled. Nonetheless, the overwhelming evidence is that the direct extrusion of Na^+ across the luminal surface by the Na^+ - K^+ -ATPase is absolutely required for CSF formation.

B. H^+ Transporting ATPases

The mRNA encoding the nongastric H^+ - K^+ -ATPase (244) was identified in rabbit choroid plexus (181). Furthermore, omeprazole applied to the ventricular side inhibited CSF secretion in the same study. These data are potentially of great importance, as the CPE seems ideally positioned for controlling the pH of the largely $\text{CO}_2/\text{HCO}_3^-$ -buffered CSF. The H^+ - K^+ -ATPase may protect CSF pH against alkalosis that is strongly associated with seizures. The expression of another ATPase, the vacuolar H^+ -ATPase, in the luminal plasma membrane has yet not been investigated directly. However, the B1 subunit normally involved in plasma membrane H^+ extrusion is not expressed at mRNA level in the choroid plexus (Christensen, Damkier, and Praetorius, unpublished data). Clearly, there is a need for further investigations to fully describe the expression of acid extruding pumps in the CPE and their possible role in controlling the pH of the CSF.

C. Cl^- and HCO_3^- Channels

As in the majority of secretory epithelia, a substantial Cl^- efflux across the luminal membrane occurs via Cl^- channels in the choroid plexus. Anion transport occurs to limit the development of the potential difference caused by Na^+ transport across the epithelium, and Cl^- is the major anion in the CSF. The majority of Cl^- moves via the transcellular route, because DIDS, an inhibitor of many Cl^- channels and Cl^- or HCO_3^- carriers, applied to the luminal or basolateral side greatly reduces Cl^- secretion (66). Both Cl^- and HCO_3^- are secreted by luminal electrogenic processes. Whole cell patch-clamp studies have identified inward-rectifying anion conductances (Clir) in CPE cells from rat (160), mouse (159), and pig (147). The inward-rectifying anion channels are constitutively active and are thought to make a significant contribution to Cl^- efflux at the luminal membrane. Channel activity is further increased by protein kinase A (160) and inhibited by protein kinase C (148). It is possible that the activation of these channels by protein kinase A modulates the rate of CSF secretion, because cholera toxin (which increases cAMP production) has been shown to stimulate CSF production in dogs (86).

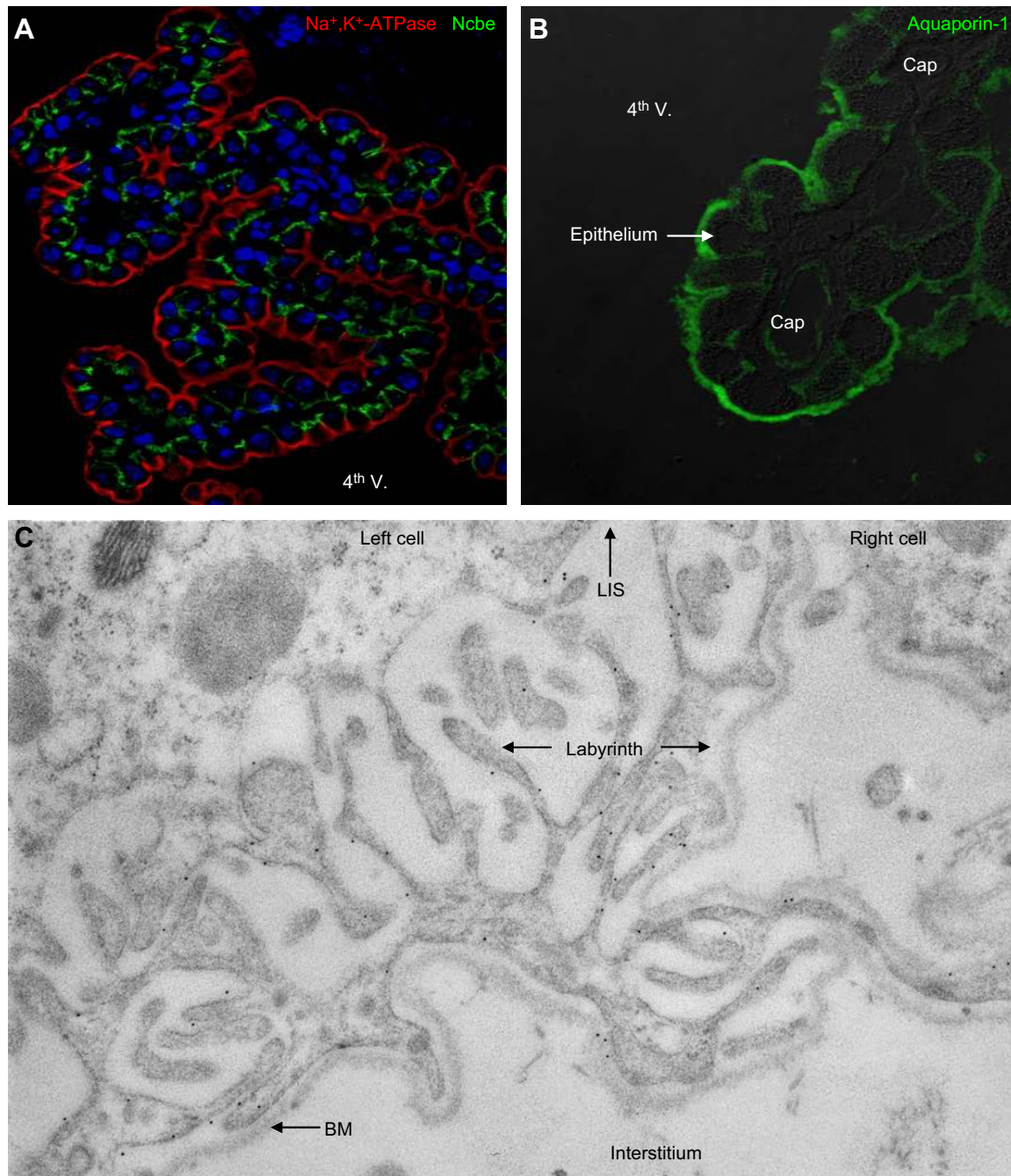


FIGURE 12. Localization of $\text{Na}^+\text{-K}^+\text{-ATPase}$, Ncbe, and aquaporin-1 in the choroid plexus. Mouse brain sections were stained with antibodies against the indicated target proteins and visualized with fluorescent secondary antibodies. *A*: the prominent luminal membrane $\text{Na}^+\text{-K}^+\text{-ATPase}$ labeling of the 4th ventricle choroid plexus epithelium is shown in red, and the strict basolateral staining for Ncbe is in green. Nuclei are labeled blue. *B*: similar labeling with antibodies against aquaporin-1 reveals that this water channel (green) is expressed in capillaries (Cap) and the basolateral membrane along with abundant luminal expression. The fluorescence image is overlaid on the corresponding differential interference contrast image. *C*: immunogold transmission electron micrograph of the basal labyrinth of rat choroid plexus. The lateral intercellular space (LIS) develops into a labyrinth of plasma membrane infoldings, and the basement membrane (BM) separates the epithelium from the interstitium. The black spots at the basolateral plasma membrane indicate Ncbe immunoreactivity.

Saito and Wright (277) proposed that HCO_3^- -conductive and cAMP-regulated ion channels form the main efflux pathway in the luminal membrane of amphibian choroid plexus. Patch-clamp studies of the mammalian choroid

plexus actually indicate that the Clr channels possess such high HCO_3^- permeability (160). This, however, may be an overestimate because the contribution of the NBCe2 (an electrogenic HCO_3^- transporter, see below) to the whole cell

current was not considered in the calculation. These channels must therefore make a much less significant contribution to HCO_3^- efflux in the mammalian choroid plexus than was previously proposed (29).

The molecular identity of the Clr channel remains to be determined. It is not, however, the cystic fibrosis transmembrane conductance regulator (CFTR), which is another epithelial anion channel regulated by cAMP. This has been determined in a number of ways: 1) the relative anion permeability for halides was different from that of CFTR (160), 2) CFTR mRNA was not expressed in the choroid plexus in the same study, and 3) the anion conductance of the choroid plexus was unaltered in a CFTR knockout model (159). The voltage dependence of the channel resembles that of ClC-2 channels, but the other properties, such as halide selectivity, differ (160). Furthermore, the Cl^- conductance is still observed in CPE cells from ClC-2 knockout mice (300).

A second class of Cl^- channels identified in choroid plexus belongs to the volume-regulated anion channel (VRAC) family of channels (159, 160). VRACs appear to be almost ubiquitously expressed, but the molecular identity of these channels has proven difficult to determine (79). These channels make only a minor contribution to the Cl^- conductance at normal cell volumes, so they are thought to make only a limited contribution to Cl^- efflux during CSF secretion (160, 212).

D. K^+ Channels

In the amphibian choroid plexus, at least 90% of K^+ pumped into the cells by the Na^+/K^+ -ATPase in the luminal membrane leaves the cells via ion channels in the same membrane (364). The K^+ channels responsible for this efflux also make a major contribution to the negative membrane potential of the CPE cells, and sustain the Na^+/K^+ -ATPase activity by providing an efflux pathway for K^+ . A similar role is also envisaged for K^+ channels expressed in the luminal membrane of the mammalian CPE cells.

K^+ channels were first identified by patch-clamp methods in the luminal membrane of choroid plexus isolated from *Necturus maculosa* (30, 44, 364). Two K^+ conductances have subsequently been identified in the mammalian choroid plexus: a time-independent, inward-rectifying conductance (Kir) and a time-dependent, outward-rectifying conductance (Kv) (166). The inward-rectifying conductance is carried by Kir7.1 channels (78), whereas Kv1.1 and Kv1.3 channels make major contributions to the Kv conductance (301). Recent data indicate that the KCNQ1/KCNE2 channels also contribute to the Kv conductance (269). All these K^+ channel proteins are exclusively expressed in the lumi-

nal membrane of rat and mouse choroid plexus: Kir7.1 (223), Kv1.1 and Kv1.3 (269, 301), and KCNQ1/KCNE2 (269).

The activity of the Kv conductance in rat choroid plexus is significantly reduced by serotonin acting at 5-HT_{2C} receptors to stimulate PKC (301). It has always been difficult to determine whether such changes in channel activity modulate choroid plexus function and CSF secretion. However, recent experiments using mice in which the KCNE2 gene is silenced (KCNE2 $-/-$) have elegantly demonstrated the importance of the luminal K^+ efflux to the overall process of ion secretion. In these animals the magnitude of the Kv conductance was increased twofold, due to an increase in the Kv1.3 and KCNQ1 components (269). These changes caused both a 9 mV hyperpolarization of V_m and an increase in the $[\text{Cl}^-]_{\text{CSF}}$ (269). They were also accompanied by the relocation of Kv1.3 and KCNQ1 channel proteins from the luminal to the basolateral membrane of CPE cells. This relocation of channels to the basolateral membrane may help explain why $[\text{K}^+]_{\text{CSF}}$ was not altered in the KCNE2 $-/-$ mice (269). It is interesting to note that mutations to the human KCNE2 gene have recently been identified which cause neonatal seizures (117). Whether changes in CSF composition have any influence on CNS activity in these individuals still remains to be determined.

E. Na^+ Channels

Leenen and co-workers have published a series of reports on the molecular and functional expression of the epithelial Na^+ channel, ENaC, in the choroid plexus (8, 9, 174, 318, 331). These data are somewhat surprising because ENaC complexes are generally restricted to tight epithelia, as e.g., renal collecting ducts, distal colon, sweat gland ducts, and airways. The mRNAs encoding ENaC α , β and γ subunits, however, have been detected by RT-PCR in the rat choroid plexus (9). Subsequent work by the same group has described immunoreactivity for all of the three subunits in the choroid plexus, and reported benzamil-sensitive $^{22}\text{Na}^+$ retention in the cells, which was suggested to be consistent with the expression of functional ENaC channels (8). The massive inward electrochemical driving force for Na^+ makes ENaC an obvious candidate as a Na^+ entry pathway at the basolateral membrane. Indeed, immunolocalization studies demonstrated basolateral membrane expression of the ENaC subunits, but expression was also reported in the luminal membrane and cytoplasm (8). The authors proposed ENaC at the basolateral membrane as an amiloride-sensitive Na^+ -loading mechanism, which they suggested may account for the relatively high intracellular $[\text{Na}^+]$ in these cells (TABLE 2).

The localization data are to some extent consistent with studies showing abundant cytoplasmic β - and γ -ENaC immunoreactivity regularly observed in renal collecting ducts.

However, α ENaC has not previously been determined in both the luminal and basolateral membranes of any epithelia. Furthermore, these studies lack appropriate controls for the immuno-gold electron microscopy and fail to describe the immunohistochemical properties of the antibodies employed, i.e., in positive control tissues, such as kidney or distal colon. In contrast to these data, we have identified only the nonpore forming γ subunit and the β subunit in the luminal membrane of rat choroid plexus (Praetorius, unpublished findings), and we have no evidence of an amiloride-sensitive component to the whole-cell conductance (Brown and Millar, unpublished data). The potential contribution of ENaC to vectorial Na^+ transport therefore remains in doubt.

F. Na^+ - K^+ - Cl^- Cotransporters

The Na^+ - K^+ - 2Cl^- cotransporter isoform 1 (NKCC1) mediates electroneutral movement of one Na^+ , one K^+ , and two Cl^- across the plasma membrane. The cotransporter is inhibited by bumetanide and to a much lesser extent by furosemide (274). In the majority of cells including other secretory epithelia, NKCC1 mediates ion influx and is situated in the basolateral membrane. In contrast, the CPE cells express NKCC1 in the luminal membrane (156, 246). Given the relatively low $[\text{K}^+]$ of CSF and the relatively high intracellular $[\text{Na}^+]$ (TABLES 1 AND 2), it has been proposed that the driving force for NKCC1 in CPE cells is close to equilibrium (156). Perhaps not surprisingly then, both inward and outward NKCC1-mediated transport has been observed in the choroid plexus. In experiments with dissociated cells, Wu et al. (353) concluded that NKCC1 in CPE cells works in the inward mode reabsorbing solute from the CSF. This was based on data showing that a high concentration of bumetanide (100 μM) caused a decrease in choroid plexus cell volume, whereas increasing $[\text{K}^+]_o$ from 3 to 25 mM produced $\sim 40\%$ increase in cell volume. CPE cells from NKCC1 knockout mice were severely shrunken, both in dissociated state in vitro as well as in situ (48) further supporting a role in ion influx. In contrast, Bairamian et al. (14) found that bumetanide applied at the luminal side of the epithelium decreased CSF secretion, suggesting the activity of NKCC1 in net ion efflux. Recently, Hughes et al. (125) were unable to demonstrate a role for NKCC1 in volume regulation studies, suggesting that at least in some conditions the transporter neither contributes to ion influx nor efflux. Such discrepancies in the data on NKCC1 activity may be due to differences in experimental conditions; alternatively, it may indicate that the activity of NKCC1 in the choroid plexus is carefully regulated. Thus we can only conclude that the significance of the robust expression of apical NKCC1 in CPE cells remains to be determined but that the cotransporter does not appear to play a direct role in CSF secretion.

G. K^+ - Cl^- Cotransporters

The K^+ - Cl^- cotransporters (KCCs) are electroneutral and facilitate outward transport of the ions driven by the huge difference in $[\text{K}^+]$ across cell membranes. Like NKCC1, the KCCs are inhibited by furosemide, but bumetanide only poorly inhibits KCC isoforms, i.e., $\sim 1,000$ times less potent than NKCC1 (274). Luminal K^+ - Cl^- cotransport was first evidenced by Zeuthen (360) as a furosemide-sensitive K^+ - and Cl^- -dependent transport in the choroid plexus (360). It now appears that the CPE expresses both KCC3a and KCC4. KCC3a is expressed in the basolateral membrane, whereas KCC4 is in the luminal membrane (152, 240). KCC4 may, therefore, contribute to the recycling of K^+ across the luminal membrane helping to sustain the Na^+ - K^+ -ATPase activity. The exact contribution of the luminal KCC4 to K^+ and Cl^- efflux, however, has yet to be evaluated using methods such as siRNA or using tissues from knockout mice.

H. Na^+ - HCO_3^- Cotransporters

The electrogenic cotransporter NBCe2 (or NBC4) mediates the transport of one Na^+ with two or three HCO_3^- depending on tissue-specific factors (280, 320). The normal electrochemical gradients for Na^+ and HCO_3^- therefore favor outward transport with the 1:3 stoichiometry, while 1:2 coupling promotes inward transport. NBCe2 was immunolocalized to the luminal membrane of rat choroid plexus (27), and mediates the export of one Na^+ for three HCO_3^- across the luminal membrane of mouse CPE (211). NBCe2 is believed to participate not only in Na^+ secretion, but also in the regulation of CSF pH by extruding HCO_3^- . In rodents, exposure to 11% CO_2 causes a significant increase in Na^+ content in CSF without a concomitant fall in CSF K^+ (225). This observation is consistent with the participation of a Na^+ -dependent acid/base transporters, such as NBCe2, in compensating for the change in CSF Pco_2 .

In a recent study, NBCe2 was ascribed a major contribution to CSF production as judged from the decreased ventricular volume and reduced intracranial pressure in NBCe2 genetrapped knockout mice (151). Furthermore, the composition of the CSF was altered in the knockouts with a significant decrease in $[\text{HCO}_3^-]$ from 24 to 20 mM, and an increase in $[\text{K}^+]$ from 3.6 to 4.7 mM (151). These differences occurred in parallel to profound changes in the localization of other transporters in the epithelium, e.g., the NBCE/NBCn2 transporter was found in the luminal and basolateral membrane expression of Na^+ - K^+ -ATPase subunits in this NBCe2 genetrapped mouse (151). Surprisingly, however, these changes in ventricular dimensions and transporter expression were not observed in CPE from a conventional NBCe2 knockout mouse model (Damkier and Praetorius, unpublished observations). Thus the full significance of NBCe2 in CSF production and to pH regulation awaits clarification.

I. Na^+/H^+ Exchangers

The almost ubiquitously expressed Na^+/H^+ exchanger NHE1 is an electroneutral acid extruder. It is driven by the inward Na^+ gradient and is inhibited by amiloride derivatives such as EIPA (233). The choroid plexus expresses NHE1 at the mRNA level (57, 149), and isolated epithelial cells display EIPA-sensitive Na^+/H^+ exchange, which is also indicative of NHE1 function (27, 57). NHE1 is normally expressed in the basolateral membrane in epithelia (233). This was also believed to be the case for the CPE, as intravenous application of amiloride was reported to inhibit the rate of CSF secretion in vivo (216). Immunohistochemical studies, however, have now demonstrated that NHE1 is located in the luminal membrane of both mouse and human choroid plexus (57, 151). Functionally, NHE1 seems to be the only plasma membrane NHE isoform in the normal choroid plexus, as NHE1 knockout mouse showed no residual Na^+ -dependent pH_i recovery from acid values in the same study. A recent transcriptome study of the choroid plexus has identified mRNA for the organellar (Na^+ or K^+)/ H^+ exchanger NHE7 (SLC9a7) in the choroid plexus (176). However, this is not a consistent observation (120, 199) so that it is far from certain that the NHE7 will have a functional role in the CPE. The luminal membrane location of the NHE1 in CPE, where it must mediate Na^+ absorption from the CSF, means that it almost certainly has a role in maintaining either intracellular or CSF pH , and that it does not directly contribute to CSF secretion.

J. Na^+ -Borate Cotransporter

NaBC1 (*slc4a11*) was shown to transport Na^+ and borate into cells but is otherwise a poorly characterized member of a gene family. The protein was localized to the ventricular membrane of choroid plexus in both rodents and humans (58). Genetic defects in NaBC1 lead to severe dysfunction of the corneal epithelium (182) and development of familial corneal dystrophy (67, 138). The significance of NaBC1 in relation to choroid plexus function is unknown.

VII. MOVEMENT OF SMALL MONOVALENT IONS ACROSS THE BASOLATERAL MEMBRANE

A. Ion Pumps and Channels

There is little evidence for the expression of either ion pumps or ion channels in the basolateral membrane of the mammalian choroid plexus. As described above, the Na^+/K^+ -ATPase is normally strictly confined to the luminal plasma membrane in the choroid plexus. Recent work, however, has suggested that $\alpha 1$ subunit Na^+/K^+ -ATPase may be expressed in both luminal and basolateral membranes of CPE from NBCe2-targeted genetrapped mice (151).

The functional significance of this observation is unknown since similar changes in protein expression were not observed in conventional NBCe2 knockouts (Damkier and Praetorius, unpublished observations). There are no other reports of ion pump expression in the basolateral membrane of the CPE.

Cl^- and HCO_3^- channels have neither been described nor hypothesized to be in the basolateral membrane of the CPE. A role for K^+ channels was suggested in amphibians (364), but to date, there are no data to support the expression of K^+ channels in the basolateral membrane of the mammalian choroid plexus. As mentioned above, the expression and function of ENaC subunits have been proposed in the choroid plexus (8, 9, 174, 318, 331), and basolateral ENaC expression would explain the amiloride sensitivity of the vectorial Na^+ transport. However, most ENaC immunoreactivity was demonstrated in the cytosol, less in the luminal membrane, and least in the basolateral membrane. Furthermore, the suggested specific regulation of choroid plexus ENaC expression by aldosterone is questionable, as the CPE does not express the 11β -hydroxysteroid dehydrogenase type 2 that inactivates cortisol. Nevertheless, the implication of ENaC in choroid plexus function remains a very interesting new development and would have an enormous impact on the understanding of Na^+ handling by the choroid plexus.

B. $\text{Na}^+/\text{HCO}_3^-$ Cotransporters

The *slc4a10* gene product was characterized as a DIDS-sensitive, electroneutral $\text{Na}^+/\text{HCO}_3^-$ cotransporter (56, 104, 238, 329), for which the inward direction of transport is determined by the Na^+ gradient. In early studies, Wang et al. (316) and Giffard et al. (97) demonstrated a dependence of HCO_3^- transport on intracellular Cl^- when heterologously expressing rodent *slc4a10* in mammalian cell lines. Furthermore, the protein was estimated to transport twice as many acid-base equivalents as Na^+ , and to mediate DIDS-sensitive net Cl^- efflux (56). Thus the transporter was called Ncbe, the Na^+ -dependent $\text{Cl}^-/\text{HCO}_3^-$ exchanger. However, compelling evidence from Parker et al. (226) working with the human *SLC4A10* gene product expressed in *Xenopus laevis* oocytes found neither a dependence on intracellular Cl^- nor any net extrusion of Cl^- . The protein was therefore renamed NBCn2 by these scientists (238). As this controversy has still not been fully resolved, we will refer to the transporter as Ncbe in rodents and NBCn2 in humans.

The Ncbe/NBCn2 protein is expressed in the basolateral membrane of the choroid plexus (252, 253), and it was therefore proposed to contribute to cellular Na^+ and HCO_3^- accumulation across the basolateral membrane (FIGURE 12, A AND C). The involvement in cellular Na^+ and HCO_3^- uptake was indirectly supported by an equivalent

reduction in both DIDS-sensitive and Na^+ -dependent HCO_3^- import into the choroid plexus cells in an Ncbe knockout mouse model (57, 137). These studies in Ncbe knockout mice indicate that the transporter is the principle route for HCO_3^- influx, with a 70% decrease in Na^+ -dependent HCO_3^- uptake in the knockouts compared with wild-type mice (137). Genetic ablation of Ncbe also caused an 80% reduction in brain ventricle size, suggesting that the rate of CSF secretion is greatly depressed in the knockout animals (137). Ncbe mediates all the inward, DIDS sensitive Na^+ -dependent HCO_3^- uptake in choroid plexus (57). Furthermore, deletion of Ncbe leads to profound rearrangement of proteins known to be critically involved in CSF secretion in the same study, e.g., the abundance of the Na^+ - K^+ -ATPase and water channel AQP1 is greatly reduced in the Ncbe knockout mouse. It is worth noting that these other changes in transport protein expression could account for the decreased ventricular volume, and the deduced reduction in CSF formation in the knockouts. Thus the apparent reduction of CSF secretion in these animals cannot be considered conclusive proof for the involvement of the Ncbe/NBCn2 transporter in CSF secretion.

NBCn1, the electroneutral Na^+ - HCO_3^- cotransporter 1, is most frequently observed in the basolateral membrane of mammalian CPE cells (252), but it is also occasionally found in the luminal membrane. The epithelial NBCn1 form is relatively DIDS insensitive, and when first identified in the rat choroid plexus much of the Na^+ -dependent HCO_3^- influx was ascribed to this transporter. This was because a large fraction of the pH recovery from acid load was mediated by DIDS-insensitive Na^+ - HCO_3^- cotransport (27). However, more recent observations indicate that NBCn1 may not play a major role in CSF secretion. First of all, the transporter is not strictly a basolateral transporter. NBCn1 was localized to the luminal membrane of the choroid plexus in certain mouse strains (57), and was even demonstrated in both membranes in human choroid plexus (253). Second, a significant fraction of the NBC activity and the CSF secretion is DIDS sensitive, and finally, the NBC activity in isolated choroid plexus cells from NBCn1 knockout mice is indistinguishable from that of wild-type littermates and do not develop any apparent CSF-related phenotype (Damkier, unpublished results). Thus NBCn1 protein is now thought to make only a minor contribution to trans-epithelial ion transport. It may, however, function to correct intracellular acidosis in the CPE.

C. $\text{Cl}^-/\text{HCO}_3^-$ Exchangers

The anion exchanger 2 (AE2) is an electroneutral antiporter of one Cl^- for one HCO_3^- . Given the prevailing ion gradients it generally mediates the uptake of Cl^- and the extrusion of HCO_3^- . The transporter is more active at alkaline pH and inhibited by DIDS (4). AE2 was first isolated from mouse choroid plexus, where it was found to be expressed

in the basolateral membrane (178). Similar expression has also been reported in choroid plexus tissue from other mammalian species (5, 253, 299).

AE2 is, at present, the only known basolateral entry mechanism for Cl^- , which is needed to sustain CSF secretion. The first indication that $\text{Cl}^-/\text{HCO}_3^-$ exchangers may be involved in CSF secretion came from experiments in which DIDS applied from the blood side inhibited Cl^- transport into the CSF (66, 97). Subsequent work suggests that a significant accumulation of Cl^- by AE2 across the basolateral membrane is possible in the choroid plexus given the inward chemical gradient for Cl^- (143). Cl^- uptake by AE2 is also supported by the ready supply of intracellular HCO_3^- accumulated by a variety of Na^+ -coupled HCO_3^- transporters (see above), and via the activity of carbonic anhydrases. Indeed, Cl^- accumulation mediated by AE2 has been observed during cell volume regulation in mouse choroid plexus cells in a HCO_3^- -dependent manner (125).

The AE2 belongs to the *slc4* gene family just like the Na^+ -dependent HCO_3^- transporters. It is also possible that membrane proteins of the *slc26* gene family could serve as anion exchangers in the CPE. To date, only mRNA encoding the *slc26a7*, *slc26a10*, and *slc26a11* members of this gene family have been detected at the mRNA level in rat and human choroid plexus (Praetorius, unpublished observations), but protein expression has not been examined. Further work is therefore required to determine whether these proteins are expressed and if they have any function in the CPE.

D. K^+ - Cl^- Cotransporters

Transport proteins that mediate K^+ efflux must be expressed in the basolateral membrane to explain the net transcellular K^+ absorption. At present, a K^+ - Cl^- cotransporter (KCC3) is the only such K^+ efflux pathway from choroid plexus cells to the blood side of the mammalian epithelium (240). There are two isoforms of KCC3: KCC3a and the truncated form KCC3b. Only the expression of KCC3a was demonstrated in mouse choroid plexus by Northern analysis. KCC3 protein was localized to the basolateral membrane of rat choroid plexus using an antibody, which did not discriminate between KCC3a and KCC3b (240). However, the authors of the study did note that the optical resolution of the methods used did not allow them to discriminate fully between the basolateral membrane and underlying vascular or connective tissue. Furthermore, the function of KCC3 in K^+ reabsorption has yet to be determined by gene knockout or knockdown methods.

E. Na^+/H^+ Exchangers

Na^+/H^+ exchange was once widely accepted to be the main basolateral Na^+ -entry mechanism in the CPE for a number

of reasons: 1) amiloride inhibited Na^+ flux into the CSF (216), 2) the secretion of CSF is dependent on pH-sensitive Na^+ uptake from the basolateral side of the epithelium (220, 221), 3) NHE1 is normally the basolateral Na^+/H^+ exchanger isoform in epithelia, and 4) mRNA encoding NHE1 was demonstrated in the choroid plexus of rat. It was therefore hypothesized that NHE1 would mediate Na^+ uptake at the basolateral membrane and also facilitate Cl^- uptake by working in parallel with AE2. To date, however, NHE1 has not been observed in the basolateral membrane of isolated CPE from wild-type animals, although it is expressed in the basolateral membrane of Ncbe/NBCn2 knockouts (57) and NBCn1 knockouts (Damkier, Aalkjaer, and Praetorius, unpublished data). In vitro, amiloride has little effect on Na^+ -dependent pH recovery in the choroid plexus in the presence of $\text{CO}_2/\text{HCO}_3^-$ (205). Thus a significant role for NHE1 at the basolateral membrane of the CPE seems very unlikely, and $\text{Na}^+/\text{HCO}_3^-$ cotransporters appear to be the main candidate route for Na^+ entry at this membrane.

VIII. TRANSCELLULAR WATER TRANSPORT

Vectorial transport of water across an epithelium, just like that of solutes, can occur by two separate pathways: 1) the transcellular route, whereby water moves in and out of the cells via water channels or the lipid bilayer itself (95); or 2) the paracellular route, by which water molecules move across the epithelium through the lateral intercellular spaces and where the major limitation for transport is the tight junctions.

In the CPE cells, the luminal membrane has high water permeability (234, 352, 361) because aquaporin-1 (AQP1), originally isolated from red blood cells (254), is abundantly expressed (228). Here, it conveys the vast majority of the luminal water permeability, as the permeability is reduced by 80% in cells from AQP1 knockout mice (234). AQP1 is also expressed in the basolateral membrane of the CPE, but at much lower levels than those in the apical membrane (228, 253) (**FIGURE 12B**). The AQP1 immunoreactivity of the basolateral membrane is similar to that of the adjacent capillary endothelium. There are, unfortunately, no measurements of the water permeability of the basolateral membrane, but it is tempting to predict that it is far exceeded by that of the luminal membrane.

Luminal membrane expression of AQP1 and the high cellular water permeability per se do not represent an absolute measure of the secretory capacity of the CPE. A driving force for water movement must be present (as mentioned above), and basolateral water entry, which remains more or less undefined, may be rate limiting. Thus, in AQP1 knockout mice, only a 20% reduction in the rate of CSF secretion is measured by ventriculocisternal perfusion, despite the

80% reduction in luminal membrane water permeability (234). This modest reduction in CSF secretion is supported by the normal appearance and dimensions of the ventricular space in AQP1 knockout mice. The discrepancy between luminal permeability and the rate of secretion has received little critical attention however; possible explanations include 1) the CPE may compensate for the decrease in (luminal) water permeability by increasing other transcellular or paracellular water pathways, or 2) the osmotic driving force for secretion may be increased. This issue remains to be clarified.

The choroid plexus may express aquaporins other than AQP1. Speake et al. (299) found immunoreactivity for AQP4 in rat choroid plexus, but the signal was largely dispersed throughout the cytoplasm. Recently, AQP7 was shown in human choroid plexus restricted to the luminal membrane (Lebeck, Damkier, and Praetorius, unpublished data). No other aquaporins have been convincingly demonstrated at the protein level in CPE. Alternative routes of H_2O transport, such as NKCC and KCC, have been suggested to contribute to transepithelial water movement. However, in the CPE, these transporters are either expressed in “the wrong membrane”, or mediate ion transport in the opposite direction to that required for transepithelial water movement. Thus the low-level expression of AQP1 in the basolateral membrane remains the best candidate to mediate water movement into the CPE from the interstitium.

IX. CURRENT MODEL FOR CSF SECRETION BY THE CHOROID PLEXUS

The bulk of ion transport from blood to the CSF occurs via the transcellular route. Thus as in other secretory epithelia, most researchers believe that transcellular transport of Na^+ and Cl^- (with HCO_3^-) generates the osmotic gradient that drives secretion of H_2O . While Na^+ and Cl^- are quantitatively by far the most important, other ions such as HCO_3^- , Ca^{2+} , and K^+ are also transported across the epithelium predominantly by the transcellular route. The transport of these ions is of considerable interest because their final concentrations within the CSF are known to be carefully regulated, and they remain relatively stable even when plasma concentrations vary (126, 127, 145, 217). Furthermore, the overall process of CSF secretion is known to have a high dependency on HCO_3^- . **FIGURE 13** represents a current model of the secretion of CSF by the CPE. This model is described in detail below.

A. Na^+ Secretion

Na^+ is quantitatively the most important ion transported by the CPE. It provides the driving force for CSF secretion, i.e., there is no secretion without Na^+ extrusion across the

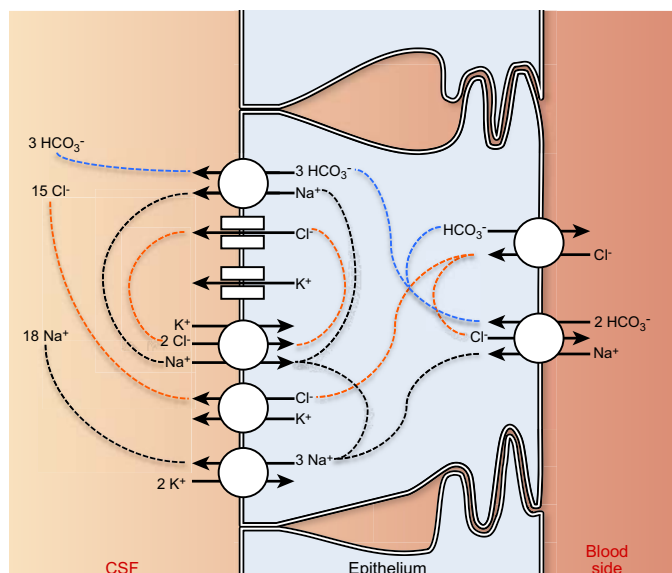


FIGURE 13. Model for the transcellular “isotonic” transport by the choroid plexus. In the simplest possible model of secretion by the choroid plexus epithelium, the main ions are taken up from the blood side by the action of AE2 and Ncbe in the basolateral membrane in a ratio $18 \text{ Na}^+ : 15 \text{ Cl}^- : 3 \text{ HCO}_3^-$. A large fraction of the Cl^- and HCO_3^- influx is recycled across the basolateral membrane. At the luminal membrane, the $\text{Na}^+ \text{--} \text{K}^+ \text{--} \text{ATPase}$ extrudes most of the Na^+ , with a small contribution from NBCe2, which mediates the HCO_3^- efflux. The KCC4 secretes the majority of Cl^- and is also a main luminal K^+ recycling pathway. A fraction of the extruded Na^+ must reenter the cell to keep the stoichiometry of the secreted ions to roughly $18 \text{ Na}^+ : 15 \text{ Cl}^- : 3 \text{ HCO}_3^-$ through the NKCC1. This small recycling of Na^+ is accompanied by the need of additional extrusion of the imported K^+ and Cl^- through their respective luminal ion channels. The transcellular movement of ions is powered by the $\text{Na}^+ \text{--} \text{K}^+ \text{--} \text{ATPase}$, which also directly pumps out net solute to the cerebrospinal fluid (CSF). Net ion flux from blood side to the CSF side creates a small difference in osmolarity, which drags water molecules across the epithelium, most likely mainly through aquaporin-1 in both the luminal and basolateral membranes.

The precise details of how Na^+ is transported into the choroid plexus cells at the basolateral membrane are still not clear despite molecular evidence for the expression of several Na^+ entry pathways in this membrane. In support of a role for Ncbe/NBCn2, knockout mice exhibit a decreased ventricular volume, and a reduction in DIDS-sensitive, Na^+ -dependent HCO_3^- uptake. However, the reduction in ventricular volume in Ncbe knockouts may also be due to a secondary decrease in the expression of $\text{Na}^+ \text{--} \text{K}^+ \text{--} \text{ATPase}$ and/or AQP1 observed in these animals. Attempts to generate inducible Ncbe knockout mice to circumvent any compensatory changes in expression of other transporters have been unsuccessful thus far. Furthermore, determinations of $^{22}\text{Na}^+$ influx and direct assessments of the rate of CSF secretion in Ncbe knockout and wild-type mice are needed to help establish Ncbe as the main Na^+ entry pathway. The NBCn1 is unlikely to be a major route for Na^+ , as it is not always situated in the basolateral membrane. Neither ENaC subunits nor NHEs have been convincingly demonstrated in the basolateral membrane using molecular or functional assays. However, given the large amount of functional data suggesting amiloride-sensitive influx, we cannot dismiss the possibility that yet undescribed Na^+/H^+ exchangers or other Na^+ transporters may contribute to Na^+ import at the basolateral membrane.

B. Cl^- Secretion

Current evidence, on balance, strongly suggests that Cl^- is transported via a transcellular rather than a paracellular route across the CPE. First, the concentration of Cl^- in CSF is much lower than predicted for simple diffusion given the lumen-positive potential difference. Second, there is no evidence that anion-selective claudins are present in this epithelium. Third, the CPE expresses anion conductances and cotransporters in the luminal membrane and anion exchangers in the basolateral membrane. Fourth, the Cl^- uptake into the choroid plexus is sensitive to the bath $[\text{HCO}_3^-]$ and is inhibited by the stilbene derivatives SITS and DIDS (295). The molecular identity of the Cl^- transport pathways, however, remains to be precisely resolved. In other epithelia, Cl^- entry at the basolateral membrane occurs via the NKCC1 (274), but this transporter is situated in the luminal membrane of CPE. At present, AE2 is the only Cl^- import mechanism described in the basolateral membrane, although it is possible that *slc26* proteins may also facilitate Cl^- entry and may also be expressed in the basolateral membrane. In the luminal membrane, Cl^- channels and KCC4 are thought to contribute significantly to Cl^- extrusion (148, 159, 160, 358, 359).

C. HCO_3^- Secretion

There is a significant body of data to show that HCO_3^- is essential for the overall process of CSF secretion. For in-

luminal membrane (7, 60, 250, 338, 351). The major Na^+ extruder to the CSF at the luminal membrane is without doubt the $\text{Na}^+ \text{--} \text{K}^+ \text{--} \text{ATPase}$ (258, 350, 365). In addition to pumping Na^+ into CSF, the $\text{Na}^+ \text{--} \text{K}^+ \text{--} \text{ATPase}$ also creates the electrochemical gradients that are exploited by a variety of other transporters involved in CSF secretion. The significance of the dual action of the $\text{Na}^+ \text{--} \text{K}^+ \text{--} \text{ATPase}$ is underscored by blockade of CSF formation by application of the inhibitor ouabain to the luminal side. NBCe2 also extrudes Na^+ into the CSF, but only at a ratio of one Na^+ for three HCO_3^- . Thus, because of this 1:3 stoichiometry, and given the rate of HCO_3^- secretion is significantly lower than that of Cl^- secretion, NBCe2 must contribute $<10\%$ to the total Na^+ extrusion. In contrast, neither the luminal NKCC1 nor ENaC (if expressed) is thought to make significant contribution to Na^+ secretion in the choroid plexus. Thus the pathways for Na^+ exit in the luminal membrane of the choroid plexus closely resemble the basolateral Na^+ transport mechanisms in the renal proximal tubule, i.e., $\text{Na}^+ \text{--} \text{K}^+ \text{--} \text{ATPase}$ supplemented with an electrogenic NBC form.

stance, CSF secretion in rats is significantly inhibited by carbonic anhydrase inhibitors (321), and in amphibians, secretion is greatly reduced and Na^+ - K^+ -ATPase inhibited in the absence of $\text{CO}_2/\text{HCO}_3^-$ (278). Furthermore, in humans, intracranial pressure (an indirect measure of the rate of CSF secretion) is reduced by the carbonic anhydrase inhibitor acetazolamide (45). Ncbe is a good candidate for importing HCO_3^- from the blood side, while NBCn1 may assist when expressed in the basolateral membrane of CPE. An unknown proportion of intracellular HCO_3^- could also be generated by the system of potent carbonic anhydrases in the cells. Luminal HCO_3^- extrusion is mainly mediated via NBCe2. Thus, in isolated choroid plexus cells, the rate of HCO_3^- extrusion by AE2 and NBCe2 seems to balance HCO_3^- import by Ncbe, NBCn1, and NHE1 (Damkier, unpublished results), leaving little room for other transport processes. However, there may also be small amounts of transport via the luminal anion conductances and possibly by *slc26* proteins if they are expressed in the luminal membrane.

D. K^+ Transport

K^+ transport by the choroid plexus is quite complex as there appears to be a precise regulation of $[\text{K}^+]_{\text{CSF}}$. K^+ is secreted into the CSF by the CPE to replace K^+ , which is lost from the ventricular system when CSF drains via the arachnoid granulations. The secretory flux of K^+ (blood to CSF) is thought to occur via the paracellular pathway, perhaps through claudin-2. K^+ transport by the paracellular route is limited, however, by the slight CSF-positive transepithelial potential difference. Thus the theoretical maximum $[\text{K}^+]_{\text{CSF}}$ which can be attained by this pathway is 3.6 mM (assuming a plasma concentration of 4.4 mM; TABLES 1 AND 2). $[\text{K}^+]_{\text{CSF}}$ however is actually only ~ 2.8 mM, and this value is achieved because the CPE also actively absorbs K^+ by a transcellular route (333). Modulation of transcellular transport is probably necessary to maintain $[\text{K}^+]_{\text{CSF}}$ at 2.8 mM, and this value remains constant even when plasma $[\text{K}^+]$ is experimentally varied (7, 113).

K^+ absorption is explained by active uptake at the luminal membrane by the Na^+ - K^+ -ATPase and possibly NKCC1. Subsequently, the vast majority of the imported K^+ is recycled across the luminal membrane by a combination of K^+ channels and the KCC4 cotransporter (331, 332). However, a minor fraction of this K^+ , $<10\%$ in the bullfrog (333), leaves the cell across the basolateral membrane accounting for K^+ absorption. In the bullfrog, basolateral efflux may be mediated by K^+ channels (333), but in mammals it is thought to occur via KCC3a, which is the only K^+ transport pathway known to be expressed in this membrane.

It is important to note that the recycling of K^+ at the luminal membrane by K^+ channels (and KCC4) serves two very

important purposes. First, it avoids the excessive accumulation of K^+ in the cells, thus preventing both the inhibition of the Na^+ - K^+ -ATPase and an increase in cell volume. Second, efflux via the channels maintains the intracellular negative membrane potential, which makes a vital contribution to the electrochemical gradient for Cl^- and HCO_3^- efflux via anion channels and the NBCe2.

E. Water Secretion

The simplest model for transepithelial water movement in the choroid plexus is a transcellular route, whereby AQP1 in both the basolateral and luminal membrane facilitates H_2O transport from the interstitium to the CSF. This movement would be driven by a small, stepwise increase in osmolarity from interstitium to cell, and from cell to CSF. While it has been established that there is a transepithelial gradient of 5 mosM, the intracellular osmolarity has not been precisely estimated. For the time being, therefore, other mechanisms cannot be completely disregarded.

The relative lack of aquaporin expression in the basolateral membrane is a matter of concern. It may be that the intrinsic water permeability of the basolateral membrane may be sufficient and reduce the need for high expression of aquaporins at this site. Nevertheless, one might equally claim that the lack of aquaporin expression in the basolateral membrane indicates a role for paracellular water transport via claudin-2. In such a scenario, the abundant luminal AQP1 would mainly become an efficient means of cell volume regulation. However, the reduced CSF formation rate in AQP1 knockouts described above currently offers a strong argument that AQP1 and transcellular water transport are crucial for CSF formation. Furthermore, there were no significant changes in the expression of other ion transporters in the AQP1 knockout animals (59), so the reduction of CSF secretion must be due to the lack of AQP1 alone. In future studies it will be interesting to investigate the water permeability and the rate of CSF secretion in claudin-2 knockout mice.

F. Carbonic Anhydrases and Solute Transport

Carbonic anhydrases catalyze the conversion of H_2O and CO_2 to H^+ and HCO_3^- . They are among the enzymes in nature with the fastest turnover and are potently inhibited by acetazolamide (196). Acetazolamide is known to reduce CSF secretion by 50–100% (7, 60, 338), and much of this inhibitory effect is thought to be due to actions on the CPE cells, but the drug also exerts the vasoconstrictor effects on cerebral vessels. This dual action may help explain why there is a large variance in the net inhibition of CSF secretion reported in the literature. At the time these experiments

were performed, only cytosolic carbonic anhydrase activity had been described. The choroid plexus, however, is now known to express the extracellular membrane-associated isoforms CAXII and CAIX, in addition to the ubiquitous cytosolic carbonic anhydrase CAII (150).

In the field of acid/base transport, there is currently much debate about the potential associations of both external membrane-bound and cytosolic carbonic anhydrases with HCO_3^- transport proteins of the *slc4a* family, e.g., AE2 and NBCe1 (24, 207). Data indicate that there may be both functional and physical coupling of the transporters with the enzymes. Furthermore, it is thought that such interactions may facilitate transport by supplying substrate to the HCO_3^- transporters (207). In the choroid plexus, CAXII is localized in the basolateral membrane where many of the key plasma membrane bicarbonate transporters are expressed. It is not yet established whether the originally reported effect of acetazolamide on CSF secretion is caused by inhibition of intracellular or extracellular carbonic anhydrases or both. In the case of intracellular conversion of CO_2 and H_2O to HCO_3^- , a potent H^+ extruder must be expressed in the basolateral membrane. However, to date, no such transporter has been identified at the molecular level, and at a functional level the pH recovery following acid loading is minimal in the absence of Na^+ or $\text{CO}_2/\text{HCO}_3^-$ (27, 57). Thus it is still possible that secreted HCO_3^- may arise directly from the plasma, and not from the intracellular conversion of CO_2 and H_2O .

X. REGULATION OF CSF WATER AND MONOVALENT ELECTROLYTE BALANCE

Many of the key hormones and their receptors, which regulate systemic water and electrolyte homeostasis, such as aldosterone, angiotensin II, and arginine vasopressin, are also present in the choroid plexus/ventricular system. These mediators are believed not only to have a local role with respect to CSF production and brain extracellular fluid volume regulation (FIGURE 14), but they may also play a role via the choroid plexus and CSF in the central regulation of blood pressure.

The mediators may arise from local production in the choroid plexus, from other regions of the brain, or from the blood plasma. They either directly target epithelial cell function, or have indirect effects on the vascular bed underlying the epithelium. In considering the choroid plexuses, it is important to remember that these tissues constitutively secrete CSF and that any hormonal actions are modulatory. This contrasts the situation in many secretory epithelia, where significant secretion only occurs upon stimulation with hormones or neurotransmitters, e.g., in the salivary gland or pancreas. In this review, we only consider hormones and mediators with direct relevance to CSF secretion, although many other substances affect the functions of the choroid plexus (229).

A. Aldosterone

Aldosterone is a mineralocorticoid hormone that plays key roles in systemic Na^+ and H_2O balance through its action primarily on the kidney. Aldosterone acts on mineralocorticoid receptors to conserve body Na^+ content. In the kidney, the distal colon, and ducts from exocrine glands, this occurs via increasing the abundance and activity of ENaC and $\text{Na}^+-\text{K}^+-\text{ATPase}$ (83, 123). In addition to production in the adrenal glands, aldosterone is also produced in the hypothalamus from where it may have local actions within the CNS (124). High-affinity aldosterone binding and mineralocorticoid receptor expression (MR) have been demonstrated in the choroid plexus (63, 335).

Concentrations of aldosterone in the CSF closely follow those in plasma (106), and the brain content of aldosterone is diminished following adrenalectomy, indicating that much of the aldosterone in CSF is derived from the adrenal glands. Aldosterone shows poor penetration of the BBB; thus the hormone is thought to enter the brain via the choroid plexus and other circumventricular organs in which the BBB is absent (201). Local production of aldosterone in the brain, however, is increased in response to increased $[\text{Na}^+]_{\text{CSF}}$ and/or increased concentrations of systemic angiotensin II and contribute to the total brain aldosterone (150). Many tissues including the choroid plexus express

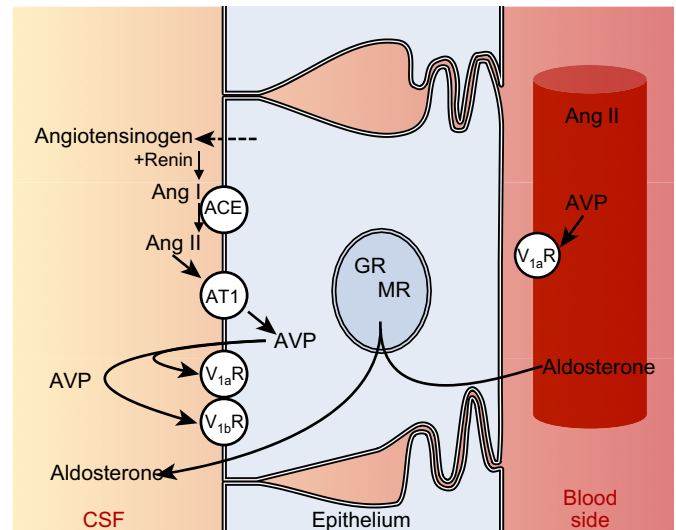


FIGURE 14. Local actions of angiotensin II, vasopressin, and aldosterone on the choroid plexus. Angiotensin II (ANG II) and arginine vasopressin (AVP) are both produced locally in the choroid plexus cell and also reach these cells and cerebrospinal fluid (CSF) from the systemic circulation. ANG II mediates release of AVP from the cell through AT_1 receptors. The systemic action of ANG II is to decrease blood flow. The epithelial cells contain both V_{1a} and V_{1b} receptors, and through these AVP mediates decreased decreased Cl^- efflux and CSF secretion. The vascular bed contains V_{1a} receptors through which AVP mediates decreased blood flow and increased capillary permeability. Central and systemic aldosterone mediates decreased $\text{Na}^+-\text{K}^+-\text{ATPase}$ activity and thereby decreased CSF secretion. MR, mineralocorticoid receptor; GR, glucocorticoid receptor.

both MR and glucocorticoid receptors (GR), and cortisol binds equally well to both receptors. Normally, plasma glucocorticoid levels exceed aldosterone levels, and MR receptor specificity is secured by the rapid intracellular conversion of cortisol to the inactive cortisone by the enzyme 11β -hydroxysteroid dehydrogenase type 2 (11β HSD2). However, the choroid plexus expresses 11β HSD type 1, and not 11β HSD2 (294). Thus it is not evident that aldosterone can exert specific MR actions in the choroid plexus.

Intracerebroventricular administration of aldosterone causes an elevation of systemic blood pressure (146, 335). This effect is believed to be caused by a reduction in $[K^+]_{CSF}$, due to an aldosterone-mediated increase in Na^+ - K^+ -ATPase activity in the luminal membrane of the CPE cells. Thus, the effect of aldosterone is abolished by 1) the infusion of K^+ into the ventricular system, 2) administration of a mineralocorticoid receptor antagonist, and 3) the presence of benzamil or digoxin (330, 335). The two latter are blockers of ENaC and Na^+ /H $^+$ exchange, and the Na^+ - K^+ -ATPase, respectively, and the data suggest a role for one or more of these transport proteins in the response to aldosterone. This notion is supported by the expression of ENaC subunits as well as ENaC-regulatory genes in the choroid plexus (9, 331). There is, however, no data to show that aldosterone binding to the mineralocorticoid receptors in choroid plexus causes an increase in ENaC abundance or activity. Thus a clear role for aldosterone in the choroid plexus still remains to be established.

B. Angiotensin II

The CPE expresses other components of the renin-angiotensin-aldosterone system: renin, angiotensinogen, and angiotensin converting enzyme (ACE) are all produced in the CPE cells (39, 40, 131, 133). Furthermore, the angiotensin II receptor, AT1, is expressed by the choroid plexus (103). Systemic administration of angiotensin II causes a decrease in blood flow to the choroid plexus (195), and intraventricular injection of both angiotensin I and II also cause a decrease in CP blood flow without affecting cerebral blood flow. Systemic administration of ACE inhibitors does not affect the blood flow to the choroid plexus (195), but intraventricular administration of ACE inhibitors causes increased CSF production in rat (322). This implies that the effects on both CP blood flow and CSF production are mediated through angiotensin II and that the AT1-dependent inhibition of CSF blood flow is mediated through the V1 receptor (42). Activating the AT1 receptor by angiotensin II is believed to lead to a production of arginine vasopressin in the choroid plexus cell. This, in turn, acts on V1 receptors in CP cell as well as in the vasculature.

C. Arginine Vasopressin

Arginine vasopressin (AVP) has been detected in samples of CSF (75). The AVP peptide present may be derived from

peripheral blood, central release from the hypothalamus, and/or from production within the CPE cells. Systemic administration of AVP is known to increase the water content of brain tissue (74), and to enhance brain edema during brain injury and hemorrhage (73, 264). The effect of AVP on the choroid plexus, however, is a decreased CSF formation rate and reduced choroid plexus blood flow (141). This decrease occurs despite a simultaneous increase in choroid plexus capillary water permeability (260). Vasopressin receptors exist as V1a, V1b, and V2 subtypes. The adult choroid plexus possesses V1a receptors (235, 245) and, albeit less abundant, V1b receptors (31). V2 receptors are not found in the adult CNS, but they are expressed in the choroid plexus in newborn rats (235).

As mentioned above, the AVP production by CPE cells is stimulated by centrally released angiotensin II through AT1 receptor-mediated activation. The resulting decrease in CSF formation rate is mediated via the V1a receptor in the luminal membrane of the CPE (312), and in the capillaries (286). Salt-loading of rats, which leads to hyperosmolarity, causes increased AVP production locally in the choroid plexus (311), as well as increased V1b receptor mRNA (357). The effect of vasopressin on the CPE cells includes a reduction of Cl^- efflux (141), but the complete understanding of the molecular mechanisms behind the effect of vasopressin on CPE cells remains to be determined. Hyponatremia induced by administration of hypotonic dextrose solution and AVP increases AQP1 and NKCC1 abundance in the luminal membrane of CPE, as well as disrupting the integrity of the BCSFB (162). The effect of hyponatremia on CSF production, blood flow, or water permeability has not been investigated. Whether the effect is mediated through CP vasopressin or angiotensin II production is unknown.

There are still many unknown factors regarding the molecular actions of aldosterone and vasopressin on CSF formation. The studies that have been conducted suggest a regulatory pathway influencing both the water and electrolyte transporters located in the luminal membrane as well as the influence of the blood flow and permeability of the capillary bed. The complexity is further enhanced by the fact that the peptides are also found in the bloodstream, making it difficult to decipher whether the effects are local or systemic.

D. CSF pH and Regulation of Ventilatory Rate

The regulation of ventilatory rate is a complex interplay between peripheral and central chemoreceptors which sense changes in the chemistry of the blood and CSF respectively, and "effectors" that modulate the ventilation of the lungs. The precise extent of the distribution of the central chemoreceptors in the brain stem is still debated and is outside the scope of this review. However, the first chemo-

receptors were identified on the ventrolateral medullary surface (214), and in the following decades other chemosensitive regions were reported across brain stem nuclei 200–400 μm below the ventral surface of the medulla (for review, see Ref. 65). The central chemoreceptors respond to changes in brain extracellular fluid H^+ concentration. The extracellular fluid pH is influenced directly by the CSF pH, then indirectly by the metabolism of the brain, plasma PCO_2 , and the local blood flow (342). The BBB and BCSFB are relatively impermeable to H^+ and HCO_3^- but not to the gaseous CO_2 . An increase in plasma PCO_2 therefore leads to the diffusion of CO_2 from the cerebral blood vessels into the CSF. The resultant change in pH in CSF is a main stimulator for the chemoreceptors.

The $[\text{HCO}_3^-]_{\text{CSF}}$ is regulated in face of plasma PCO_2 changes (126, 154, 325), and this is of particular importance to the control of ventilation. In the short term (e.g., seconds to minutes), $[\text{HCO}_3^-]_{\text{CSF}}$ is tightly regulated at ~ 22 mM. This relatively constant concentration is vital for maintaining the responsiveness of the central respiratory chemoreceptors to changes of the CO_2 concentration (25), i.e., the central chemoreceptors would be much less responsive if $[\text{HCO}_3^-]_{\text{CSF}}$ was not controlled. However, prolonged exposure to PCO_2 changes (i.e., hours to days) causes a so-called “resetting” of the central chemoreceptors. This involves gradual changes in the $[\text{HCO}_3^-]_{\text{CSF}}$ which accommodate the altered CO_2 concentration. Thus the pH of the CSF returns towards pH 7.4, and the activity of the central chemoreceptors and ventilatory rate return to normal. At high altitudes with decreased PCO_2 , the $[\text{HCO}_3^-]_{\text{CSF}}$ is reduced over a period of days as the individual acclimatizes to the new environment (93), whereas individuals chronically exposed to high concentrations of CO_2 , e.g., in chronic obstructive pulmonary disease, have increased $[\text{HCO}_3^-]_{\text{CSF}}$ (135). These changes in $[\text{HCO}_3^-]_{\text{CSF}}$ may simply be the result of prolonged changes in plasma $[\text{HCO}_3^-]$ which gradually influence the CSF. However, it is also possible that these changes result from regulation of HCO_3^- transport activity by the choroid plexus. This view is now supported by data from the NBCe2 knockout mice that have reduced $[\text{HCO}_3^-]_{\text{CSF}}$ (151). It will be interesting to learn whether changes in Na^+ - HCO_3^- cotransport in the choroid plexus are part of the physiological response to changes in ambient PCO_2 .

XI. MECHANISMS AND REGULATION OF CALCIUM TRANSPORT BY THE CHOROID PLEXUS

An evolving topic in choroid plexus physiology is their potential role in Ca^{2+} transport into the CNS. The recent observation that α -klotho (an antiageing protein with key roles in balancing systemic Ca^{2+} homeostasis) is highly expressed by the choroid plexus (132, 175) has focused attention on Ca^{2+} transport into the brain. Ca^{2+} is known to

play many key roles in the CNS, e.g., it controls neurotransmitter release, contributes to depolarizing currents, and modulates the activity of ion channels (21). It also regulates processes such as long-term potentiation, neuronal plasticity, and cell death (17, 186, 326). The regulation of the intracellular $[\text{Ca}^{2+}]$ in neurons has been extensively studied and is well understood (21). Ultimately, however, the stability of all these signaling pathways is dependent on the long-term control of $[\text{Ca}^{2+}]$ in the CSF ($[\text{Ca}^{2+}]_{\text{CSF}}$) and the interstitial fluid of the brain in general, e.g., experimentally induced changes in $[\text{Ca}^{2+}]_{\text{CSF}}$ have profound effects on neuronal excitability (92, 296, 354). To prevent these unwanted changes in excitability, the cells of the BBB and BCSFB regulate Ca^{2+} transport into the CNS. This was demonstrated in studies in which $[\text{Ca}^{2+}]_{\text{CSF}}$ remained relatively stable (1.0–1.5 mM) when plasma $[\text{Ca}^{2+}]$ was experimentally varied in the range from 1 to 5 mM (145, 217). How this regulation of Ca^{2+} is achieved is still very poorly understood, but Imura et al. (132) recently suggested that α -klotho may be at least partially responsible.

In humans, a minimum of 34 mg Ca^{2+} is lost each day from the CNS in the CSF as it drains from the subarachnoid space into the vascular system. This amount, together with any other Ca^{2+} lost from the brain interstitial fluid, must be replaced in order for homeostasis to be maintained. Flux studies indicate that the CPE are the main route of Ca^{2+} entry to the CNS, and that the transport of Ca^{2+} across the CPE occurs via a saturable pathway (219). This suggests that carrier-mediated transport is involved and that Ca^{2+} transport is not by simple diffusion via the paracellular pathway. This conclusion is further supported by the fact that claudin-16, which renders junctional complexes permeable to Ca^{2+} , is not expressed in the epithelium (199, 347). A recent *in vitro* study (284) demonstrated the net secretion of Ca^{2+} across monolayers of primary cultures of rat choroid plexus cells. The mechanisms by which Ca^{2+} is transported was not elucidated, but interactions between Ca^{2+} and Mn^{2+} were reported which suggest that these ions may be transported by similar pathways (284).

Imura (132) proposed that Ca^{2+} transport by the choroid plexus may occur by a mechanism similar to that which accounts for transcellular Ca^{2+} absorption in some other epithelia, e.g., renal distal tubule and the small intestine (122). In this proposed model, the first step is Ca^{2+} entry by either or both the TRPV5 and TRPV6 ion channels in the basolateral membrane. Once in the cell the Ca^{2+} must be bound to binding proteins such as the calbindins, which are present in the cytoplasm and facilitate the transition of the Ca^{2+} from basolateral to luminal membrane (122). Finally, extrusion of Ca^{2+} into the CSF at the luminal membrane is mediated by a combination of Ca^{2+} -ATPase (PMCA) and $\text{Na}^+/\text{Ca}^{2+}$ exchange (NCX) (122). This model is theoretically plausible for the choroid plexus; however, it is not really supported by the existing evidence, and

alternative mechanisms must be considered. The following sections summarize what is currently known about Ca^{2+} transport by the choroid plexus, and then suggests alternative mechanisms for Ca^{2+} transport.

A. Expression of Proteins Mediating Entry or Exit of Ca^{2+}

There are no data in support of the expression of either TRPV5 or TRPV6 in the choroid plexus (Brown, Millar, and Hoenderop, unpublished data). Patch-clamp experiments have identified a Ca^{2+} -permeant nonselective cation conductance in the choroid plexuses (210). The conductance may be carried at least in part by TRPV4 (177) and TRPM3 channels (231), because mRNA for both is expressed in the choroid plexus. The TRPV4 channel protein, however, appears to be predominantly localized in the luminal membrane of the cells (132) where it cannot contribute directly to Ca^{2+} secretion, i.e., it can only mediate an absorptive influx of Ca^{2+} from the CSF. In contrast, the current-voltage relationship for the conductance has similarities to that of heterologously expressed TRPM3. It is not yet known, however, whether the TRPM3 channel protein is expressed in basolateral membrane of the choroid plexus.

PMCA mediates the primary active transport of ions by hydrolyzing ATP and exchanging intracellular Ca^{2+} for extracellular H^+ . Two isoforms, PMCA3 and PMCA4, are expressed in the luminal membrane of the human, cat, and rat CPE (23, 306, 307). This pump is normally involved in maintaining a suitable intracellular Ca^{2+} level in collaboration with $\text{Na}^+/\text{Ca}^{2+}$ exchangers (NCX), and in certain epithelia it plays a role in vectorial transport of Ca^{2+} . There are no data to support the expression of NCX of the SLC8 family in the choroid plexus, although these transporters are expressed elsewhere in the CNS (36). Expression of SLC25a5 mRNA, encoding a $\text{Na}^+/\text{Ca}^{2+}\text{-K}^+$ exchanger has been reported (120), but whether functional proteins are expressed in the luminal membrane has not been determined. Several studies have examined calbindin expression in the choroid plexus, but they have produced equivocal data on calbindin-D_{28K} expression. It is expressed in dogfish (268) but not in rat choroid plexus (101). The expression of calbindin-D_{9K} expression has not been investigated in the choroid plexus.

B. An Alternative Model for Ca^{2+} Transport

The current lack of evidence for key components of the conventional Ca^{2+} transepithelial transport model, e.g., TRPV5 or TRPV6, intracellular calbindins, and luminal NCX, suggest that transport may not occur by this arrangement. Furthermore, the in vitro observation that Ca^{2+} and Mn^{2+} may share a common pathway across the epithelium (284) also argues against the conventional route for a sig-

nificant component of the transport (since Mn^{2+} is transported neither by the NCX nor the PMCA). An alternative model may be that Ca^{2+} is secreted by mechanisms similar to those observed in the mammary gland epithelium (319). Here, the precise route of basolateral Ca^{2+} entry remains to be determined, but once in the cell much of the Ca^{2+} is sequestered into the Golgi apparatus by secretory pathway ATPases (SPCA1 and/or SPCA2), which transport Mn^{2+} in addition to Ca^{2+} . From here, the Ca^{2+} is "trafficked" across the cell in vesicles, and extruded at the luminal membrane by exocytosis (319). It remains to be determined whether such mechanisms contribute to Ca^{2+} transport by the choroid plexus. However, both SPCA1 and SPCA2 mRNA are expressed in rat and pig choroid plexus (243). Furthermore, there are data demonstrating that exocytosis of proteins containing vesicles occurs at the luminal membrane of the choroid plexus (41).

C. Regulation of Ca^{2+} Transport

In the systemic circulation, Ca^{2+} homeostasis is governed by hormones such as 1,25(OH)₂-cholecalciferol (the activated form of vitamin D), parathyroid hormone (PTH) (122), and the recently identified modulator α -klotho (170). Data on whether Ca^{2+} transport by the choroid plexus is modulated by these factors are very limited and equivocal. For instance, an increase in the rate of Ca^{2+} entry was observed in studies of hypocalcaemic rats in which both plasma 1,25(OH)₂-cholecalciferol and PTH concentrations would be elevated (18, 218). A slight decrease in the rate of entry was observed in hypercalcaemic rats (218). However, these changes in the rate of transport appeared to be independent of directly administered vitamin D₃ (218), even though receptors for 1,25(OH)₂-cholecalciferol are expressed (328). Keep et al. (155) on the other hand demonstrated a large increase in PMCA protein expression in brain microvessels, suggesting increased transport by the BBB, but there were no significant changes in expression in the choroid plexus. The direct effect of PTH on transport into the brain, however, has not been investigated, although the PTH receptor is expressed in the CPE (334).

While our knowledge of the regulation of Ca^{2+} transport by conventional messengers such as 1,25(OH)₂-cholecalciferol and PTH remains rather confused, there are more definitive data on the role of α -klotho. For example, the $[\text{Ca}^{2+}]_{\text{CSF}}$ is reduced by over 25% in transgenically modified mice in which the klotho genes has been silenced (132). The reduction in $[\text{Ca}^{2+}]_{\text{CSF}}$ in the absence of α -klotho was suggested to be caused by a decrease in Ca^{2+} extrusion via NCX as $\text{Na}^+\text{-K}^+\text{-ATPase}$ activity is also reduced (132). However, if NCX does not contribute to Ca^{2+} transport in the choroid plexus (see above), alternative explanations must now be sought.

XII. PATHOPHYSIOLOGY RELATING TO CHOROID PLEXUS CSF FORMATION

A. Age-Related Changes of the Choroid Plexus and Alzheimer's Disease

The CPE cells undergo flattening with age, and this in humans amounts to an 11% decrease in cell height from infancy to 88 yr of age (255). In rats, Serot et al. (287) showed that the decrease in cell height started after 18 mo of age, indicating that it is not a normal phenomenon in the younger animals (287). In addition to the changes in height, the basement membranes of both the endothelial and epithelial cells thicken (287) and the thickness of the underlying connective tissue increases. Furthermore, increases in the number of intracellular inclusions of both lipid byproducts and protein tangles that resemble the plaques found in Alzheimer's disease in the content of amyloid- β protein epitopes are observed (341). Most of these changes, however, are also seen in non-Alzheimer's patients, and the general increase in number of these inclusions reaches a plateau at the age of 70 yr in humans.

The rate of CSF secretion by the choroid plexus decreases with ageing, as demonstrated in both sheep and humans (55, 255). The volume of CSF, however, increases with age due to moderate brain atrophy and increased CSF drainage resistance (2). The increased resistance is at least partially due to fibrosis of the meninges, which probably reduces outflow via the arachnoid granulations (20). Elevated central venous pressure due to vascular disease has also been implicated in the increased resistance of CSF drainage (272). The increased CSF volume, the lower rate of CSF secretion, and reduced drainage all result in a general decrease in the rate of CSF turnover. This leads to age-dependent increases in CSF/plasma concentration ratios of many compounds normally removed from the brain by CSF drainage, including proteins such as IgG and albumin (102). These age-related changes in CSF composition should not be misinterpreted as a simple mechanical breakdown of the BBB or BCSFB functions.

Alzheimer's disease is a detrimental neurodegenerative disease, which is normally fatal within a few years after diagnosis. The incidence of the disease increases with age, and late-onset Alzheimer's disease (observed after 65 years of age) is the most common form. Although Alzheimer's disease has been studied in great detail, the role of the choroid plexus in Alzheimer's disease is not fully understood. In recent years, a number of studies have suggested that changes in the rate of CSF turnover may be important in the progression of the disease.

Basically, Alzheimer's disease is known to present two types of lesions: extracellular amyloid plaques and intracellular neurofibrillary aggregation (81). The amyloid plaques con-

sist of extracellular deposits of amyloid- β ($A\beta$) peptide fibrils. $A\beta$ is generally considered to be a waste product, and it is normally produced at low levels, which act positively on brain synapses at picomolar concentrations (257). The intracellular neurofibrillary tangles consist of abnormally phosphorylated tau, a microtubule-associated protein (MAP) (81). The accumulation of tau is believed to have severe consequences for neuronal function, and the density of these accumulations is correlated to severity of symptoms. Both $A\beta$ and tau are normally present in CSF, and the drainage of CSF is believed to be the main pathway by which $A\beta$ is removed from the CNS (314). In late-onset Alzheimer's disease, concentrations of $A\beta$ in CSF are decreased, but those of tau are increased and probably reflect neuronal damage (136). These changes can be measured in CSF before the onset of any other symptoms, and they can therefore be used as a diagnostic marker for the disease (315).

In Alzheimer's disease (341) and systemic amyloidosis (279), the number of amyloid deposits increases in the epithelial and endothelial cells, respectively. The impact of the deposits on choroid plexus function may be abnormal CSF secretion. It was also suggested that $A\beta$ found in cerebrospinal fluid may be produced by the choroid plexuses and may contribute to the deposits in the brain seen in Alzheimer's disease (256). A general decrease in CSF turnover is thought to be important in the development of Alzheimer's disease, because it decreases the rate at which waste products are cleared from the brain. It is also thought to increase the contact time for proteins with glucose in the CSF, which promotes the glycosylation of CSF proteins and increased oxidative stress (289). In patients suffering from Alzheimer's disease, CSF turnover and thereby also CSF clearance is indeed decreased by 50% (292). Although it has not yet been determined, the decrease in CSF turnover may be related to a decrease in the activity of the Na^+K^+ -ATPase in the choroid plexus with age. In contrast, the opposite effect, i.e., decreased deposition of $A\beta$ and an increase in Na^+K^+ -ATPase, were observed in mice after the administration of caffeine (11, 115).

CPE cells may also play a direct role in removal of proteins from the CSF by receptor-mediated endocytosis via receptors such as the low-density lipoprotein receptor related protein-1 (LRP-1) and -2 (megalin). The abundance of LRP-1 in the choroid plexus increases with age, whereas the abundance of megalin is reduced. LRP-1 seems to be shed from the membrane upon stimulation of $A\beta$. This leads to $A\beta$ accumulation in CSF by binding to LRP-1 and thereby preventing aggregation. The bound $A\beta$ can be cleared from the central nervous system to be degraded in the systemic circulation (183). Megalin is thought to contribute to the clearance of $A\beta$ protein through the choroid plexus (114), and a decrease in megalin was shown in the CPE cell of Alzheimer's disease (6, 239). Megalin has been shown to transport solutes both from blood and CSF into the choroid

plexus, but the fate of the solutes is not known. One explanation could be that they are degraded in the choroid plexus or transcytosed through the cells. For both LRP1 and megalin, altered expression can lead to accumulation of A β in the CSF. However, it is not clear whether these changes are the cause or effect of the pathological changes observed in Alzheimer's patients. Changes in vitamin transport into the CSF by the choroid plexuses may also play a role in the development of Alzheimer's disease. Decreased concentrations of vitamin B₁₂ and folate within the CSF have been observed (130), which in vitro has been shown to increase plasma tau levels (121). Reduced antioxidant levels in the CSF, primarily ascorbic acid, are also predicted to cause a cognitive deterioration with age (28).

B. Role of the Choroid Plexuses in the Control of Intracranial Pressure

The intracranial pressure (ICP) is normally between 7 and 13 mmHg, and it is equal throughout the brain parenchyma and the cerebrospinal fluid (25). In a supine position, the ICP is equal to the pressure in the spinal canal, while it decreases in the erect position, and increases in response to the Valsalva maneuver. ICP can be monitored by invasive ICP measurements through the skull. Alternatively, CSF pressure can be measured as the opening pressure when performing lumbar puncture with the patient placed completely horizontal. However, this latter measurement can be complicated by the anxiety often experienced in conscious patients during this procedure (356).

After closing of the skull sutures during neonatal development, the rigid bone structure of the skull hinders any expansion of the volume inside. According to the Monro-Kellie doctrine, this means that changes in volume of one compartment of the brain (brain tissue, blood, CSF) must entail an opposite change in another compartment (54). A venous plexus surrounds the dura in the spinal canal, and sudden increases in pressure (e.g., when coughing) are followed by compression of this venous plexus. Depletion of CSF, on the other hand, leads to an accumulation of venous blood in the plexus and expansion of the vascular volume. Loss of CSF volume is seen in individuals with dural defects or as a consequence of the lumbar puncture procedure, e.g., patients often experience headaches after a lumbar puncture. These headaches are most likely the consequence of the decrease in CSF content and a subsequent increase in vascularization (89). Increases in CSF volume or other space-occupying lesions, on the other hand, cause effacement of cerebral sulci and potentially brain herniation.

A number of clinical conditions lead to an elevated ICP, e.g., traumatic brain injury, stroke, edema, tumors, infection, or hydrocephalus. Increases in ICP to 30 mmHg are considered pathological, whereas a pressure above 40 mmHg is life threatening. The relationship between ICP and

the secretion of cerebrospinal fluid has been investigated with varying results. Increased ICP in infant hydrocephalus was shown not to affect the cerebrospinal fluid formation (332). In calves, however, an increase in ICP was shown to decrease CSF formation by 50% (35). Later studies suggest that chronic elevations of ICP decrease CSF formation rate, but acute ICP changes do not have such an effect (291).

In other cases of increased ICP where damage to the brain occurs as seen in traumatic brain injury or stroke, the BCSFB can be disturbed either by direct damage to the CPE with consequences for the barrier function; or by the accumulation of cellular debris in the ventricular system that can interfere with the reabsorption of the CSF in the arachnoid granulations. The damage to the CPE can cause an increased permeability of solutes into the CSF with consequences for the osmotic pressure (153). This results in an increase of osmotically driven water transport into the ventricle system. The choroid plexuses have a reabsorptive role in these instances; following traumatic brain injury an extensive vacuolar appearance is found in the CP that was shown to reflect great lysosomal activity and digestion of the waste products accumulating in the cerebrospinal fluid (153, 236). Following brain injury, the CPE cells show other structural changes indicative of their role in protecting the brain. This includes widening of intercellular spaces and enlargement of the luminal microvilli. Following hemorrhage into the CSF, immune cells (monocytes) appear in the intercellular clefts (204) and CSF where they differentiate into macrophages (Kolmer cells). The macrophages in CSF bind to the apical membrane glycocalyx where they most likely affect the clearance of debris through the CPE cells. Additional removal of waste occurs via the arachnoid granulations into the venous system (111, 248). The CNS lacks a true lymphatic system, which makes the process of removing toxic substances important for the CPE and CSF.

When ICP increases, the compression causes a decrease in the blood flow to the entire brain, including the choroid plexuses. Although a decrease in blood flow does not in itself reduce the rate of CSF production, the substrate availability from the vasculature can become rate-limiting. In addition, atrial natriuretic peptide (ANP) is released into the CSF when ICP is increased (355). ANP binds to the choroid plexus cell and inhibits CSF production by up to 35% (308). Other peptides released in response to increased ICP include AVP and basic fibroblast growth factor, both of which are known to decrease CSF formation (185, 285).

C. Hydrocephalus

Hydrocephalus is a condition in which there is an enlargement of the brain ventricular size with an abnormally increased volume of CSF. Several criteria are used to discriminate between a variety of different classes of hydrocephalus. The disease complex is divided into infantile, juvenile, or adult forms.

Hydrocephalus can be further classified into either high-pressure or normal-pressure hydrocephalus. The disease complex exists in communicating or noncommunicating forms depending on whether there is free passage between the ventricles and the subarachnoid space (87). Finally, hydrocephalus is also divided into active or arrested hydrocephalus depending on the progression of symptoms.

Hydrocephalus can arise from an increase in the rate of CSF secretion, an obstruction of flow in the ventricular-subarachnoidal pathway, or a decrease in drainage to the venous system (232). Increased CSF secretion by the choroid plexus is rare and mainly described in the case of choroid plexus-papillomas. Cessation of the ventricular-subarachnoidal flow can occur after obstruction of any of the narrow parts of the CSF flow system, i.e., the foramina Monroi, the third ventricle, the aqueduct of Sylvius, or the fourth ventricle (**FIGURE 1**). These obstructions are observed after a subarachnoidal hemorrhage or an infection (meningitis) because of accumulation of debris. A blockage to flow in the narrow parts of the ventricle system will lead to an accumulation of CSF proximal to the blockage. Finally, the absorption of CSF through the arachnoidal granulations to the venous system can be disturbed either through congenital malformations in the villi or through neoplasms or inflammation in the arachnoid granulations (232).

The treatment for hydrocephalus is dependent on the extent to which the ICP is elevated. As mentioned in the previous section, increases in ICP can be life threatening. In the current context, it is worth noting that hydrocephalus can be alleviated in the short term by targeting carbonic anhydrase with acetazolamide or KCCs with furosemide. Both of these drugs are thought to reduce ICP by inhibiting CSF secretion by the choroid plexus (247). The hemodynamic effects of the drugs are unlikely to explain the decrease in CSF production, as they are secondary to actions on the kidney, and are also observed in nephrectomized animals (263). Furthermore, the immediate reduction in CSF secretion cannot be explained by development of acid-base disturbances, as this would require a longer time to develop (206). Finally, intraventricular furosemide decreases CSF formation (208), which cannot be secondary to renal effects of the drug. In the long term, hydrocephalus is almost always alleviated by insertion of a ventricular shunt to either the heart atrium or to the peritoneum. Endoscopic removal of tumors or debris causing blockage of the flow can in some cases alleviate the hydrocephalus.

The impact of hydrocephalus on the choroid plexus is similar to what is seen in other conditions of increased ICP. In an animal model, the epithelial cells appear flattened and vacuolized, and the lateral intercellular spaces are dilated (194). In humans with chronic hydrocephalus, the CP has a sclerotic stroma and the epithelium is atrophied (288). The CP is also found to contain a larger number of macrophages (Kolmer

cells) than normal, and this is believed to reflect local inflammation and appearance of debris in the CSF (189). Other studies, however, have shown that the changes that occur in CP after the onset of hydrocephalus are reversible after a day of pressure and volume relief by shunting (76).

The increased ICP in hydrocephalus causes a decrease in blood flow to the CP. It also causes the central release of AVP, which reduces blood flow and probably also decreases the rate of CSF secretion (91, 164). Other studies show decreased atrial natriuretic peptide (ANP) binding sites in rats with congenital hydrocephalus, but increased binding in rats with kaolin-induced hydrocephalus (215). In human CSF, ANP increases proportionally with intracranial pressure and independently of serum ANP levels (355). In a rabbit kaolin-induced hydrocephalus model, the CSF formation rate is decreased both 3 h and 3 wk after onset of hydrocephalus (180).

D. Idiopathic Intracranial Hypertension

Idiopathic intracranial hypertension (IIH), or pseudotumor cerebri, is a condition in which the intracranial pressure is raised, but there are no signs of any intracranial expansion. Thus brain ventricular volume is normal (108). The criteria for diagnosis include the presence of increased CSF pressure (above 20–25 cmH₂O) with normal composition of CSF and normal CT/MRI scans of the ventricular system. Patients present with symptoms associated with elevated ICP, i.e., papilledema (optic disc swelling), headache, and visual disturbances (108). The condition is most prevalent in women between 20 and 50 yr and is strongly associated with obesity. The incidence is low at between 1–3 per 100,000 per year (80). The condition can be quite detrimental to the vision, and vision field losses occur in up to 50–75% of patients (271, 327).

The pathogenesis of the condition is not precisely known, but IIH may be caused by an increased resistance to CSF absorption, an increased CSF production, or increased venous sinus pressure (128, 129). In all instances, the result is an increase in CSF pressure. Medical treatment aims at lowering ICP using acetazolamide and in some cases, but less effectively, furosemide, both of which are known to decrease CSF formation as mentioned earlier (273). The condition can also in some cases be relieved by serial lumbar punctures or on a more long-term basis through surgical intervention with insertion of a CSF draining shunt. Surgical intervention is particularly necessary when the increase in pressure is acutely threatening vision. When obesity is present, the condition may also be alleviated through weight loss (317).

E. Neoplasms of the Choroid Plexus

Neoplasms of the choroid plexus are rare (0.4–0.6% of all intracranial neoplasms; 1); however, the prevalence is

higher in early childhood. Thus, throughout childhood, choroid plexus tumors constitute 2–3% of all tumors (105), whereas in infants these tumors make up 13.1% (267). Congenital papillomas make up 7.9% of tumors diagnosed prenatally by ultrasound (266). Choroid plexus tumors are associated with hydrocephalus due to either CSF overproduction or blockage of CSF circulation through the ventricular system (98). Choroid plexus papillomas are five times more common than carcinomas (1). Most primary tumors of the choroid plexus are derived from the epithelial cells, whereas angiomas are described rarely.

Papillomas in the choroid plexus are benign papillary tumors (WHO grade I neoplasm) that resemble the normal CP epithelium, but the cells are more tightly packed and elongated. The cells have tight junctions, microvilli, cilia, and a basement membrane. Additionally, papilloma cells show accumulation of glycogen granules (172). The papillomas do not invade the brain parenchyma and, unlike the carcinomas, they are not necrotic. The choroid plexus carcinomas are invasive tumors that can be solid, hemorrhagic, and necrotic. They are most commonly located in the lateral and fourth ventricles. The malignancy diagnosis, choroid plexus carcinoma (WHO grade III tumor) is based on cytological changes: the cells show increased mitotic figures, nuclear pleomorphism and necrosis. The carcinomas are fast growing, and the 5-yr survival rate is ~40%. The tumor spreads through the cerebrospinal fluid, and systemic metastases have been shown in patients with longer survival (134). The treatment is aimed at complete resection of the tumor. Adjuvant chemotherapy or radiation therapy is also generally considered for the individual patient (261, 283, 348, 349).

Other tumor types have been described in the choroid plexus including the papillary meningioma (WHO III neoplasm) that in rare cases can arise in the choroid plexus (12). In adults, tumors found in the choroid plexus are most often metastatic neoplasms. The incidence of these is low (0.14% of all cerebral metastasis). The origin is most commonly renal cell carcinoma and lung cancer, but also primary tumors in breast, stomach, and colon have been described (165).

XIII. PERSPECTIVES AND FUTURE INVESTIGATIONS

Many aspects of choroid plexus biology have an impact far beyond the simple secretory function of this modestly sized tissue. From a cell biological perspective, the atypical polarization of the CPE is of major interest. Paradigms of polarized cell growth and differentiation are largely based on model epithelia grown in cell culture, but these paradigms are challenged by data from the CPE. These data suggest that many of the proposed rules of polarization may not be global after all. The unique mechanisms of membrane targeting of ion transporting

proteins and anchoring proteins in the CPE may have bearing for diseases of cell polarization such as cystic fibrosis and polycystic kidney disease.

At the same level of fundamental cell biology, the architecture and permeability of the tight junctions and tricellular junctions in the choroid plexus may hold important information on the contribution of claudins to unidirectional ion and/or water movement. At present, the claudins are believed to permit ion flux in single file just like most cellular ion channels. It is unknown whether the same claudin can mediate H₂O secretion and K⁺ transport simultaneously. If the tricellular junctions do not form large pores between cells, the morphological basis for the idea of “solvent drag” in leaky epithelia is centrally challenged. It also remains to be determined whether the very well developed lateral infoldings of the basolateral membrane have any importance for transepithelial H₂O or solute movement. Finally, the existence of the kinocilia or primary cilia on the luminal membrane may vary between species, and their respective functions may therefore also differ. One role of kinocilia could be preventing a functional unstirred layer to develop and/or to ascertain proper mixing of nascent and bulk CSF for proper CPE cell sensing of CSF. In turn, the primary cilia could serve sensory functions.

The pathway for H₂O through the CPE needs to be determined in more detail by transport physiologists. It is critical to know the water permeability basolateral membrane to determine whether the paracellular pathway may also contribute to secretion. The surface area of the tight junctions is orders of magnitude lower than the permeable luminal membrane, but tight junction H₂O permeability may be important if the basolateral membrane is relatively impermeable to water. We should also keep an open mind regarding the potential contribution of KCC4-mediated water transport. Answers to these question may soon be determined as both claudin-2 and KCC4 knockout mouse models are available for testing these central issues. Moreover, estimation of the intracellular osmolarity is also warranted to firmly establish whether there is an expected stepwise increase in osmolarity from interstitium to cytoplasm and from cytoplasm to CSF as the basic paradigm for osmotic water transport dictates.

The molecular mechanism for basolateral Na⁺ entry needs to be identified with greater certainty. This should be possible by combining flux studies with the genetically modified mice in existence. At the opposite side of the epithelium, an interesting development is the idea of CPE sensing the CSF and modulating the composition of the nascent CSF accordingly. For example, changes in CSF pH, HCO₃⁻, or CO₂ may be sensed by the CPE, and the cells might react by extruding more acid or base equivalents to sustain a suitable intraventricular milieu. Both the study of sensor proteins

and the cellular response in terms of transport will need to be investigated in the future.

There is significant interest in being able to manipulate the rate of CSF production. In conditions with high intracranial pressure or volume, it would be most helpful if further CSF volume secretion could be prevented by pharmacological means. Conversely, there is some evidence of lower CSF volume that perhaps would increase the risk of brain damage because of the greater mechanical forces acting on the brain parenchyma. Obvious targets for future therapy would include AQP1, Ncbe, AE2, and the V1a vasopressin receptors. Thus there are plenty of reasons for a continued strong interest in choroid plexus biology from the point of view of the cell polarization biologist, the epithelial transport physiologist, as well as the neurologist/neurosurgeon.

ACKNOWLEDGMENTS

We thank Drs. Kenneth R. Spring and Francisco J Alvarez-Leefmans for helpful discussion and valuable comments.

Address for reprint requests and other correspondence: J. Praetorius, Dept. of Biomedicine, Aarhus University-Health, Wilhelm Meyers Allé 3, Bldg 1233/1234, 8000 Aarhus C, Denmark.

DISCLOSURES

No conflicts of interest, financial or otherwise, are declared by the authors.

REFERENCES

- Aguzzi ABS, Paulus W. Choroid plexus tumours. In: *World Health Organization Classification of Tumours. Pathology and Genetics of Tumours of the Nervous System*, edited by Kleihues P, Cavenee WK. Lyon: IARC, 2000, p. 84–86.
- Albeck MJ, Skak C, Nielsen PR, Olsen KS, Borgesen SE, Gjerris F. Age dependency of resistance to cerebrospinal fluid outflow. *J Neurosurg* 89: 275–278, 1998.
- Alberts B, Johnson A, Lewis J, Raff M, Roberts K, Walter P. *Molecular Biology of the Cell*. New York: Garland Science, 2007.
- Alper SL. Molecular physiology and genetics of Na⁺-independent SLC4 anion exchangers. *J Exp Biol* 212: 1672–1683, 2009.
- Alper SL, Stuart-Tilley A, Simmons CF, Brown D, Drenckhahn D. The fodrin-ankyrin cytoskeleton of choroid plexus preferentially colocalizes with apical Na⁺K⁺-ATPase rather than with basolateral anion exchanger AE2. *J Clin Invest* 93: 1430–1438, 1994.
- Alvira-Butero X, Carro EM. Clearance of amyloid-beta peptide across the choroid plexus in Alzheimer's disease. *Curr Aging Sci* 3: 219–229, 2010.
- Ames A 3rd, Higashi K, Nesbitt FB. Effects of pCO₂ acetazolamide and ouabain on volume and composition of choroid-plexus fluid. *J Physiol* 181: 516–524, 1965.
- Amin MS, Reza E, Wang H, Leenen FH. Sodium transport in the choroid plexus and salt-sensitive hypertension. *Hypertension* 54: 860–867, 2009.
- Amin MS, Wang H, Reza E, Whitman SC, Tuana BS, Leenen FHH. Distribution of epithelial sodium channels and mineralocorticoid receptors in cardiovascular regulatory centers in rat brain. *Am J Physiol Regul Integr Comp Physiol* 289: R1787–R1797, 2005.
- Andreoli TE, Schafer JA, Troutman SL. Perfusion rate-dependence of transepithelial osmosis in isolated proximal convoluted tubules: estimation of the hydraulic conductance. *Kidney Int* 14: 263–269, 1978.
- Arendash GW, Schleif W, Rezai-Zadeh K, Jackson EK, Zacharia LC, Cracchiolo JR, Shippy D, Tan J. Caffeine protects Alzheimer's mice against cognitive impairment and reduces brain beta-amyloid production. *Neuroscience* 142: 941–952, 2006.
- Avninder S, Vermani S, Shruti S, Chand K. Papillary meningioma: a rare but distinct variant of malignant meningioma. *Diagnostic Pathol* 2: 2007.
- Baines AJ. The spectrin-ankyrin-4.1-adducin membrane skeleton: adapting eukaryotic cells to the demands of animal life. *Protoplasma* 244: 99–131, 2010.
- Bairamian D, Johanson CE, Parmelee JT, Epstein MH. Potassium cotransport with sodium and chloride in the choroid plexus. *J Neurochem* 56: 1623–1629, 1991.
- Banizs B, Komlosi P, Bevensee MO, Schwiebert EM, Bell PD, Yoder BK. Altered pH_i regulation and Na⁺/HCO₃⁻ transporter activity in choroid plexus of cilia-defective Tg737(orp) mutant mouse. *Am J Physiol Cell Physiol* 292: C1409–C1416, 2007.
- Banizs B, Pike MM, Millican CL, Ferguson WB, Komlosi P, Sheetz J, Bell PD, Schwiebert EM, Yoder BK. Dysfunctional cilia lead to altered ependyma and choroid plexus function, and result in the formation of hydrocephalus. *Development* 132: 5329–5339, 2005.
- Bano D, Nicotera P. Ca²⁺ signals and neuronal death in brain ischemia. *Stroke* 38: 674–676, 2007.
- Barkai AI, Meltzer HL. Regulation of calcium entry into the extracellular environment of the rat brain. *J Neurosci* 2: 1322–1328, 1982.
- Begley DJ, Brightman MW. Structural and functional aspects of the blood-brain barrier. *Prog Drug Res* 61: 39–78, 2003.
- Bellur SN, Chandra V, McDonald LW. Arachnoidal cell hyperplasia. Its relationship to aging and chronic renal failure. *Arch Pathol Lab Med* 104: 414–416, 1980.
- Berridge MJ. Neuronal calcium signaling. *Neuron* 21: 13–26, 1998.
- Berry CA. Water permeability and pathways in the proximal tubule. *Am J Physiol Renal Physiol* 245: F279–F294, 1983.
- Borke JL, Caride AJ, Yaksh TL, Penniston JT, Kumar R. Cerebrospinal fluid calcium homeostasis: evidence for a plasma membrane Ca²⁺-pump in mammalian choroid plexus. *Brain Res* 489: 355–360, 1989.
- Boron WF. Evaluating the role of carbonic anhydrases in the transport of HCO₃⁻-related species. *Biochim Biophys Acta* 1804: 410–421, 2010.
- Boron WF, Boulpaep EL. *Medical Physiology*. Philadelphia, PA: Saunders, 2012.
- Boulpaep EL. Ion permeability of the peritubular and luminal membrane of the renal tubular cell. In: *Transport und Funktion Intracellulärer Elektrolyte*, edited by Kruck F. Munich: Urban und Schwarzenberg, 1967, p. 98–107.
- Bouzinova EV, Praetorius J, Virkki LV, Nielsen S, Boron WF, Aalkjaer C. Na⁺-dependent HCO₃⁻ uptake into the rat choroid plexus epithelium is partially DIDS sensitive. *Am J Physiol Cell Physiol* 289: C1448–C1456, 2005.
- Bowman GL, Dodge H, Frei B, Calabrese C, Oken BS, Kaye JA, Quinn JF. Ascorbic acid and rates of cognitive decline in Alzheimer's disease. *J Alzheimers Dis* 16: 93–98, 2009.
- Brown PD, Davies SL, Speake T, Millar ID. Molecular mechanisms of cerebrospinal fluid production. *Neuroscience* 129: 957–970, 2004.
- Brown PD, Loo DD, Wright EM. Ca²⁺-activated K⁺ channels in the apical membrane of *Necturus* choroid plexus. *J Membr Biol* 105: 207–219, 1988.
- Burbach JP, van Schaick HS, de Bree FM, Lopes da Silva S, Adan RA. Functional domains in the oxytocin gene for regulation of expression and biosynthesis of gene products. *Adv Exp Med Biol* 395: 9–21, 1995.
- Burg MB, Orloff J. Control of fluid absorption in the renal proximal tubule. *J Clin Invest* 47: 2016–2024, 1968.

33. Burghardt B, Elkaer ML, Kwon TH, Racz GZ, Varga G, Steward MC, Nielsen S. Distribution of aquaporin water channels AQP1 and AQP5 in the ductal system of the human pancreas. *Gut* 52: 1008–1016, 2003.
34. Burghardt B, Nielsen S, Steward MC. The role of aquaporin water channels in fluid secretion by the exocrine pancreas. *J Membr Biol* 210: 143–153, 2006.
35. Calhoun MC, Hurt HD, Eaton HD, Rousseau JE Jr, Hall RC Jr. Rates of formation and absorption of cerebrospinal fluid in bovine hypovitaminosis A. *J Dairy Sci* 50: 1489–1494, 1967.
36. Canitano A, Papa M, Boscia F, Castaldo P, Sellitti S, Tagliatela M, Annunziato L. Brain distribution of the $\text{Na}^+/\text{Ca}^{2+}$ exchanger-encoding genes NCX1, NCX2, and NCX3 and their related proteins in the central nervous system. *Ann NY Acad Sci* 976: 394–404, 2002.
37. Carmosino M, Valenti G, Caplan M, Svelto M. Polarized traffic towards the cell surface: how to find the route. *Biol Cell* 102: 75–91, 2010.
38. Case RM, Harper AA, Scratcherd T. Water and electrolyte secretion by the perfused pancreas of the cat. *J Physiol* 196: 133–149, 1968.
39. Chai SY, McKinley MJ, Mendelsohn FA. Distribution of angiotensin converting enzyme in sheep hypothalamus and medulla oblongata visualized by in vitro autoradiography. *Clin Exp Hypertens A* 9: 449–460, 1987.
40. Chai SY, Mendelsohn FA, Paxinos G. Angiotensin converting enzyme in rat brain visualized by quantitative in vitro autoradiography. *Neuroscience* 20: 615–627, 1987.
41. Chodobski A, Szmydynger-Chodobska J. Choroid plexus: target for polypeptides and site of their synthesis. *Microsc Res Tech* 52: 65–82, 2001.
42. Chodobski A, Szmydynger-Chodobska J, Johanson CE. Vasopressin mediates the inhibitory effect of central angiotensin II on cerebrospinal fluid formation. *Eur J Pharmacol* 347: 205–209, 1998.
43. Choe S, Rosenberg JM, Abramson J, Wright EM, Grabe M. Water permeation through the sodium-dependent galactose cotransporter vSGLT. *Biophys J* 99: L56–58, 2010.
44. Christensen O, Zeuthen T. Maxi K^+ channels in leaky epithelia are regulated by intracellular Ca^{2+} , pH and membrane potential. *Pflügers Arch* 408: 1987.
45. Cowan F, Whitelaw A. Acute effects of acetazolamide on cerebral blood flow velocity and pCO_2 in the newborn infant. *Acta Paediatr Scand* 80: 22–27, 1991.
46. Crambert G, Fuzesi M, Garty H, Karlsh S, Geering K. Phospholemman (FXDI) associates with Na,K-ATPase and regulates its transport properties. *Proc Natl Acad Sci USA* 99: 11476–11481, 2002.
47. Crambert G, Hasler U, Beggah AT, Yu C, Modyanov NN, Horisberger JD, Lelievre L, Geering K. Transport and pharmacological properties of nine different human Na,K-ATPase isozymes. *J Biol Chem* 275: 1976–1986, 2000.
48. Crum JM, Alvarez FJ, Alvarez-Leefmans FJ. The apical NKCC1 cotransporter debate (Abstract). *FASEB J* 26: 881–814, 2012.
49. Cserr HF. Physiology of the choroid plexus. *Physiol Rev* 51: 273–311, 1971.
50. Cserr HF, Harling-Berg CJ, Knopf PM. Drainage of brain extracellular fluid into blood and deep cervical lymph and its immunological significance. *Brain Pathol* 2: 269–276, 1992.
51. Curran PF, Macintosh JR. A model system for biological water transport. *Nature* 193: 347–348, 1962.
52. Curran PF, Solomon AK. Ion and water fluxes in the ileum of rats. *J Gen Physiol* 41: 143–168, 1957.
53. Cushing H. Studies on the cerebro-spinal fluid. I. Introduction. *J Med Res* 31: 1–19, 1914.
54. Cushing H. *The Third Circulation in Studies in Intracranial Circulation and Surgery*. London: Oxford Univ. Press, 1926.
55. Cutler RW, Page L, Galicich J, Watters GV. Formation and absorption of cerebrospinal fluid in man. *Brain* 91: 707–720, 1968.
56. Damkier HH, Aalkjaer C, Praetorius J. Na^+ -dependent HCO_3^- import by the *slc4a10* gene product involves Cl^- export. *J Biol Chem* 285: 26998–27007, 2010.
57. Damkier HH, Prasad V, Hubner CA, Praetorius J. Nhe1 is a luminal Na^+/H^+ exchanger in mouse choroid plexus and is targeted to the basolateral membrane in Ncbe/Nbcn2-null mice. *Am J Physiol Cell Physiol* 296: C1291–C1300, 2009.
58. Damkier HH, Nielsen S, Praetorius J. Molecular expression of *SLC4*-derived Na^+ -dependent anion transporters in selected human tissues. *Am J Physiol Regul Integr Comp Physiol* 293: R2136–R2146, 2007.
59. Damkier HH, Praetorius J. Genetic ablation of *Slc4a10* alters the expression pattern of transporters involved in solute movement in the mouse choroid plexus. *Am J Physiol Cell Physiol* 302: C1452–C1459, 2012.
60. Davson H, Segal MB. The effects of some inhibitors and accelerators of sodium transport on the turnover of ^{22}Na in the cerebrospinal fluid and the brain. *J Physiol* 209: 131–153, 1970.
61. Davson H, Segal MB. *Physiology of the CSF and Blood-Brain Barriers*. Boca Raton, FL: CRC, 1996, p. 1832.
62. Davson H, Welch K, Segal MB. *Physiology and Pathophysiology of the CSF*. Edinburgh: Churchill Livingstone, 1987.
63. De Kloet ER, Van Acker SA, Sibug RM, Oitzl MS, Meijer OC, Rahmouni K, de Jong W. Brain mineralocorticoid receptors and centrally regulated functions. *Kidney Int* 57: 1329–1336, 2000.
64. De RJ, Ames A 3rd, Nesbitt FB, Hofmann HF. Fluid formed by choroid plexus; a technique for its collection and a comparison of its electrolyte composition with serum and cisternal fluids. *J Neurophysiol* 23: 485–495, 1960.
65. Dean JB, Nattie EE. Central CO_2 chemoreception in cardiorespiratory control. *J Appl Physiol* 108: 976–978, 2010.
66. Deng QS, Johanson CE. Stilbenes inhibit exchange of chloride between blood, choroid plexus and the cerebrospinal fluid. *Brain Res* 510: 183–187, 1989.
67. Desir J, Moya G, Reish O, Van Regemorter N, Deconinck H, David KL, Meire FM, Abramowicz MJ. Borate transporter *SLC4A11* mutations cause both Harboyan syndrome and non-syndromic corneal endothelial dystrophy. *J Med Genet* 44: 322–326, 2007.
68. Desmond ME. Description of the occlusion of the spinal cord lumen in early human embryos. *Anat Rec* 204: 89–93, 1982.
69. Diamond JM. The reabsorptive function of the gall-bladder. *J Physiol* 161: 442–473, 1962.
70. Diamond JM. Transport of salt and water in rabbit and guinea pig gall bladder. *J Gen Physiol* 48: 1–14, 1964.
71. Diamond JM, Bossert WH. Standing-gradient osmotic flow. A mechanism for coupling of water and solute transport in epithelia. *J Gen Physiol* 50: 2061–2083, 1967.
72. Dockray GJ. The action of secretin, cholecystokinin-pancreozymin and caerulein on pancreatic secretion in the rat. *J Physiol* 225: 679–692, 1972.
73. Doczi T, Laszlo FA, Szerdahelyi P, Joo F. Involvement of vasopressin in brain edema formation: further evidence obtained from the Brattleboro diabetes insipidus rat with experimental subarachnoid hemorrhage. *Neurosurgery* 14: 436–441, 1984.
74. Doczi T, Szerdahelyi P, Gulya K, Kiss J. Brain water accumulation after the central administration of vasopressin. *Neurosurgery* 11: 402–407, 1982.
75. Dogterom J, van Wimersma Greidanus TB, De Wied D. Vasopressin in cerebrospinal fluid and plasma of man, dog, and rat. *Am J Physiol Endocrinol Metab Gastrointest Physiol* 234: E463–E467, 1978.
76. Dohrmann GJ. The choroid plexus in experimental hydrocephalus. A light and electron microscopic study in normal, hydrocephalic, and shunted hydrocephalic dogs. *J Neurosurg* 34: 56–69, 1971.
77. Dohrmann GJ, Bucy PC. Human choroid plexus: a light and electron microscopic study. *J Neurosurg* 33: 506–516, 1970.
78. Döring F, Derst C, Wischmeyer E, Karschin C, Schneggenburger R, Daut J, Karschin A. The epithelial inward rectifier channel Kir 7.1 displays unusual K^+ permeation properties. *J Neurosci* 18: 8625–8636, 1998.
79. Duran C, Thompson CH, Xiao Q, Hartzell HC. Chloride channels: often enigmatic, rarely predictable. *Annu Rev Physiol* 72: 95–121, 2010.

80. Durcan FJ, Corbett JJ, Wall M. The incidence of pseudotumor cerebri. Population studies in Iowa and Louisiana. *Arch Neurol* 45: 875–877, 1988.
81. Duyckaerts C, Delatour B, Potier MC. Classification and basic pathology of Alzheimer disease. *Acta Neuropathol* 118: 5–36, 2009.
82. Dziegielewska KM, Ek J, Habgood MD, Saunders NR. Development of the choroid plexus. *Microsc Res Tech* 52: 5–20, 2001.
83. Eaton DC, Malik B, Saxena NC, Al-Khalili OK, Yue G. Mechanisms of aldosterone's action on epithelial Na^+ transport. *J Membr Biol* 184: 313–319, 2001.
84. Ek CJ, Dziegielewska KM, Habgood MD, Saunders NR. Barriers in the developing brain and neurotoxicology. *Neurotoxicology* 33: 586–604, 2012.
85. Ellis DZ, Nathanson JA, Sweadner KJ. Carbachol inhibits Na^+/K^+ -ATPase activity in choroid plexus via stimulation of the NO/cGMP pathway. *Am J Physiol Cell Physiol* 279: C1685–C1693, 2000.
86. Epstein MH, Feldman AM, Brusilow SW. Cerebrospinal fluid production: stimulation by cholera toxin. *Science* 196: 1012–1013, 1977.
87. Epstein MH, Johanson CE. The Dandy-Walker syndrome. In: *Handbook of Clinical Neurology*, edited by Myrianthopoulos N. Amsterdam: Elsevier, 1987, p. 1–14.
88. Ernst SA, Palacios JR, Siegel GJ. Immunocytochemical localization of Na^+/K^+ -ATPase catalytic polypeptide in mouse choroid plexus. *J Histochem Cytochem* 34: 189–195, 1986.
89. Eversole UH, Rokowski WJ. Spinal puncture headache. *Calif Med* 81: 59–64, 1954.
90. Faivre J. Structure du conarium et des plexus choroïde chez l'homme et des animaux. *Gaz Med Paris* 9: 555–556, 1854.
91. Faraci FM, Kinzenbaw D, Heistad DD. Effect of endogenous vasopressin on blood flow to choroid plexus during hypoxia and intracranial hypertension. *Am J Physiol Heart Circ Physiol* 266: H393–H398, 1994.
92. Feldberg W, Sherwood SL. Effects of calcium and potassium injected into the cerebral ventricles of the cat. *J Physiol* 139: 408–416, 1957.
93. Fencel V, Gabel RA, Wolfe D. Composition of cerebral fluids in goats adapted to high altitude. *J Appl Physiol* 47: 508–513, 1979.
94. Feschenko MS, Donnet C, Wetzell RK, Asinowski NK, Jones LR, Sweadner KJ. Phospholemman, a single-span membrane protein, is an accessory protein of Na^+/K^+ -ATPase in cerebellum and choroid plexus. *J Neurosci* 23: 2161–2169, 2003.
95. Finkelstein A. *Water Movement Through Lipid Bilayers, Pores, and Plasma Membranes: Theory and Reality*. New York: Wiley Interscience, 1987.
96. Fischberg J. Fluid transport across leaky epithelia: central role of the tight junction and supporting role of aquaporins. *Physiol Rev* 90: 1271–1290, 2010.
97. Frankel H, Kazemi H. Regulation of CSF composition: blocking chloride-bicarbonate exchange. *J Appl Physiol* 55: 177–182, 1983.
98. Fujimoto Y, Matsushita H, Plese JP, Marino RJr. Hydrocephalus due to diffuse villous hyperplasia of the choroid plexus. Case report and review of the literature. *Pediatr Neurosurg* 40: 32–36, 2004.
99. Furuse M, Fujita K, Hiragi T, Fujimoto K, Tsukita S. Claudin-1 and -2: novel integral membrane proteins localizing at tight junctions with no sequence similarity to occludin. *J Cell Biol* 141: 1539–1550, 1998.
100. Galen C. *Opera Omnia*. Leipzig: Lipsiae Cnoblock, 1826.
101. Garcia-Segura LM, Baetens D, Roth J, Norman AW, Orci L. Immunohistochemical mapping of calcium-binding protein immunoreactivity in the rat central nervous system. *Brain Res* 296: 75–86, 1984.
102. Garton MJ, Keir G, Lakshmi MV, Thompson EJ. Age-related changes in cerebrospinal fluid protein concentrations. *J Neurol Sci* 104: 74–80, 1991.
103. Gehlert DR, Speth RC, Wamsley JK. Distribution of [^{125}I]angiotensin II binding sites in the rat brain: a quantitative autoradiographic study. *Neuroscience* 18: 837–856, 1986.
104. Giffard RG, Lee YS, Ouyang YB, Murphy SL, Monyer H. Two variants of the rat brain sodium-driven chloride bicarbonate exchanger (NCBE): developmental expression and addition of a PDZ motif. *Eur J Neurosci* 18: 2935–2945, 2003.
105. Gjerris F, Agerlin N, Borgesen SE, Buhl L, Haase J, Klinken L, Mortensen AC, Olsen JH, Ovesen N, Reske-Nielsen E, Schmidt K. Epidemiology and prognosis in children treated for intracranial tumours in Denmark 1960–1984. *Childs Nerv Syst* 14: 302–311, 1998.
106. Gomez-Sanchez EP, Ahmad N, Romero DG, Gomez-Sanchez CE. Is aldosterone synthesized within the rat brain? *Am J Physiol Endocrinol Metab* 288: E342–E346, 2005.
107. Green R, Giebisch G. Luminal hypotonicity: a driving force for fluid absorption from the proximal tubule. *Am J Physiol Renal Physiol* 246: F167–F174, 1984.
108. Greenberg MS. *Handbook of Neurosurgery*. Stuttgart, Germany: Thieme, 2001.
109. Gresz V, Kwon TH, Gong H, Agre P, Steward MC, King LS, Nielsen S. Immunolocalization of AQP-5 in rat parotid and submandibular salivary glands after stimulation or inhibition of secretion in vivo. *Am J Physiol Gastrointest Liver Physiol* 287: G151–G161, 2004.
110. Gresz V, Kwon TH, Hurley PT, Varga G, Zelles T, Nielsen S, Case RM, Steward MC. Identification and localization of aquaporin water channels in human salivary glands. *Am J Physiol Gastrointest Liver Physiol* 281: G247–G254, 2001.
111. Grzybowski DM, Holman DW, Katz SE, Lubow M. In vitro model of cerebrospinal fluid outflow through human arachnoid granulations. *Invest Ophthalmol Vis Sci* 47: 3664–3672, 2006.
112. Hajdu SI. A note from history: discovery of the cerebrospinal fluid. *Ann Clin Lab Sci* 33: 334–336, 2003.
113. Hallback DA, Jodal M, Lundgren O. Villous tissue osmolality, water and electrolyte transport in the cat small intestine at varying luminal osmolalities. *Acta Physiol Scand* 110: 95–100, 1980.
114. Hammad SM, Ranganathan S, Loukinova E, Twa WO, Argraves WS. Interaction of apolipoprotein J-amyloid beta-peptide complex with low density lipoprotein receptor-related protein-2/megalin. A mechanism to prevent pathological accumulation of amyloid beta-peptide. *J Biol Chem* 272: 18644–18649, 1997.
115. Han ME, Kim HJ, Lee YS, Kim DH, Choi JT, Pan CS, Yoon S, Baek SY, Kim BS, Kim JB, Oh SO. Regulation of cerebrospinal fluid production by caffeine consumption. *BMC Neurosci* 10: 110, 2009.
116. Held D, Fencel V, Pappenheimer JR. Electrical potential of cerebrospinal fluid. *J Neurophysiol* 27: 942–959, 1964.
117. Heron SE, Hernandez M, Edwards C, Edkins E, Jansen FE, Scheffer IE, SFB, Mulley JC. Neonatal seizures and long QT syndrome: a cardiocerebral channelopathy? *Epilepsia* 51: 293–296, 2010.
118. Hill AE, Shachar-Hill B. A new approach to epithelial isotonic fluid transport: an osmosensor feedback model. *J Membr Biol* 210: 77–90, 2006.
119. Hippocrates. *Hippocrates/Collected Works with an English translation by W. H.S. Jones*. London: Heinemann, 1923.
120. Ho HT, Dahlin A, Wang J. Expression profiling of solute carrier gene families at the blood-CSF barrier. *Front Pharmacol* 3: 154, 2012.
121. Ho PI, Ashline D, Dhitavat S, Ortiz D, Collins SC, Shea TB, Rogers E. Folate deprivation induces neurodegeneration: roles of oxidative stress and increased homocysteine. *Neurobiol Dis* 14: 32–42, 2003.
122. Hoenderop JG, Nilius B, Bindels RJ. Calcium absorption across epithelia. *Physiol Rev* 85: 373–422, 2005.
123. Horisberger JD, Rossier BC. Aldosterone regulation of gene transcription leading to control of ion transport. *Hypertension* 19: 221–227, 1992.
124. Huang BS, Leenen FH. Mineralocorticoid actions in the brain and hypertension. *Curr Hypertens Rep* 13: 214–220, 2011.
125. Hughes AL, Pakhomova A, Brown PD. Regulatory volume increase in epithelial cells isolated from the mouse fourth ventricle choroid plexus involves Na^+/H^+ exchange but not $\text{Na}^+/\text{K}^+/\text{2Cl}^-$ cotransport. *Brain Res* 1323: 1–10, 2010.
126. Husted RF, Reed DJ. Regulation of cerebrospinal fluid bicarbonate by the cat choroid plexus. *J Physiol* 267: 411–428, 1977.

127. Husted RF, Reed DJ. Regulation of cerebrospinal fluid potassium by the cat choroid plexus. *J Physiol* 259: 213–221, 1976.
128. Iencean SM. Idiopathic intracranial hypertension and idiopathic normal pressure hydrocephalus: diseases with opposite pathogenesis? *Med Hypotheses* 61: 526–528, 2003.
129. Iencean SM. Simultaneous hypersecretion of CSF and of brain interstitial fluid causes idiopathic intracranial hypertension. *Med Hypotheses* 61: 529–532, 2003.
130. Ikeda T, Furukawa Y, Mashimoto S, Takahashi K, Yamada M. Vitamin B₁₂ levels in serum and cerebrospinal fluid of people with Alzheimer's disease. *Acta Psychiatr Scand* 82: 327–329, 1990.
131. Imboden H, Harding JW, Hilgenfeldt U, Celio MR, Felix D. Localization of angiotensinogen in multiple cell types of rat brain. *Brain Res* 410: 74–77, 1987.
132. Imura A, Tsuji Y, Murata M, Maeda R, Kubota K, Iwano A, Obuse C, Togashi K, Tominaga M, Kita N, Tomiyama K, Iijima J, Nabeshima Y, Fujioka M, Asato R, Tanaka S, Kojima K, Ito J, Nozaki K, Hashimoto N, Ito T, Nishio T, Uchiyama T, Fujimori T. α -Klotho as a regulator of calcium homeostasis. *Science* 316: 1615–1618, 2007.
133. Inagami T, Celio MR, Clemens DL, Lau D, Takii Y, Kasselberg AG, Hirose S. Renin in rat and mouse brain: immunohistochemical identification and localization. *Clin Sci* 59 Suppl 6: 49s–51s, 1980.
134. Ironside JW. *Diagnostic Pathology of Nervous System Tumours*. Edinburgh: Churchill Livingstone, 2002, p. 651.
135. Irsigler GB, Severinghaus JW. Clinical problems of ventilatory control. *Annu Rev Med* 31: 109–126, 1980.
136. Jack CR Jr, Knopman DS, Jagust WJ, Shaw LM, Aisen PS, Weiner MW, Petersen RC, Trojanowski JQ. Hypothetical model of dynamic biomarkers of the Alzheimer's pathological cascade. *Lancet Neurol* 9: 119–128, 2010.
137. Jacobs S, Ruusuvaari E, Sipilä ST, Haapanen A, Damkier HH, Kurth I, Hentschke M, Schweizer M, Rudhard Y, Laatikainen LM, Tyynelä J, Praetorius J, Voipio J, Hubner CA. Mice with targeted *Slc4a10* gene disruption have small brain ventricles and show reduced neuronal excitability. *Proc Natl Acad Sci USA* 105: 311–316, 2008.
138. Jiao X, Sultana A, Garg P, Ramamurthy B, Vemuganti GK, Gangopadhyay N, Hejtmancik JF, Kannabiran C. Autosomal recessive corneal endothelial dystrophy (CHED2) is associated with mutations in *SLC4A11*. *J Med Genet* 44: 64–68, 2007.
139. Johanson CE, Duncan JA, Stopa EG, Baird A. Enhanced prospects for drug delivery and brain targeting by the choroid plexus-CSF route. *Pharm Res* 22: 1011–1037, 2005.
140. Johanson CE, Murphy VA. Acetazolamide and insulin alter choroid plexus epithelial cell [Na⁺], pH, and volume. *Am J Physiol Renal Physiol* 258: F1538–F1546, 1990.
141. Johanson CE, Preston JE, Chodobski A, Stopa EG, Szmydynger-Chodobska J, McMillan PN. AVP V1 receptor-mediated decrease in Cl[−] efflux and increase in dark cell number in choroid plexus epithelium. *Am J Physiol Cell Physiol* 276: C82–C90, 1999.
142. Johanson CE, Reed DJ, Woodbury DM. Active transport of sodium and potassium by the choroid plexus of the rat. *J Physiol* 241: 359–372, 1974.
143. Johanson CE, Sweeney SM, Parmelee JT, Epstein MH. Cotransport of sodium and chloride by the adult mammalian choroid plexus. *Am J Physiol Cell Physiol* 258: C211–C216, 1990.
144. Johansson PA, Dziegielewska KM, Ek CJ, Habgood MD, Mollgard K, Potter A, Schuliga M, Saunders NR. Aquaporin-1 in the choroid plexuses of developing mammalian brain. *Cell Tissue Res* 322: 353–364, 2005.
145. Jones HC, Keep RF. Brain fluid calcium concentration and response to acute hypercalcaemia during development in the rat. *J Physiol* 402: 579–593, 1988.
146. Kageyama Y, Bravo EL. Hypertensive mechanisms associated with centrally administered aldosterone in dogs. *Hypertension* 11: 750–753, 1988.
147. Kajita H, Omori K, Matsuda H. The chloride channel ClC-2 contributes to the inwardly rectifying Cl[−] conductance in cultured porcine choroid plexus epithelial cells. *J Physiol* 523: 313–324, 2000.
148. Kajita H, Whitwell C, Brown PD. Properties of the inward-rectifying Cl[−] channel in rat choroid plexus: regulation by intracellular messengers and inhibition by divalent cations. *Pflügers Arch* 440: 933–940, 2000.
149. Kalaria RN, Premkumar DR, Lin CW, Kroon SN, Bae JY, Sayre LM, LaManna JC. Identification and expression of the Na⁺/H⁺ exchanger in mammalian cerebrovascular and choroidal tissues: characterisation by amiloride-sensitive [³H]MIA binding and RT-PCR analysis. *Brain Res* 58: 178–187, 1998.
150. Kallio H, Pastorekova S, Pastorek J, Waheed A, Sly WS, Mannisto S, Heikinheimo M, Parkkila S. Expression of carbonic anhydrases IX and XII during mouse embryonic development. *BMC Dev Biol* 6: 22, 2006.
151. Kao L, Kurtz LM, Shao X, Papadopoulos MC, Liu L, Bok D, Nusinowitz S, Chen B, Stella SL, Andre M, Weinreb J, Luong SS, Piri N, JMK, Newman D, Kurtz I. Severe neurologic impairment in mice with targeted disruption of the electrogenic sodium bicarbonate cotransporter NBCe2 (*Slc4a5* gene). *J Biol Chem* 286: 32563–32574, 2011.
152. Karadsheh MF, Byun N, Mount DB, Delpire E. Localization of the KCC4 potassium-chloride cotransporter in the nervous system. *Neuroscience* 123: 381–391, 2004.
153. Kaur C, Singh J, Lim MK, Ng BL, Yap EP, Ling EA. Studies of the choroid plexus and its associated ependymal cells in the lateral ventricles of rats following an exposure to a single non-penetrative blast. *Arch Histol Cytol* 59: 239–248, 1996.
154. Kazemi H, Choma L. H⁺ transport from CNS in hypercapnia and regulation of CSF [HCO₃[−]]. *J Appl Physiol* 42: 667–672, 1977.
155. Keep RF, Ulanski LJ, Xiang J, Ennis SR, Lorris Betz A. Blood-brain barrier mechanisms involved in brain calcium and potassium homeostasis. *Brain Res* 815: 200–205, 1999.
156. Keep RF, Xiang J, Betz AL. Potassium cotransport at the rat choroid plexus. *Am J Physiol Cell Physiol* 267: C1616–C1622, 1994.
157. Keep RF, Jones HC. A morphometric study on the development of the lateral ventricle choroid plexus, choroid plexus capillaries and ventricular ependyma in the rat. *Brain Res* 56: 47–53, 1990.
158. Keep RF, Smith DE. Choroid plexus transport: gene deletion studies. *Fluids Barriers CNS* 8: 26, 2011.
159. Kibble JD, Garner C, Kajita H, Colledge WH, Evans MJ, Radcliff R, Brown PD. Whole-cell Cl[−] conductances in mouse choroid plexus epithelial cells do not require CFTR expression. *Am J Physiol Cell Physiol* 272: C1899–C1907, 1997.
160. Kibble JD, Tresize AO, Brown PD. Properties of the cAMP-activated Cl[−] conductance in choroid plexus epithelial cells isolated from the rat. *J Physiol* 496: 69–80, 1996.
161. Kida S, Yamashita T, Kubota T, Ito H, Yamamoto S. A light and electron microscopic and immunohistochemical study of human arachnoid villi. *J Neurosurg* 69: 429–435, 1988.
162. Kim J, Jung Y. Increased aquaporin-1 and Na⁺-K⁺-2Cl[−] cotransporter 1 expression in choroid plexus leads to blood-cerebrospinal fluid barrier disruption and necrosis of hippocampal CA1 cells in acute rat models of hyponatremia. *J Neurosci Res* 90: 1437–1444, 2012.
163. Klarr SA, Ulanski LJ, Stummer W, Xiang J, Betz AL, Keep RF. The effects of hypo- and hyperkalemia on choroid plexus potassium transport. *Brain Res* 758: 39–44, 1997.
164. Knuckey NW, Preston J, Palm D, Epstein MH, Johanson C. Hydrocephalus decreases chloride efflux from the choroid plexus epithelium. *Brain Res* 618: 313–317, 1993.
165. Kohno M, Matsutani M, Sasaki T, Takakura K. Solitary metastasis to the choroid plexus of the lateral ventricle. Report of three cases and a review of the literature. *J Neurooncol* 27: 47–52, 1996.
166. Kotera T, Brown PD. Two types of potassium current in rat choroid plexus epithelial cells. *Pflügers Arch* 237: 1994.
167. Kratzer I, Vasiljevic A, Rey C, Fevre-Montange M, Saunders N, Strazielle N, Ghersi-Egea JF. Complexity and developmental changes in the expression pattern of claudins at the blood-CSF barrier. *Histochem Cell Biol* 138: 861–879, 2012.
168. Kriegs JO, Homann V, Kinne-Saffran E, Kinne RK. Identification and subcellular localization of paracellin-1 (claudin-16) in human salivary glands. *Histochem Cell Biol* 128: 45–53, 2007.

169. Krug SM, Gunzel D, Conrad MP, Lee IF, Amasheh S, Fromm M, Yu AS. Charge-selective claudin channels. *Ann NY Acad Sci* 1257: 20–28, 2012.
170. Kuro-o M. Klotho. *Pflügers Arch* 459: 333–343, 2010.
171. Kuro-o M, Matsumura Y, Aizawa H, Kawaguchi H, Suga T, Utsugi T, Ohyama Y, Kurabayashi M, Kaname T, Kume E, Iwasaki H, Iida A, Shiraki-Iida T, Nishikawa S, Nagai R, Nabeshima YI. Mutation of the mouse klotho gene leads to a syndrome resembling ageing. *Nature* 390: 45–51, 1997.
172. Lach B, Scheithauer BW. Colloid cyst of the third ventricle: a comparative ultrastructural study of neuraxis cysts and choroid plexus epithelium. *Ultrastruct Pathol* 16: 331–349, 1992.
173. Larsen EH, Willumsen NJ, Mobjerg N, Sorensen JN. The lateral intercellular space as osmotic coupling compartment in isotonic transport. *Acta Physiol* 195: 171–186, 2009.
174. Leenen FH. The central role of the brain aldosterone-“ouabain” pathway in salt-sensitive hypertension. *Biochim Biophys Acta* 1802: 1132–1139, 2010.
175. Li SA, Watanabe M, Yamada H, Nagai A, Kinuta M, Takei K. Immunohistochemical localization of Klotho protein in brain, kidney, and reproductive organs of mice. *Cell Struct Funct* 29: 91–99, 2004.
176. Liddelow SA, Temple S, Mollgard K, Gehwolf R, Wagner A, Bauer H, Bauer HC, Phoenix TN, Dziegielewska KM, Saunders NR. Molecular characterisation of transport mechanisms at the developing mouse blood-CSF interface: a transcriptome approach. *PLoS One* 7: e33554, 2012.
177. Liedtke W, Friedman JM. Abnormal osmotic regulation in *trpv4* $-/-$ mice. *Proc Natl Acad Sci USA* 100: 13698–13703, 2003.
178. Lindsey AE, Schneider K, Simmons DM, Baron R, Lee BS, Kopito RR. Functional expression and subcellular localization of an anion exchanger cloned from choroid plexus. *Proc Natl Acad Sci USA* 87: 5278–5282, 1990.
179. Lindvall M, Owman C. Autonomic nerves in the mammalian choroid plexus and their influence on the formation of cerebrospinal fluid. *J Cereb Blood Flow Metab* 1: 245–266, 1981.
180. Lindvall M, Owman C. Sympathetic nervous control of cerebrospinal fluid production in experimental obstructive hydrocephalus. *Exp Neurol* 84: 606–615, 1984.
181. Lindvall-Axelsson M, Nilsson C, Owman C, Winblad B. Inhibition of cerebrospinal fluid formation by omeprazole. *Exp Neurol* 115: 394–399, 1992.
182. Liu J, Seet LF, Koh LW, Venkatraman A, Venkataraman D, Mohan RR, Praetorius J, Bonanno JA, Aung T, Vithana EN. Depletion of *SLC4A11* causes cell death by apoptosis in an immortalized human corneal endothelial cell line. *Invest Ophthalmol Vis Sci* 53: 3270–3279, 2012.
183. Liu Q, Zhang J, Tran H, Verbeek MM, Reiss K, Estus S, Bu G. LRP1 shedding in human brain: roles of ADAM10 and ADAM17. *Mol Neurodegener* 4: 17, 2009.
184. Lobas MA, Helsper L, Vernon CG, Schreiner D, Zhang Y, Holtzman MJ, Thedens DR, Weiner JA. Molecular heterogeneity in the choroid plexus epithelium: the 22-member gamma-protocadherin family is differentially expressed, apically localized, and implicated in CSF regulation. *J Neurochem* 120: 913–927, 2012.
185. Logan A, Frautschy SA, Baird A. Basic fibroblast growth factor and central nervous system injury. *Ann NY Acad Sci* 638: 474–476, 1991.
186. Lohmann C, Wong ROL. Regulation of dendritic growth and plasticity by local and global calcium dynamics. *Cell Calcium* 37: 403–409, 2005.
187. Lourenco SV, Coutinho-Camillo CM, Buim ME, Uyekita SH, Soares FA. Human salivary gland branching morphogenesis: morphological localization of claudins and its parallel relation with developmental stages revealed by expression of cytoskeleton and secretion markers. *Histochem Cell Biol* 128: 361–369, 2007.
188. Lowery LA, Sive H. Totally tubular: the mystery behind function and origin of the brain ventricular system. *Bioessays* 31: 446–458, 2009.
189. Lu J, Kaur C, Ling EA. An immunohistochemical study of the intraventricular macrophages in induced hydrocephalus in prenatal rats following a maternal injection of 6-aminocotinamide. *J Anat* 188: 491–495, 1996.
190. Lundberg A. Anionic dependence of secretion and secretory potentials in the perfused sublingual gland. *Acta Physiol Scand* 40: 101–112, 1957.
191. Lundberg A. Secretory potentials and secretion in the sublingual gland of the cat. *Nature* 177: 1080–1081, 1956.
192. Ma T, Song Y, Gillespie A, Carlson EJ, Epstein CJ, Verkman AS. Defective secretion of saliva in transgenic mice lacking aquaporin-5 water channels. *J Biol Chem* 274: 20071–20074, 1999.
193. MacAulay N, Zeuthen T. Water transport between CNS compartments: contributions of aquaporins and cotransporters. *Neuroscience* 168: 941–956, 2010.
194. Madhavi C, Jacob M. Light and electron microscopic structure of choroid plexus in hydrocephalic guinea pig. *Indian J Med Res* 101: 217–224, 1995.
195. Maktabi MA, Heistad DD, Faraci FM. Effects of angiotensin II on blood flow to choroid plexus. *Am J Physiol Heart Circ Physiol* 258: H414–H418, 1990.
196. Maren TH. The binding of inhibitors to carbonic anhydrase in vivo: drugs as markers for enzyme. *Biochem Pharmacol* 9: 39–48, 1962.
197. Maria OM, Kim JW, Gerstenhaber JA, Baum BJ, Tran SD. Distribution of tight junction proteins in adult human salivary glands. *J Histochem Cytochem* 56: 1093–1098, 2008.
198. Mariano C, Sasaki H, Brites D, Brito MA. A look at tricellulin and its role in tight junction formation and maintenance. *Eur J Cell Biol* 90: 787–796, 2011.
199. Marques F, Sousa JC, Coppola G, Gao F, Puga R, Brentani H, Geschwind DH, Sousa N, Correia-Neves M, Palha JA. Transcriptome signature of the adult mouse choroid plexus. *Fluids Barriers CNS* 8: 10, 2011.
200. Marrs JA, Napolitano EW, Murphy-Erdosh C, Mays RW, Reichardt LF, Nelson WJ. Distinguishing roles of the membrane-cytoskeleton and cadherin mediated cell-cell adhesion in generating different Na^+ , K^+ -ATPase distributions in polarized epithelia. *J Cell Biol* 123: 149–164, 1993.
201. Mason BL, Pariante CM, Jamel S, Thomas SA. Central nervous system (CNS) delivery of glucocorticoids is fine-tuned by saturable transporters at the blood-CNS barriers and nonbarrier regions. *Endocrinology* 151: 5294–5305, 2010.
202. Masuzawa T, Ohta T, Kawamura M, Nakahara N, Sato F. Immunohistochemical localization of Na^+ , K^+ -ATPase in the choroid plexus. *Brain Res* 302: 357–362, 1984.
203. Maxwell DS, Pease DC. The electron microscopy of the choroid plexus. *J Biophys Biochem Cytol* 2: 467–474, 1956.
204. Maxwell WL, Hardy IG, Watt C, McGadey J, Graham DI, Adams JH, Gennarelli TA. Changes in the choroid plexus, responses by intrinsic ependymal cells and recruitment from monocytes after experimental head acceleration injury in the non-human primate. *Acta Neuropathol* 84: 78–84, 1992.
205. Mayer SE, Sanders-Bush E. Sodium-dependent antiporters in choroid plexus epithelial cultures from rabbit. *J Neurochem* 60: 1308–1316, 1993.
206. McCarthy KD, Reed DJ. The effect of acetazolamide and furosemide on cerebrospinal fluid production and choroid plexus carbonic anhydrase activity. *J Pharmacol Exp Ther* 189: 194–201, 1974.
207. McMurtrie HL, Cleary HJ, Alvarez BV, Loiselle FB, Sterling D, Morgan PE, Johnson DE, Casey JR. The bicarbonate transport metabolon. *J Enzyme Inhib Med Chem* 19: 231–236, 2004.
208. Melby JM, Miner LC, Reed DJ. Effect of acetazolamide and furosemide on the production and composition of cerebrospinal fluid from the cat choroid plexus. *Can J Physiol Pharmacol* 60: 405–409, 1982.
209. Mellman I, Nelson WJ. Coordinated protein sorting, targeting and distribution in polarized cells. *Nat Rev Mol Cell Biol* 9: 833–845, 2008.
210. Millar ID, Brown PD. Characterisation of a non-selective cation channel in mouse choroid plexus epithelial cells (Abstract). *Proc Physiol Soc* 2: PC16, 2006.
211. Millar ID, Brown PD. NBCe2 exhibits a 3 HCO_3^- :1 Na^+ stoichiometry in mouse choroid plexus epithelial cells. *Biochem Biophys Res Commun* 373: 550–554, 2008.
212. Millar ID, Bruce JI, Brown PD. Ion channel diversity, channel expression and function in the choroid plexuses. *Cerebrospinal Fluid Res* 4: 2007.
213. Millgard K, Milinowska DH, Saunders NR. Lack of correlation between tight junction morphology and permeability properties in developing choroid plexus. *Nature* 264: 293–294, 1976.

214. Mitchell RA. Respiratory chemosensitivity in the medulla oblongata. *J Physiol* 202: 3P–4P, 1969.
215. Mori K, Tsutsumi K, Kurihara M, Kawaguchi T, Niwa M. Alteration of atrial natriuretic peptide receptors in the choroid plexus of rats with induced or congenital hydrocephalus. *Childs Nerv Syst* 6: 190–193, 1990.
216. Murphy VA, Johanson CE. Alteration of sodium transport by the choroid plexus with amiloride. *Biochim Biophys Acta* 979: 187–192, 1989.
217. Murphy VA, Smith QR, Rapoport SI. Homeostasis of brain and cerebrospinal fluid calcium concentrations during chronic hypo- and hypercalcemia. *J Neurochem* 47: 1735–1741, 1986.
218. Murphy VA, Smith QR, Rapoport SI. Regulation of brain and cerebrospinal fluid calcium by brain barrier membranes following vitamin D-related chronic hypo- and hypercalcemia in rats. *J Neurochem* 51: 1777–1782, 1988.
219. Murphy VA, Smith QR, Rapoport SI. Saturable transport of Ca into CSF in chronic hypo- and hypercalcemia. *J Neurosci Res* 30: 421–426, 1991.
220. Murphy VA, Johanson CE. Acidosis, acetazolamide, and amiloride: effects on ^{22}Na transfer across the blood-brain and blood-CSF barriers. *J Neurochem* 52: 1058–1063, 1989.
221. Murphy VA, Johanson CE. $\text{Na}^+\text{-H}^+$ exchange in choroid plexus and CSF in acute metabolic acidosis or alkalosis. *Am J Physiol Renal Physiol* 258: F1528–F1537, 1990.
222. Muto S, Hata M, Taniguchi J, Tsuruoka S, Moriwaki K, Saitou M, Furuse K, Sasaki H, Fujimura A, Imai M, Kusano E, Tsukita S, Furuse M. Claudin-2-deficient mice are defective in the leaky and cation-selective paracellular permeability properties of renal proximal tubules. *Proc Natl Acad Sci USA* 107: 8011–8016, 2010.
223. Nakamura N, Suzuki Y, Sakuta H, Ookata K, Kawahara K, Hirose S. Inwardly rectifying K^+ channel Kir7.1 is highly expressed in thyroid follicular cells, intestinal epithelial cells and choroid plexus epithelial cells: implication for a functional coupling with $\text{Na}^+\text{-K}^+\text{-ATPase}$. *Biochem J* 342: 329–336, 1999.
224. Narita K, Kawate T, Kakinuma N, Takeda S. Multiple primary cilia modulate the fluid transcytosis in choroid plexus epithelium. *Traffic* 11: 287–301, 2010.
225. Nattie EE. Brain and cerebrospinal fluid ionic composition and ventilation in acute hypercapnia. *Respir Physiol* 40: 309–322, 1980.
226. Nejsum LN, Kwon TH, Jensen UB, Fumagalli O, Frokiaer J, Krane CM, Menon AG, King LS, Agre PC, Nielsen S. Functional requirement of aquaporin-5 in plasma membranes of sweat glands. *Proc Natl Acad Sci USA* 99: 5111–5116, 2002.
227. Neukirchen D, Bradke F. Neuronal polarization and the cytoskeleton. *Semin Cell Dev Biol* 22: 825–833, 2011.
228. Nielsen S, Smith BL, Christensen EI, Agre P. Distribution of the aquaporin CHIP in secretory and resorptive epithelia and capillary endothelia. *Proc Natl Acad Sci USA* 90: 7275–7279, 1993.
229. Nilsson C, Lindvall-Axelsson M, Owman C. Neuroendocrine regulatory mechanisms in the choroid plexus-cerebrospinal fluid system. *Brain Res* 17: 109–138, 1992.
230. O'Rahilly R, Muller F. Neurulation in the normal human embryo. *Ciba Found Symp* 181: 70–82, 1994.
231. Oberwinkler J, Lis A, Giehl KM, Flockerzi V, Philipp SE. Alternative splicing switches the divalent cation selectivity of TRPM3 channels. *J Biol Chem* 280: 22540–22548, 2005.
232. Oi S. Classification of hydrocephalus: critical analysis of classification categories and advantages of "Multi-categorical Hydrocephalus Classification" (Mc HC). *Childs Nerv Syst* 27: 1523–1533, 2011.
233. Orłowski J, Grinstein S. Diversity of the mammalian sodium/proton exchanger SLC9 gene family. *Pflügers Arch* 447: 549–565, 2004.
234. Oshio K, Watanabe H, Song Y, Verkman AS, Manley GT. Reduced cerebrospinal fluid production and intracranial pressure in mice lacking choroid plexus water channel Aquaporin-1. *FASEB J* 19: 76–78, 2005.
235. Ostrowski NL, Lolait SJ, Bradley DJ, O'Carroll AM, Brownstein MJ, Young WS 3rd. Distribution of V1a and V2 vasopressin receptor messenger ribonucleic acids in rat liver, kidney, pituitary and brain. *Endocrinology* 131: 533–535, 1992.
236. Palm D, Knuckey N, Guglielmo M, Watson P, Primiano M, Johanson C. Choroid plexus electrolytes and ultrastructure following transient forebrain ischemia. *Am J Physiol Regul Integr Comp Physiol* 269: R73–R79, 1995.
237. Pappenheimer JR, Heisey SR, Jordan EF, Downer Jd. Perfusion of the cerebral ventricular system in unanesthetized goats. *Am J Physiol* 203: 763–774, 1962.
238. Parker MD, Musa-Aziz R, Rojas JD, Choi I, Daly CM, Boron WF. Characterization of human SLC4A10 as an electroneutral Na/HCO_3 cotransporter (NBCn2) with Cl^- self-exchange activity. *J Biol Chem* 283: 12777–12788, 2008.
239. Pascale CL, Miller MC, Chiu C, Boylan M, Caralopoulos IN, Gonzalez L, Johanson CE, Silverberg GD. Amyloid-beta transporter expression at the blood-CSF barrier is age-dependent. *Fluids Barriers CNS* 8: 21, 2011.
240. Pearson MM, Lu J, Mount DB, Delpire E. Localization of the $\text{K}^+\text{-Cl}^-$ cotransporter, KCC3, in the central and peripheral nervous systems: expression in the choroid plexus, large neurons and white matter tracts. *Neuroscience* 103: 481–491, 2001.
241. Peppi M, Ghabriel MN. Tissue-specific expression of the tight junction proteins claudins and occludin in the rat salivary glands. *J Anat* 205: 257–266, 2004.
242. Persson BE, Spring KR. Gallbladder epithelial cell hydraulic water permeability and volume regulation. *J Gen Physiol* 79: 481–505, 1982.
243. Pestov NB, Dmitriev RI, Kostina MB, Korneenko TV, Shakhparonov MI, Modyanov NN. Structural evolution and tissue-specific expression of tetrapod-specific second isoform of secretory pathway $\text{Ca}^{2+}\text{-ATPase}$. *Biochem Biophys Res Commun* 417: 1298–1303, 2012.
244. Pestov NB, Romanova LG, Korneenko TV, Egorov MV, Kostina MB, Sverdllov VE, Askari A, Shakhparonov MI, Modyanov NN. Ouabain-sensitive H,K-ATPase: tissue-specific expression of the mammalian genes encoding the catalytic alpha subunit. *FEBS Lett* 440: 320–324, 1998.
245. Phillips PA, Abrahams JM, Kelly J, Paxinos G, Grzonka Z, Mendelsohn FA, Johnston CI. Localization of vasopressin binding sites in rat brain by in vitro autoradiography using a radioiodinated V1 receptor antagonist. *Neuroscience* 27: 749–761, 1988.
246. Plotkin MD, Kaplan MR, Peterson LN, Gullans SR, Hebert SC, Delpire E. Expression of the $\text{Na}^+\text{-K}^+\text{-2Cl}^-$ cotransporter BSC2 in the nervous system. *Am J Physiol Cell Physiol* 272: C173–C183, 1997.
247. Poca MA, Sahuquillo J. Short-term medical management of hydrocephalus. *Expert Opin Pharmacother* 6: 1525–1538, 2005.
248. Pollay M. The function and structure of the cerebrospinal fluid outflow system. *Cerebrospinal Fluid Res* 7: 9, 2010.
249. Pollay M, Hisey B, Reynolds E, Tomkins P, Stevens FA, Smith R. Choroid plexus Na^+/K^+ -activated adenosine triphosphatase and cerebrospinal fluid formation. *Neurosurgery* 17: 768–772, 1985.
250. Pollay M, Curl F. Secretion of cerebrospinal fluid by the ventricular ependyma of the rabbit. *Am J Physiol* 213: 1031–1038, 1967.
251. Praetorius J. Water and solute secretion by the choroid plexus. *Pflügers Arch* 454: 1–18, 2007.
252. Praetorius J, Nejsum LN, Nielsen S. A SLC4A10 gene product maps selectively to the basolateral membrane of choroid plexus epithelial cells. *Am J Physiol Cell Physiol* 286: C601–C610, 2004.
253. Praetorius J, Nielsen S. Distribution of sodium transporters and aquaporin-1 in the human choroid plexus. *Am J Physiol Cell Physiol* 291: C59–C67, 2006.
254. Preston GM, Agre P. Isolation of the cDNA for erythrocyte integral membrane protein of 28 kilodaltons: member of an ancient channel family. *Proc Natl Acad Sci USA* 88: 11110–11114, 1991.
255. Preston JE. Ageing choroid plexus-cerebrospinal fluid system. *Microsc Res Tech* 52: 31–37, 2001.
256. Preston JE, Hipkiss AR, Himsworth DT, Romero IA, Abbott JN. Toxic effects of beta-amyloid(25–35) on immortalised rat brain endothelial cell: protection

- by carnosine, homocarnosine and beta-alanine. *Neurosci Lett* 242: 105–108, 1998.
257. Puzzo D, Privitera L, Leznik E, Fa M, Staniszewski A, Palmeri A, Arancio O. Picomolar amyloid-beta positively modulates synaptic plasticity and memory in hippocampus. *J Neurosci* 28: 14537–14545, 2008.
 258. Quinton PM, Wright EM, Tormey JM. Localization of sodium pumps in the choroid plexus epithelium. *J Cell Biol* 58: 724–730, 1973.
 259. Rahner C, Mitic LL, Anderson JM. Heterogeneity in expression and subcellular localization of claudins 2, 3, 4, and 5 in the rat liver, pancreas, and gut. *Gastroenterology* 120: 411–422, 2001.
 260. Raichle ME, Grubb RL Jr. Regulation of brain water permeability by centrally-released vasopressin. *Brain Res* 143: 191–194, 1978.
 261. Raimondi AJ, Gutierrez FA. Diagnosis and surgical treatment of choroid plexus papillomas. *Childs Brain* 1: 81–115, 1975.
 262. Redzic ZB, Preston JE, Duncan JA, Chodobski A, Szmydynger-Chodobska J. The choroid plexus-cerebrospinal fluid system: from development to aging. *Curr Top Dev Biol* 71: 1–52, 2005.
 263. Reed DJ. The effect of furosemide on cerebrospinal fluid flow in rabbits. *Arch Int Pharmacodyn Ther* 178: 324–330, 1969.
 264. Reeder RF, Nattie EE, North WG. Effect of vasopressin on cold-induced brain edema in cats. *J Neurosurg* 64: 941–950, 1986.
 265. Reid EW. Intestinal absorption of solutions. *J Physiol* 28: 241–256, 1902.
 266. Rickert CH. Neuropathology and prognosis of foetal brain tumours. *Acta Neuropathol* 98: 567–576, 1999.
 267. Rickert CH, Probst-Cousin S, Gullotta F. Primary intracranial neoplasms of infancy and early childhood. *Childs Nerv Syst* 13: 507–513, 1997.
 268. Rodriguez-Moldes I, Timmermans JP, Adriaensen D, De Groodt-Lasseel MH, Scheuermann DW, Anadon R. Immunohistochemical localization of calbindin-D28K in the brain of a cartilaginous fish, the dogfish (*Scyliorhinus canicula* L.). *Acta Anat* 137: 293–302, 1990.
 269. Roepke TK, Kanda VA, Purtell K, King EC, Lerner DJ, Abbott GW. KCNE2 forms potassium channels with KCNA3 and KCNQ1 in the choroid plexus epithelium. *FASEB J* 25: 4264–4273, 2011.
 270. Rosenthal R, Milatz S, Krug SM, Oelrich B, Schulzke JD, Amasheh S, Gunzel D, Fromm M. Claudin-2, a component of the tight junction, forms a paracellular water channel. *J Cell Sci* 123: 1913–1921, 2010.
 271. Rowe FJ, Sarkies NJ. Assessment of visual function in idiopathic intracranial hypertension: a prospective study. *Eye* 12: 111–118, 1998.
 272. Rubenstein E. Relationship of senescence of cerebrospinal fluid circulatory system to dementias of the aged. *Lancet* 351: 283–285, 1998.
 273. Rubin RC, Henderson ES, Ommaya AK, Walker MD, Rall DP. The production of cerebrospinal fluid in man and its modification by acetazolamide. *J Neurosurg* 25: 430–436, 1966.
 274. Russell JM. Sodium-potassium-chloride cotransport. *Physiol Rev* 80: 211–276, 2000.
 275. Sackin H, Boulpaep EL. Models for coupling of salt and water transport: proximal tubular reabsorption in *Necturus* kidney. *J Gen Physiol* 66: 671–733, 1975.
 276. Sadler TW. *Langman's Medical Embryology*. Baltimore, MD: Williams & Wilkins, 1995.
 277. Saito Y, Wright E. Regulation of bicarbonate transport across the brush border membrane of the bull-frog choroid plexus. *J Physiol* 350: 327–342, 1984.
 278. Saito Y, Wright EM. Bicarbonate transport across the frog choroid plexus and its control by cyclic nucleotides. *J Physiol* 336: 635–648, 1983.
 279. Sasaki A, Iijima M, Yokoo H, Shoji M, Nakazato Y. Human choroid plexus is an uniquely involved area of the brain in amyloidosis: a histochemical, immunohistochemical and ultrastructural study. *Brain Res* 755: 193–201, 1997.
 280. Sassani P, Pushkin A, Gross E, Gomer A, Abuladze N, Dukkupati R, Carpenito G, Kurtz I. Functional characterization of NBC4: a new electrogenic sodium-bicarbonate cotransporter. *Am J Physiol Cell Physiol* 282: C408–C416, 2002.
 281. Sasseville LJ, Cuervo JE, Lapointe JY, Noskov SY. The structural pathway for water permeation through sodium-glucose cotransporters. *Biophys J* 101: 1887–1895, 2011.
 282. Schafer JA, Troutman SL, Watkins ML, Andreoli TE. Flow dependence of fluid transport in the isolated superficial pars recta: evidence that osmotic disequilibrium between external solutions drives isotonic fluid absorption. *Kidney Int* 20: 588–597, 1981.
 283. Schijman E, Monges J, Raimondi AJ, Tomita T. Choroid plexus papillomas of the III ventricle in childhood. Their diagnosis and surgical management. *Childs Nerv Syst* 6: 331–334, 1990.
 284. Schmitt C, Stazielle N, Richaud P, Bouron A, Ghersi-Egea JF. Active transport at the blood-CSF barrier contributes to manganese influx into the brain. *J Neurochem* 117: 474–756, 2011.
 285. Segal MB, Burgess AM. A combined physiological and morphological study of the secretory process in the rabbit choroid plexus. *J Cell Sci* 14: 339–350, 1974.
 286. Segal MB, Chodobski A, Szmydynger-Chodobska J, Cammish H. Effect of arginine vasopressin on blood vessels of the perfused choroid plexus of the sheep. *Prog Brain Res* 91: 451–453, 1992.
 287. Serot JM, Foliguet B, Bene MC, Faure GC. Choroid plexus and ageing in rats: a morphometric and ultrastructural study. *Eur J Neurosci* 14: 794–798, 2001.
 288. Shuangshoti S, Roberts MP, Netsky MG. Neuroepithelial (colloid) cysts: pathogenesis and relation to choroid plexus and ependyma. *Arch Pathol* 80: 214–224, 1965.
 289. Shuvaev VV, Laffont I, Serot JM, Fujii J, Taniguchi N, Siest G. Increased protein glycation in cerebrospinal fluid of Alzheimer's disease. *Neurobiol Aging* 22: 397–402, 2001.
 290. Siegel GJ, Holm C, Schreiber JH, Desmond T, Ernst SA. Purification of mouse brain ($\text{Na}^+ + \text{K}^+$)-ATPase catalytic unit, characterization of antiserum, and immunocytochemical localization in cerebellum, choroid plexus, and kidney. *J Histochem Cytochem* 32: 1309–1318, 1984.
 291. Silverberg GD, Huhn S, Jaffe RA, Chang SD, Saul T, Heit G, Von Essen A, Rubenstein E. Downregulation of cerebrospinal fluid production in patients with chronic hydrocephalus. *J Neurosurg* 97: 1271–1275, 2002.
 292. Silverberg GD, Mayo M, Saul T, Rubenstein E, McGuire D. Alzheimer's disease, normal-pressure hydrocephalus, and senescent changes in CSF circulatory physiology: a hypothesis. *Lancet Neurol* 2: 506–511, 2003.
 293. Simon DB, Lu Y, Choate KA, Velazquez H, Al-Sabban E, Praga M, Casari G, Bettinelli A, Colussi G, Rodriguez-Soriano J, McCredie D, Milford D, Sanjad S, Lifton RP. Paracellin-1, a renal tight junction protein required for paracellular Mg^{2+} resorption. *Science* 285: 103–106, 1999.
 294. Sinclair AJ, Onyimba CU, Khosla P, Vijapurapu N, Tomlinson JW, Burdon MA, Stewart PM, Murray PI, Walker EA, Rauz S. Corticosteroids, 11β -hydroxysteroid dehydrogenase isozymes and the rabbit choroid plexus. *J Neuroendocrinol* 19: 614–620, 2007.
 295. Smith QR, Johanson CE. Active transport of chloride by lateral ventricle choroid plexus of the rat. *Am J Physiol Renal Physiol* 249: F470–F477, 1985.
 296. Somjen GG. Ion regulation in the brain: implications for pathophysiology. *Neuroscientist* 8: 254–267, 2002.
 297. Song Y, Sonawane N, Verkman AS. Localization of aquaporin-5 in sweat glands and functional analysis using knockout mice. *J Physiol* 541: 561–568, 2002.
 298. Sorensen PS, Thomsen C, Gjerris F, Henriksen O. Brain water accumulation in pseudotumour cerebri demonstrated by MR-imaging of brain water self-diffusion. *Acta Neurochir Suppl* 51: 363–365, 1990.
 299. Speake T, Freeman LJ, Brown PD. Expression of aquaporin 1 and aquaporin 4 water channels in rat choroid plexus. *Biochim Biophys Acta* 1609: 80–86, 2003.
 300. Speake T, Kajita H, Smith CP, Brown PD. Inward-rectifying anion channels are expressed in the epithelial cells of choroid plexus isolated from CIC-2 “knock-out” mice. *J Physiol* 539: 385–390, 2002.
 301. Speake T, Kibble JD, Brown PD. Kv1.1, Kv1.3 channels contribute to the delayed-rectifying K^+ conductance in rat choroid plexus epithelial cells. *Am J Physiol Cell Physiol* 286: C611–C620, 2004.

302. Spector R. Nature and consequences of mammalian brain and CSF efflux transporters: four decades of progress. *J Neurochem* 112: 13–23, 2010.
303. Spring KR. Fluid transport by gallbladder epithelium. *J Exp Biol* 106: 181–194, 1983.
304. Spring KR. Routes and mechanism of fluid transport by epithelia. *Annu Rev Physiol* 60: 105–119, 1998.
305. Spring KR, Siebens AW. Solute transport and epithelial cell volume regulation. *Comp Biochem Physiol A Comp Physiol* 90: 557–560, 1988.
306. Stahl WL, Eakin TJ, Owens JW, Breininger JF, Filuk PE, Anderson WR. Plasma membrane Ca^{2+} -ATPase isoforms: distribution of mRNAs in rat brain by in situ hybridization. *Brain Res* 16: 223–231, 1992.
307. Stauffer TP, Guerini D, Carafoli E. Tissue distribution of the four gene products of the plasma membrane Ca^{2+} pump. A study using specific antibodies. *J Biol Chem* 270: 12184–12190, 1995.
308. Steardo L, Nathanson JA. Brain barrier tissues: end organs for atriopeptins. *Science* 235: 470–473, 1987.
309. Swiderski RE, Agassandian K, Ross JL, Bugge K, Cassell MD, Yeaman C. Structural defects in cilia of the choroid plexus, subfornical organ and ventricular ependyma are associated with ventriculomegaly. *Fluids Barriers CNS* 9: 22, 2012.
310. Szentistvanyi I, Patlak CS, Ellis RA, Cserr HF. Drainage of interstitial fluid from different regions of rat brain. *Am J Physiol Renal Physiol* 246: F835–F844, 1984.
311. Szymdynger-Chodobska J, Chung I, Chodobski A. Chronic hypernatremia increases the expression of vasopressin and voltage-gated Na channels in the rat choroid plexus. *Neuroendocrinology* 84: 339–345, 2006.
312. Szymdynger-Chodobska J, Chung I, Kozniowska E, Tran B, Harrington FJ, Duncan JA, Chodobski A. Increased expression of vasopressin v1a receptors after traumatic brain injury. *J Neurotrauma* 21: 1090–1102, 2004.
313. Szymdynger-Chodobska J, Pascale CL, Pfeffer AN, Coulter C, Chodobski A. Expression of junctional proteins in choroid plexus epithelial cell lines: a comparative study. *Cerebrospinal Fluid Res* 4: 11, 2007.
314. Tanzi RE, Moir RD, Wagner SL. Clearance of Alzheimer's A β peptide: the many roads to perdition. *Neuron* 43: 605–608, 2004.
315. Tapiola T, Alafuzoff I, Herukka SK, Parkkinen L, Hartikainen P, Soininen H, Pirttilä T. Cerebrospinal fluid β -amyloid 42 and tau proteins as biomarkers of Alzheimer-type pathologic changes in the brain. *Arch Neurol* 66: 382–389, 2009.
316. Thaysen JH, Thorn NA, Schwartz IL. Excretion of sodium, potassium, chloride and carbon dioxide in human parotid saliva. *Am J Physiol* 178: 155–159, 1954.
317. Thurtell MJ, Wall M. Idiopathic intracranial hypertension (pseudotumor cerebri): recognition, treatment, and ongoing management. *Curr Treat Options Neurol* 15: 1–12, 2013.
318. Van Huysse JW, Amin MS, Yang B, Leenen FH. Salt-induced hypertension in a mouse model of Liddle syndrome is mediated by epithelial sodium channels in the brain. *Hypertension* 60: 691–696, 2012.
319. VanHouten JN, Wysolmerski JJ. Transcellular calcium transport in mammary epithelial cells. *J Mammary Gland Biol Neoplasia* 12: 223–235, 2007.
320. Virkki LV, Wilson DA, Vaughan-Jones RD, Boron WF. Functional characterization of human NBC4 as an electrogenic Na^{+} - HCO_3^{-} cotransporter (NBCe2). *Am J Physiol Cell Physiol* 282: C1278–C1289, 2002.
321. Vogh BP, Godman DR, Maren TH. Effect of AlCl_3 and other acids on cerebrospinal fluid production: a correction. *J Pharmacol Exp Ther* 243: 35–39, 1987.
322. Vogh BP, Godman DR. Effects of inhibition of angiotensin converting enzyme and carbonic anhydrase on fluid production by ciliary process, choroid plexus, and pancreas. *J Ocul Pharmacol* 5: 303–311, 1989.
323. Vogh BP, Godman DR. Timolol plus acetazolamide: effect on formation of cerebrospinal fluid in cats and rats. *Can J Physiol Pharmacol* 63: 340–343, 1985.
324. Vogh BP, Langham MR Jr. The effect of furosemide and bumetanide on cerebrospinal fluid formation. *Brain Res* 221: 171–183, 1981.
325. Vogh BP, Maren TH. Sodium, chloride, and bicarbonate movement from plasma to cerebrospinal fluid in cats. *Am J Physiol* 228: 673–683, 1975.
326. Voronin LL, Cherubini E. “Deaf, mute and whispering” silent synapses: their role in synaptic plasticity. *J Physiol* 557: 3–22, 2004.
327. Wall M. Idiopathic intracranial hypertension. *Neurol Clin* 9: 73–95, 1991.
328. Walters MR, Fischette CT, Fetzer C, May B, Riggall PC, Tibaldo-Bongiorno M, Christakos S. Specific 1,25-dihydroxyvitamin D_3 binding sites in choroid plexus. *Eur J Pharmacol* 213: 309–311, 1992.
329. Wang CZ, Yano H, Nagashima K, Seino S. The Na^{+} -driven $\text{Cl}^{-}/\text{HCO}_3^{-}$ exchanger. Cloning, tissue distribution, and functional characterization. *J Biol Chem* 275: 35486–35490, 2000.
330. Wang H, Huang BS, Leenen FH. Brain sodium channels and ouabainlike compounds mediate central aldosterone-induced hypertension. *Am J Physiol Heart Circ Physiol* 285: H2516–H2523, 2003.
331. Wang HW, Amin MS, El-Shahat E, Huang BS, Tuana BS, Leenen FH. Effects of central sodium on epithelial sodium channels in rat brain. *Am J Physiol Regul Integr Comp Physiol* 299: R222–R233, 2010.
332. Watters GV, Page L, Lorenzo AV, Cutler RW, Barlow CF. Relationship between cerebrospinal fluid (CSF) formation, absorption and pressure in human hydrocephalus. *Trans Am Neurol Assoc* 94: 153–156, 1969.
333. Watts AG, Sanchez-Watts G, Emanuel JR, Levenson R. Cell-specific expression of mRNAs encoding Na^{+} , K^{+} -ATPase α - and β -subunit isoforms within the rat central nervous system. *Proc Natl Acad Sci USA* 88: 7425–7429, 1991.
334. Weaver DR, Deeds JD, Lee K, Segre GV. Localization of parathyroid hormone-related peptide (PTHrP) and PTHrP receptor mRNAs in rat brain. *Brain Res* 28: 296–310, 1995.
335. Weber KT, Sun Y, Wodi LA, Munir A, Jahangir E, Ahokas RA, Gerling IC, Postlethwaite AE, Warrington KJ. Toward a broader understanding of aldosterone in congestive heart failure. *J Renin Angiotensin Aldosterone Syst* 4: 155–163, 2003.
336. Weinstein AM. Convective paracellular solute flux. A source of ion-ion interaction in the epithelial transport equations. *J Gen Physiol* 89: 501–518, 1987.
337. Weinstein AM, Stephenson JL. Models of coupled salt and water transport across leaky epithelia. *J Membr Biol* 60: 1–20, 1981.
338. Welch K. Secretion of cerebrospinal fluid by choroid plexus of the rabbit. *Am J Physiol* 205: 617–624, 1963.
339. Welch K. The secretion of cerebrospinal fluid by lamina epithelialis. *Monogr Surg Sci* 4: 155–192, 1967.
340. Welch K, Sadler K. Electrical potentials of choroid plexus of the rabbit. *J Neurosurg* 22: 344–351, 1965.
341. Wen GY, Wisniewski HM, Kascsak RJ. Biondi ring tangles in the choroid plexus of Alzheimer's disease and normal aging brains: a quantitative study. *Brain Res* 832: 40–46, 1999.
342. West JB. *Respiratory Physiology: The Essentials*. Baltimore, MD: Lippincott Williams & Wilkins, 2011.
343. Whitlock RT, Wheeler HO. Coupled transport of solute and water across rabbit gallbladder epithelium. *J Clin Invest* 43: 2249–2265, 1964.
344. Whitembury G, Paz-Aliaga A, Biondi A, Carpi-Medina P, Gonzalez E, Linares H. Pathways for volume flow and volume regulation in leaky epithelia. *Pflügers Arch* 405 Suppl 1: S17–S22, 1985.
345. Will C, Fromm M, Müller D. Claudin tight junction proteins: novel aspects in paracellular transport. *Perit Dial Int* 28: 577–584, 2008.
346. Windhager EE, Whitembury G, Oken DE, Schatzmann HJ, Solomon AK. Single proximal tubules of the Necturus kidney. III. Dependence of H_2O movement on NaCl concentration. *Am J Physiol* 197: 313–318, 1959.
347. Wolburg H, Wolburg-Buchholz K, Liebner S, Engelhardt H. Claudin-1, claudin-2 and claudin-11 are present in tight junctions of choroid plexus epithelium of the mouse. *Neurosci Lett* 307: 77–80, 2001.
348. Wolff JE, Sajedi M, Coppes MJ, Anderson RA, Egeler RM. Radiation therapy and survival in choroid plexus carcinoma. *Lancet* 353: 2126, 1999.

349. Wrede B, Liu P, Wolff JE. Chemotherapy improves the survival of patients with choroid plexus carcinoma: a meta-analysis of individual cases with choroid plexus tumors. *J Neurooncol* 85: 345–351, 2007.
350. Wright EM. Mechanisms of ion transport across the choroid plexus. *J Physiol* 226: 545–571, 1972.
351. Wright EM. Transport processes in the formation of the cerebrospinal fluid. *Rev Physiol Biochem Pharmacol* 83: 3–34, 1978.
352. Wright EM, Wiedner G, Rumrich G. Fluid secretion by the frog choroid plexus. *Exp Eye Res* 25 Suppl: 149–155, 1977.
353. Wu Q, Delpire E, Hebert SC, Strange K. Functional demonstration of $\text{Na}^+/\text{K}^+/\text{2Cl}^-$ cotransporter activity in isolated, polarized choroid plexus cells. *Am J Physiol Cell Physiol* 275: C1565–C1572, 1998.
354. Xiong ZG, MacDonald JF. Sensing of extracellular calcium by neurones. *Can J Physiol Pharmacol* 77: 715–721, 1999.
355. Yamasaki H, Sugino M, Ohsawa N. Possible regulation of intracranial pressure by human atrial natriuretic peptide in cerebrospinal fluid. *Eur Neurol* 38: 88–93, 1997.
356. Yuh EL, Dillon WP. Intracranial hypotension and intracranial hypertension. *Neuroimaging Clin N Am* 20: 597–617, 2010.
357. Zemo DA, McCabe JT. Salt-loading increases vasopressin and vasopressin 1b receptor mRNA in the hypothalamus and choroid plexus. *Neuropeptides* 35: 181–188, 2001.
358. Zeuthen T. Cotransport of K^+ , Cl^- and H_2O by membrane proteins from choroid plexus epithelium of *Necturus maculosus*. *J Physiol* 478: 203–219, 1994.
359. Zeuthen T. The effects of chloride ions on electrodiffusion in the membrane of a leaky epithelium. Studies of intact tissue by microelectrodes. *Pflügers Arch* 408: 267–274, 1987.
360. Zeuthen T. Secondary active transport of water across ventricular cell membrane of choroid plexus epithelium of *Necturus maculosus*. *J Physiol* 444: 153–173, 1991.
361. Zeuthen T. Water permeability of ventricular cell membrane in choroid plexus epithelium from *Necturus maculosus*. *J Physiol* 444: 133–151, 1991.
362. Zeuthen T. Water-transporting proteins. *J Membr Biol* 234: 57–73, 2010.
363. Zeuthen T. Cotransport of K^+ , Cl^- and H_2O by membrane proteins from choroid plexus epithelium of *Necturus maculosus*. *J Physiol* 478: 203–219, 1994.
364. Zeuthen T, Wright EM. Epithelial potassium transport: tracer and electrophysiological studies in choroid plexus. *J Membr Biol* 60: 105–128, 1981.
365. Zeuthen T, Wright EM. An electrogenic Na^+/K^+ pump in the choroid plexus. *Biochim Biophys Acta* 511: 517–522, 1978.
366. Zlokovic BV, Mackic JB, Wang L, McComb JG, McDonough A. Differential expression of Na,K-ATPase alpha and beta subunit isoforms at the blood-brain barrier and the choroid plexus. *J Biol Chem* 268: 8019–8025, 1993.